ANALYSIS OF A VACCINE-ELICITED ANTI-H5N1 ANTIBODY AND ITS UNMUTATED COMMON ANCESTOR

By

Katie Lynn Winarski

Dissertation

Submitted to the Faculty of the

Graduate School of Vanderbilt University

In partial fulfillment of the requirements

for the degree of

DOCTOR OF PHILOSOPHY

in

Microbiology and Immunology

August, 2016

Nashville, Tennessee

Approved:

Mark R. Denison, M.D.

James E. Crowe Jr., M.D.

Melanie D. Ohi, Ph.D.

James W. Thomas, M.D

Benjamin W. Spiller, Ph.D.

To my parents.

ACKNOWLEDGMENTS

First, I would like to thank my mentor Dr. Benjamin Spiller. I am thankful for the opportunity to complete my dissertation research in your laboratory. And I am grateful for the introduction into the world of antibody antigen interactions and x-ray crystallography. You has always been both an encouraging and supportive, and have made me a better scientist.

I would like to thank my committee members, Drs. Mark Denison, Jim Crowe, Melanie Ohi, and Tom Thomas. I am forever appreciative for their helpful insight into my project and the encouragement they have given me over the years.

My project was a collaboration with Jim Crowe's lab. I am thankful to him and various members of his lab, including Natalie, Gopal, David, Jessica, Andrew, and Sandhya, for the opportunity to work on this project and all of their help in completing this project.

I would like to thank the members of Ben's lab who were there when I began graduate school, (Old) Katie, Lisa, Tara, and Michele. You are a wonderful group people who made me feel at home in lab. You have done so much. Thank you for teaching me. Thank you for answering my endless questions. And most of all thank you for becoming amazing friends.

I would like to thank my family, who supported me in this endeavor, and though they did not always understand what I was doing, they were always there for me. And thank you to all of the friends I have made along the way at Vanderbilt and in Nashville. There are too many people and too many memories to list, but in the end, y'all made Nashville feel like home.

I would like to thank my department Pathology, Microbiology, and Immunology and my second department the Center for Structural Biology for all

the support they have provided. And finally I would like to thank my funding sources. This project was supported by institutional funds from the National Institutes of Health R01 AI106002, HHSN272200900047C, and R21 AI092268. Additionally, I was supported by the Molecular Biophysics Training Grant.

TABLE OF CONTENTS

Page

LIST OF TABLES

LIST OF FIGURES

LIST OF ABBREVIATIONS

Å	Angstrom
α2,3-SLN	3′-sialyl-N-acetyllactosamine
Ab	Antibody
AID	Activation-induced cytidine deaminase
APCs	Antigen presenting cells
ASU	Asymmetric unit
BCR	B cell receptor
bnAbs	Broadly neutralizing antibodies
CDC	Centers for Disease Control
CDRs	Complementarity determining regions
CDRH1/2/3	Heavy chain complementarity determining region 1/2/3
CDRL1/2/3	Light chain complementarity determining region 1/2/3
CTL	Cytotoxic T lymphocyte
D	Diversity
DNA	Deoxyribonucleic acid
DTT	Dithiothreitol
EC_{50}	Half maximal effective concentration
Fab	Fragment antigen binding
Fc	Fragment crystallizable
FDA	Federal Drug Administration
FR	Framework
H-bonding	Hydrogen bonding
H5	Hemagglutinin 5
H5hd	Hemagglutinin 5 head domain
HA	Hemagglutinin

HA1	Hemagglutinin subunit 1
HA2	Hemagglutinin subunit 2
HC	Heavy chain
hH5.3	Hybridoma produced H5.3
$H5.3_{m}$	Mature H5.3
$H5.3_{uca}$	Unmutated common ancestor of H5.3
HMG1/2	High mobility group protein 1/2
hr	Hour
IC_{50}	Half inhibitory concentration
IG	Immunoglobulin
IPTG	Isopropyl β-D-1-thiogalactopyranoside
J	Joining
kD	Kilodalton
LB	Luria broth
LC	Light chain
M1	Matrix protein 1
M2	Matrix protein 2
mAb	Monoclonal antibody
MHC	Major histocompatibility complex
mL	Milliliter
mM	Millimolar
NA	Neuraminidase
NHEJ	Non-homologous end joining
NLPR3	Nucleotide oligomerization domain (NOD)-like receptor family pyrin domain containing 3
NP	Nucleoprotein

NS1	Nonstructural protein 1
NS2	Nonstructural protein 2
OH	Hydroxyl group
ORF	Open reading frame
PA	Polymerase acidic
PAMPs	Pathogen associated molecular pattern
PB1	Polymerase basic 1
PB2	Polymerase basic 2
PBS	Phosphate buffered saline
PCC	Post cleavage complex
PCR	Polymerase chain reaction
PDB	Protein data bank
PMSF	Phenylmethylsulfonyl fluoride
PRRs	Pattern recognition receptors
RAG	Recombination activating gene
RBS	Receptor binding site
rdt	Respiratory droplet transmissible
*rdt*_In	Thr160Ala, Gln226Leu, Gly228Ser mutations in H5
*rdt*_Vn	Asn158Asp, Asn224Lys, Gln226Leu mutations in H5
rH5.3	Recombinantly expressed H5.3
RIG-1	Retinoic acid-inducible gene 1
RNA	Ribonucleic acid
s	Seconds
SA	Sialic acid
SHM	Somatic hypermutation
Th1/2	Helper T cell 1/2

TLS	Torsion/libration/screw
UCA	Unmutated common ancestor
µg	Micrograms
µM	Micromolar
V	variable
VN/1203	A/Vietnam/1203/2004 (H5N1)
WHO	World Health Organization
wt	Wild-type

CHAPTER I

INTRODUCTION

Overview

Seasonal influenza remains a worldwide health concern, causing the death of between 250,000 – 500,000 people each year (WHO, 2014a). Recently, avian influenza viruses, novel to the human population have breached the host species barrier, and infected and caused disease in humans, though they are not currently capable of direct transmission in humans (Claas et al., 1998; Class et al., 1998; WHO, 2014a). Since 2003, ~850 human cases of the novel avian influenza virus H5N1 have been reported with a ~50% mortality rate (WHO, 2016). Recently two labs have shown very few mutations in the influenza glycoprotein hemagglutinin (HA) may be necessary for H5N1 to be efficiently transmitted in humans (Herfst et al., 2012; Imai et al., 2012).

In order to examine the immune response to H5N1, a panel of antibodies was isolated from subjects in a phase I clinical trial of an experimental H5N1 vaccine trial and characterized (Thornburg et al., 2013). We chose a potent and specific antibody, H5.3, that binds the H5 head domain to study further.

The key questions for this project were how does a vaccine-elicited antibody neutralize a novel influenza virus and what role did affinity maturation play in the development of this antibody?

The key results are the structure of the H5.3 Fab H5 head domain complex showed H5.3 uses all six complementarity determining regions (CDRs) to interact with the highly conserved receptor binding site (RBS) and polymorphic residues on the edges of the interface. This indicates the breadth and potency of the antibody

conflict due to the variability outside the RBS. Secondly, as evidenced by the structures of H5.3 in complex with H5 respiratory droplet transmissible variants, the receptor specificity of the virus, different in avian and human type HAs, may not be important for recognition by a RBS-directed antibody. Thirdly, the H5N1 vaccine primarily elicited a naïve B cell response, where the H5-specific antibodies had a lower average number of somatic mutations compared to broadly neutralizing influenza antibodies. Finally, the H5.3 somatic mutations do not stabilize the protein conformation, as it remains flexible after affinity maturation, and do not have large effect on increasing the affinity of H5.3 for H5. This indicates the somatic mutations perform another function, such as decreasing the polyspecificity or increasing the stability of the antibody. Taken together these data will help inform future vaccine design.

Antibody Overview

Antibodies are specialized proteins that allow B lymphocytes to recognize antigens. An antibody is composed of 2 large heavy chains (HCs; ~55kD) and 2 smaller light chains (LCs; ~24kD) (Figure I-1). Each antibody is composed of three structural domains connected by a flexible hinge region, including two Fragments antigen binding (Fabs) and one Fragment crystallizable (Fc). These domains can be separated into Fab and Fc fragments by protease cleavage. The Fc is composed of a dimer of the constant heavy chain 2 (C_H2) and C_H3 domains of each HC, and the Fab is comprised of a dimer of the variable light chain (V_L) and constant light chain (C_L), and variable heavy chain (V_H) and C_H1 domains.

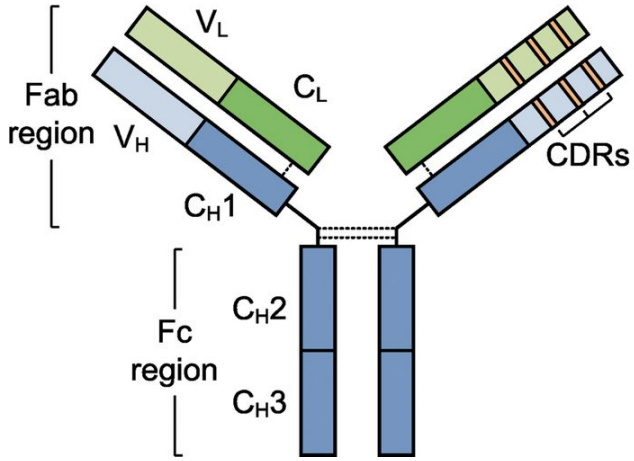

Figure I-1. Antibody Structure. The heavy chains are shown in blue, the light chains in green. The dark colors represent the constant regions (dark blue, HC; dark green, LC), which are important for antibody effector function. Both the HC and LC variables regions (light colors) contain three complementarity determining regions (yellow, CDRs), important for antigen recognition and binding. The Fab region (Fab) consists of one LC and the HC variable region and C_H1 (constant heavy chain 1). The Fc region is a dimer of C_H2 and C_H3 of both HCs. Figure adapted from (Ruigrok et al., 2011).

The variable region contains 6 complementarity-determining regions (CDRs), involved in antigen recognition, and frameworks (FR), which provide structural support.

Antibody diversity

Antibody diversity is generated by pairing the heavy and light chains, V(D)J recombination, somatic hypermutation, and class switching. During V(D)J recombination one each variable (V), diversity (D), and joining (J) segment on the IGH gene locus form the variable region of the HC, and one each V and J gene segment on the IGL (or IGK) gene locus form the variable region on the LC. The heavy and light chain genes are located on chromosomes 14 (heavy chain; IGH), 22 (light chain lambda; IGL), and 2 (light chain kappa; IGK). Not all of the gene segments are functional; some have mutations that prevent them from encoding a functional protein. Of the 123-129 IGHV gene segments, 44 contain open reading frames (ORFs); 25 of 27 of the D segments and 6 of the 9 J segments are used for somatic recombination (Herfst et al., 2012; Imai et al., 2012; Lefranc and Lefranc, 2001; WHO, 2016). The IGHV and IGHD genes are each grouped into 7 families based on sequence homology.

The standard nomenclature for antibody V and D genes is as follows: the chain and gene descriptions (IGHV, IGHD), the family number, the gene number (determined by the position from 5' to 3' on the gene locus), and allele number; the family and gene number are separated by a hyphen and an asterisk precedes the allele (Lefranc et al., 1999; Lefranc, 1998). For example, IGHV4-4*02.

V(D)J recombination

Recombination signal sequences (RSSs) are composed of conserved heptamer or nonomer elements separated by either 12 or 23 nucleotide spacers that flank the V, D, and J gene segments. The synaptic complex, composed of one RSS of each type, the lymphoid-specific V(D)J recombinase, RAG1 and RAG2, and the high-mobility group protein 1 (HMG1) or HMG2 which act as cofactors, must be formed for recombination to occur (Oettinger et al., 1990; Ruigrok et al., 2011; Schatz et al., 1989; Thornburg et al., 2013).

To form the complex synapse, the RAG proteins bind to an RSS and introduce a single-stranded nick, creating a hydroxyl (OH) group (Figure I-2). This complex synapses with another RSS and the OH group attacks the other strand, causing a double-stranded break. The coding ends and blunt ends remain connected with RAG in a post-cleavage complex (PCC), which serves as a scaffold for the DNA ends and may recruit factors from the non-homologous end joining (NHEJ) pathway to ligate the ends and form signal and coding joints (Lieber et al., 2003; Roth and Roth, 2000).

During this process nucleotides are randomly inserted or deleted at segment junctions leading to more diversity. Every naïve B cell has an unique B cell receptor (BCR), and models predict there are 10^{18} possible BCR sequences (Elhanati et al., 2015).

Class-switching

Class switching is the process by which the constant region of the heavy chain can be altered (from IgM or IgD), changing the function of the BCR. Each C_H gene segment (IgA, IgG, IgE) is preceded by a switch region, which contains transcribed repetitive DNA elements.

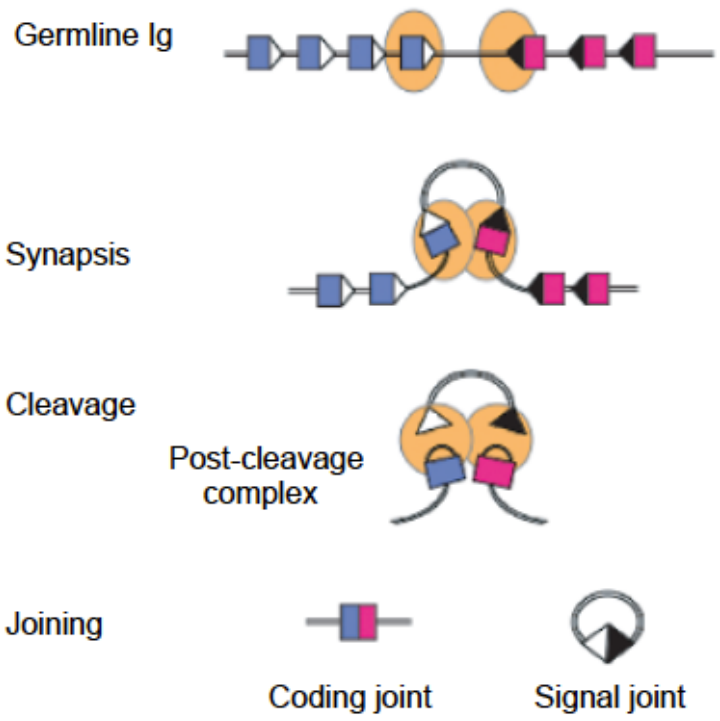

Figure I-2. V(D)J Recombination. The top panel shows germline Ig genes, where the colored boxes represent coding segments, flanked by 12- and 23-RSSs (white and black triangles), and one of each is bound by RAG proteins (orange ovals). The RAG proteins introduce a single-stranded nick and the synapse forms leading to a double-stranded break. This leads to the formation of the PCC, followed by ligation of the ends by the NHEJ pathway to form signal and coding joints. Figure adapted from (Brandt and Roth, 2004).

Activation-induced cytidine deanimase (AID) deaminates cytosines to uracils resulting in double-stranded DNA breaks upstream of the donor and downstream of the acceptor switch regions (Xu et al., 2012). The donor and acceptor regions are joined together, resulting in a new constant region and a new function for the antibody.

Affinity maturation

Naïve and memory B cells are activated by foreign antigens and migrate to the germinal centers to undergo somatic hypermutation (SHM) and clonal selection. The B cells move between the dark zone where they undergo SHM and proliferate; and the light zone where they undergo selection.

During SHM, mutations are introduced into the variable region, and the BCR is rapidly altered (Figure I-3). AID is the enzyme responsible for the mutations during SHM, it deaminates cytosine to uracil during transcription (Muramatsu et al., 2000; Teng and Papavasiliou, 2007). This process typically involves ~one mutation/cell division (Teng and Papavasiliou, 2007; Victora and Nussenzweig, 2012) and the identity of neighboring nucleotides influences the likelihood a residue will be mutated (Elhanati et al., 2015; Shapiro et al., 2003; Yaari et al., 2013).

During clonal selection, the somatically altered B cells compete for survival signals from T follicular helper cells by competitively binding foreign antigen on follicular dendritic cells (Peled et al., 2008). During this process around 90% of the selected B cells repeat this cycle, and 10% exit the cycle to serve as memory cells or plasma cells (Oprea and Perelson, 1997).

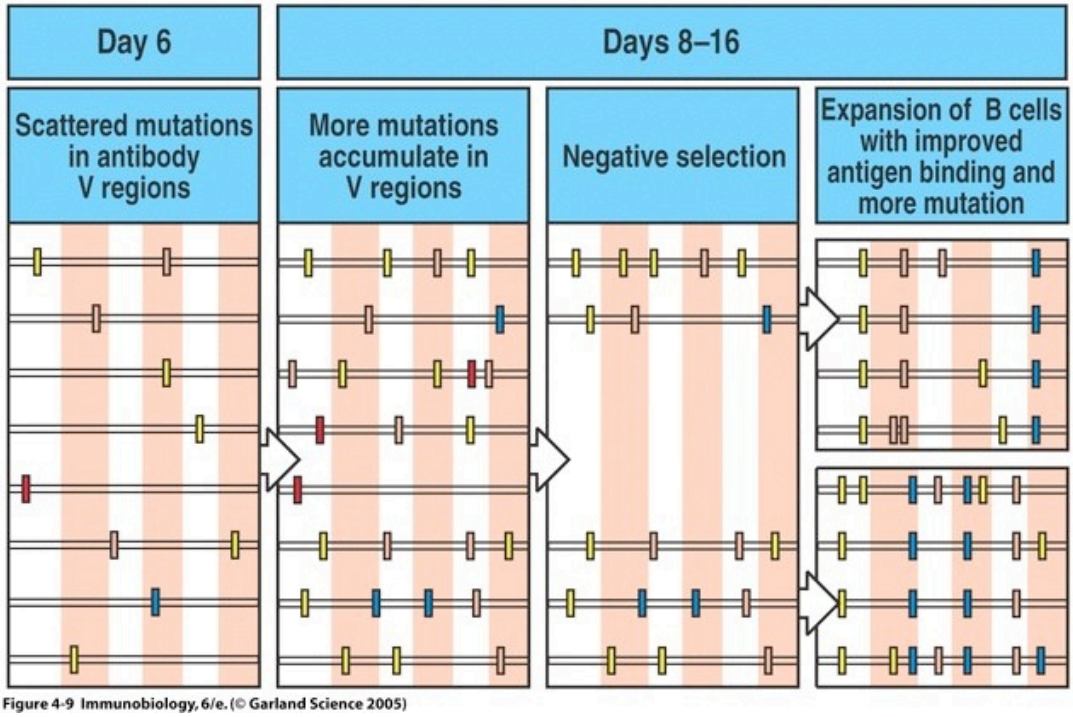

Figure I-3. Affinity maturation. BCRs accumulate mutations in the variable regions. Antibodies are selected on the basis of affinity for antigen and B cells with improved antigen binding are selected and expanded. Figure from (Murphy et al., 2007)

Influenza

The *Orthomyxoviridae* virus family includes Influenza A, B, C, D, Thogotavirus, Isavirus, and Quaranfilvirus (Lefranc, 1998; Palese and Shaw, 2007). Influenza A can infect a large range of species, including humans and swine, though wild aquatic birds are the natural reservoir (Webster et al., 1992). The host range of Influenza B is limited to humans and seals (Osterhaus et al., 2000; Webster et al., 1992), and it is classified into 2 linages, Yamagata and Victoria (Yamashita et al., 1988). Influenza A is further divided into subtypes based on the hemagglutinin (HA) and neuraminidase (NA) glycoproteins on the viral surface; 18 HA and 11 NA subtypes have been identified, two subtypes, H17N10 and H18N11, are specific to bats (Fouchier et al., 2005; Tong et al., 2012; 2013). The HA glycoprotein is further divided into two groups based on sequence homology, group 1 (H1, H2, H5, H6, H8, H9, H11, H12, H13, H16, H17, H18) and group 2 (H3, H4, H7, H10, H14, H15) (Figure I-4).

The standard nomenclature for influenza is as follows: antigenic type of influenza, host of origin (unless human), geographic origin, strain number, year (2 numbers before 2000, and 4 numbers after 2000), and antigenic description of the HA and NA in parenthesis (only for influenza A) (WHO, 1980). For example, A/Vietnam/1203/2004 (H5N1).

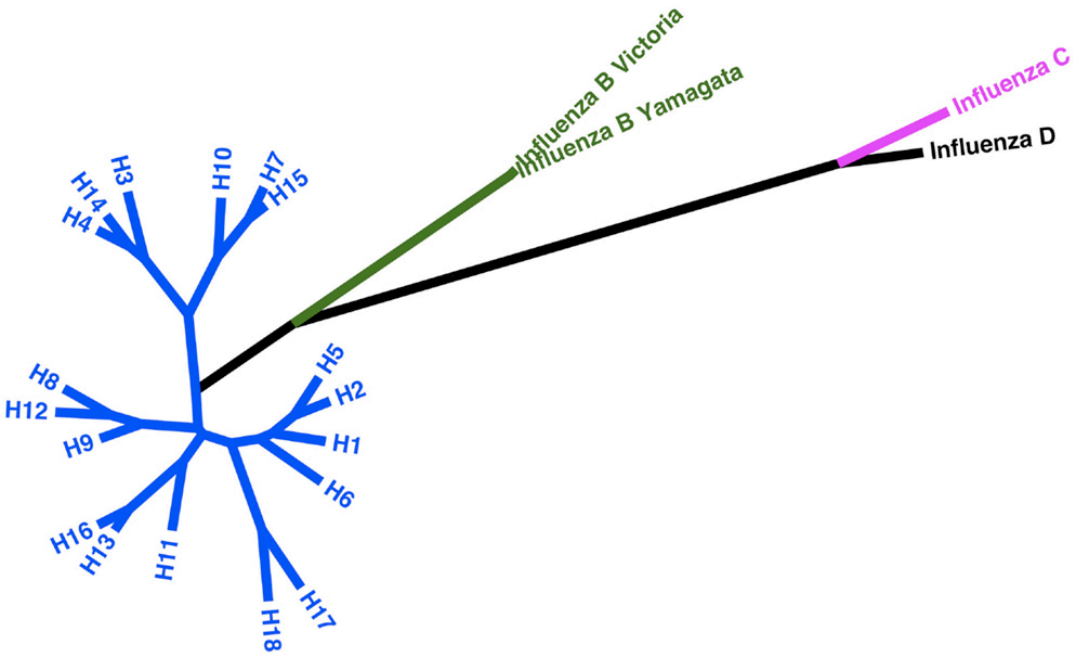

Figure I-4. Influenza HA phylogenetic tree. Phylogenetic analysis of HA sequences from Influenza A (blue; group 1, bottom; group 2, top), B (green), C (magenta), and putative Influenza D (black). Figure from (Carnell et al., 2015).

Influenza infects 2-5 million people annually and results in the death of 250,000-500,000 people each year (WHO, 2014a). It is a seasonal infection, causing disease during the winter in areas with temperate climates and during the rainy season in tropical climates (Tamerius et al., 2011). Influenza is transmitted person-to-person by respiratory droplets and is maintained by person-to-person contact. The incubation period for influenza A is 1-4 days, and those infected may be able to transmit the virus one day prior to exhibiting symptoms (Cox and Subbarao, 1999). Influenza is an acute respiratory disease, with symptoms including fever, coughing, sore throat, malaise, muscle fatigue, and headache, ranging from mild to severe (Centers for Disease Control and Prevention (CDC), 2008). Infection can exacerbate underlying conditions, cause primary viral pneumonia, lead to secondary bacteria pneumonia, or add to co-infections with other viral or bacterial pathogens (Ho et al., 2009; Lieber et al., 2003; Roth and Roth, 2000; Xu et al., 2012).

Influenza A virus genome and structure

Influenza A is an enveloped virus containing eight, negative-sense single-stranded RNA segments (Figure I-5A) (Palese and Shaw, 2007). The virus particles can be spherical (~100 mm) or filamentous (1μm or longer) (Figure I-5B) (Bouvier and Palese, 2008). There are twelve proteins encoded by the influenza genome, surface glycoproteins, HA and NA, two matrix proteins (M1 and M2), the nucleoprotein (NP), three polymerase proteins, PA (polymerase acid), PB1 (polymerase basic 1), and PB2; and four nonstructural proteins NS1, NS2, PA-X, and PB1-F2 (Teng and Papavasiliou, 2007; Victora and Nussenzweig, 2012).

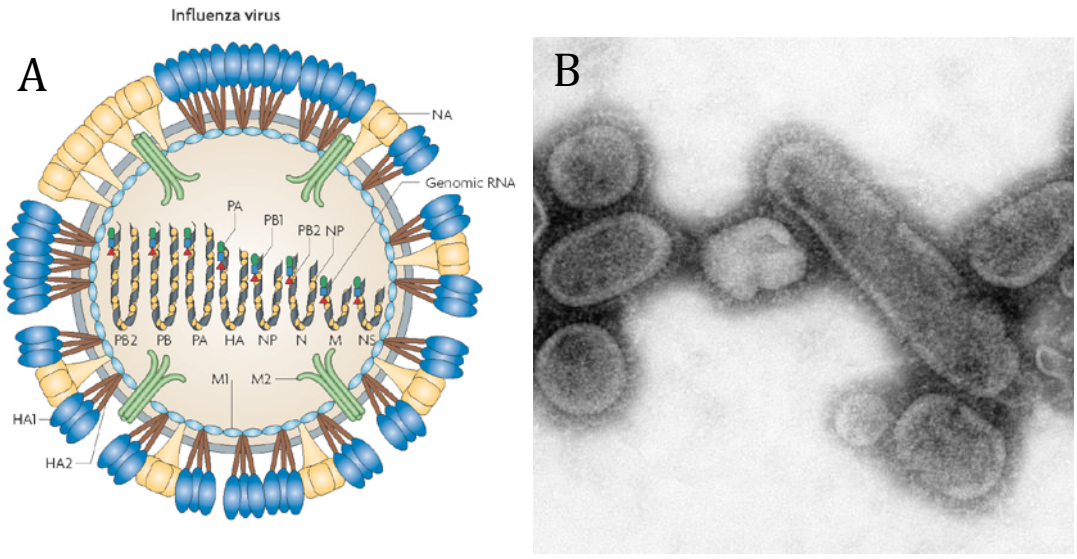

Figure I-5. Influenza A virus structure. (A) Influenza has a lipid envelope derived from the host cell membrane, three glycoproteins, HA (HA1, blue; HA2, brown), NA (light yellow), and M2 (green), are inserted into the viral membrane and M1 (light blue) lines the viral interior. The virus contains 8 negative sense single stranded RNA segments (grey); they are encapsulated with NP (yellow) and coupled with three RNA polymerase proteins, PA (green), PB1 (blue), and PB2 (red). Figure adapted from (Karlsson Hedestam et al., 2008). (B) Electron micrograph of reconstructed 1918 H1N1 influenza virus. Imaged adapted from http://phil.cdc.gov/phil/details.asp?pid=8243.

Hemagglutinin binds host-cell sialic acid receptors leading to endocytosis of the virus. Endosome acidification, partially catalyzed by the M2 proton channel, promotes viral fusion and entry of the virus into the host cell. Protons enter and acidify the virus interior through the M2 ion channel, allowing the viral payload to be released into the cell (Zhirnov, 1990). The virus replicates in the nucleus and new virus is assembled at the cell membrane (Banerjee et al., 2013; Leser and Lamb, 2005). NA is responsible for cleaving the interaction between HA and the influenza receptor, sialic acid (SA), NA enzymatically cleaves sialic acid groups from host glycoproteins, releasing newly formed virus from the infected cell (Colman, 1994).

Hemagglutinin

Hemagglutinin is a type I integral membrane protein composed of three identical protomers. HA is initially expressed as an HA0 precursor, then cleaved by host proteases at the cell surface into HA1, composed of the membrane distal globular head domain and part of the membrane-proximal stem domain, and HA2, contributing only to the stem domain (Figure I-6). In 1981 the Wiley lab determined the first structure of HA, the bromelain-released HA ectodomain of A/Aichi/68 (H3N2) (Wilson et al., 1981).

The HA receptor binding site (RBS) is a conserved shallow pocket surrounded by hypervariable regions, and is located on the HA1 globular head domain. The influenza receptor, SA, binds HA at this site (Weis et al., 1988). Influenza viruses that replicate in different species contain HAs with different SA linkage preferences.

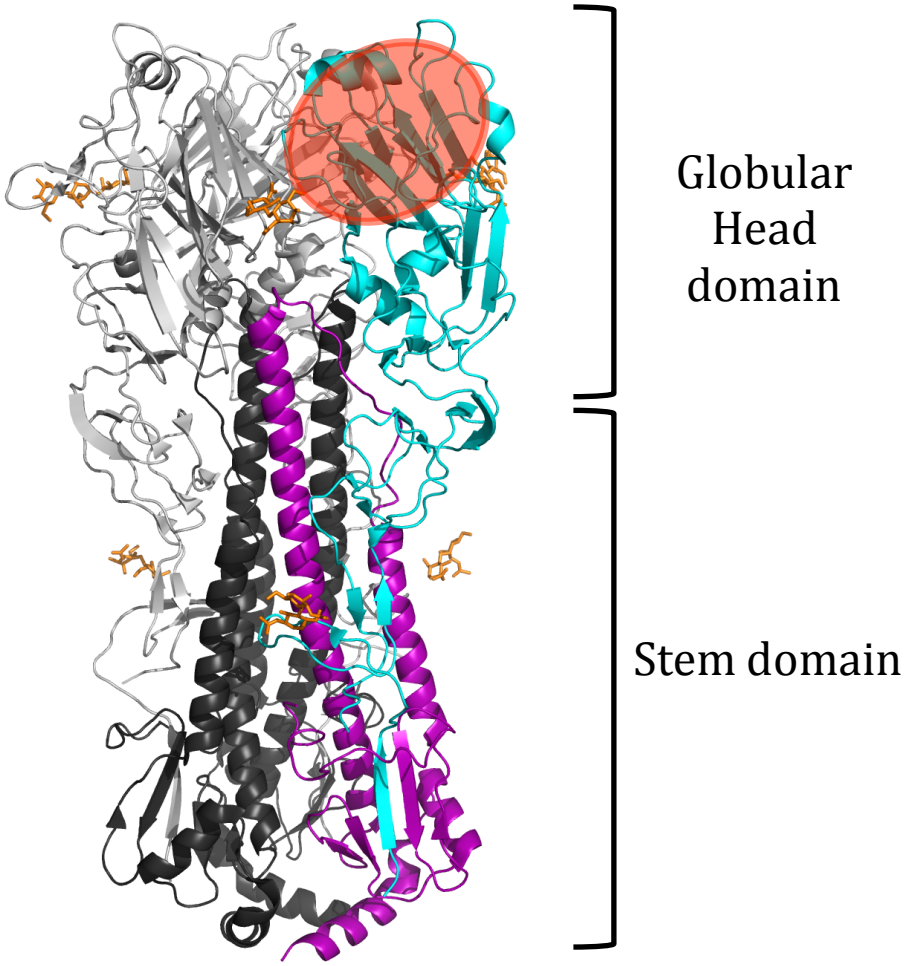

Figure I-6. Overview of hemagglutinin structure. Crystal structure of the A/Vietnam/1203/2004 (H5N1) HA trimer ectodomain. Each protomer is colored by HA1 (light grey) and HA2 (black); one protomer is colored differently (HA1 cyan; HA2 purple) for clarity. The globular head domain consists of a portion of HA1, and the stem domain contains of the rest of HA1 and HA2. The red circle indicates the location of the RBS. Carbohydrates are shown in orange. PDB ID 2FK0.

Human-type influenza HAs preferentially recognize an α2,6-SA linkage, located in the human upper respiratory tract, while avian-type influenza HAs recognize an α2,3-SA linkage, located in the avian gut epithelium (Connor et al., 1994). The situation may be complicated in humans, with α2,3-SA linkages on ciliated cells and α2,6-SA linkages on non-ciliated cells in the human respiratory tract (Elhanati et al., 2015; Matrosovich et al., 2004; Shapiro et al., 2003; Yaari et al., 2013).

The membrane proximal stem domain is responsible for viral membrane fusion. Following endocytosis, the exposure of the virus to the low pH of the endosome triggers HA to undergo large-scale conformational rearrangements where HA1 disassociates from HA2, remaining linked through a disulfide tether (Figure I-7A,B) (Bullough et al., 1994; Chen et al., 1999; Peled et al., 2008; Skehel et al., 1982). This exposes the fusion peptide, which inserts into the endosomal membrane, forming the extended intermediate (Figure I-7C) (Carr and Kim, 1993; Oprea and Perelson, 1997). Collapse of the extended intermediate causes the fusion peptide and transmembrane anchor to fold together into a stable coiled coil domain and consequently the viral and endosomal membranes fuse (Figure I-7D,E). The action of several HAs form a pore allowing the release of the viral payload into the host cell.

Influenza immune response

The primary defense system against influenza infection is the non-specific response of the innate immune system, formed by physical barriers and innate immune cells (Holt et al., 2008; Murphy et al., 2007).

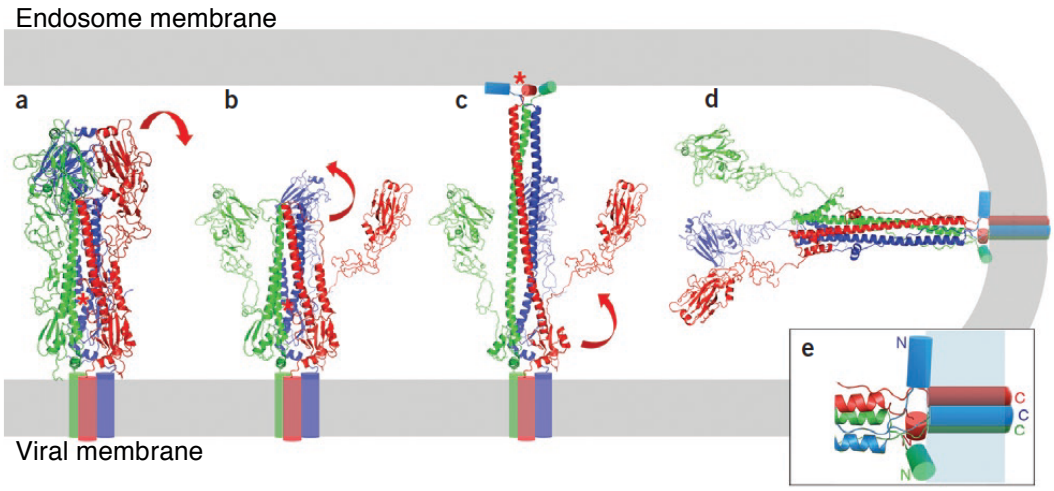

Figure I-7. Viral membrane fusion. (A) The pre-fusion HA conformation with each protomer shown in a different color. (B) The low pH of the endosome causes HA1 to separate from HA2, remaining linked through a disulfide tether. (C) The fusion peptide flips up into the endosomal membrane, forming an extended helix intermediate. (D, E) Collapse of the intermediate brings the fusion peptide and transmembrane anchor together, fusing the endosome and viral membranes. The action of multiple HAs forms pores allowing the release of the viral payload. Figure adapted from (Harrison, 2008).

As a result of influenza infections, interferons, cytokines, and chemokines are produced following recognition of pathogen-associated molecular patterns (PAMPs) by pattern recognition receptors (PRRs) (Sanders et al., 2011). Retinoic acid inducible gene-I (RIG-I) receptors, toll like receptors (TLRs), and nucleotide oligomerization domain (NOD)-like receptor family pyrin domain containing 3 (NLRP3) are the main PRR categories involved in the detection of influenza infection and the induction of the interferon response (Pang and Iwasaki, 2011). These pathways lead to the activation of the antiviral response and the recruitment of neutrophils, activation of macrophages, and maturation of dendritic cells (Sanders et al., 2011).

The secondary defense system is the highly specific adaptive immune system, which consists of the humoral (antibodies; discussed in the Neutralizing Antibodies Against Influenza section) and cellular (CD4+ and CD8+ T cells) immune responses. CD4+ T cells are activated after recognition of viral epitopes associated with MCH class II antigen-presenting cells (APCs). Naïve CD4+ T cells differentiate into CD4+ T helper 1 (Th1) cells, which produce IFN-γ and IL-2, promote cytotoxic T lymphocyte (CTL) responses, and induce memory CD8+ T cell formation (Deliyannis et al., 2002; Mosmann et al., 1986; Osterhaus et al., 2000; Riberdy et al., 2000; Webster et al., 1992; Zhu and Paul, 2010); or Th2 cells, which produce IL-4, -5, and -13, and promote the activation and differentiation of B cells (Eichelberger et al., 1991; Lamb et al., 1982; Okoye and Wilson, 2011; Yamashita et al., 1988).

After activation by MCH class I APCs, CD8+ T cells differentiate into CTLs, migrate to the site of infection where they recognize the conserved internal influenza proteins (M1, NP, PA, PB2; cross-reactive), and eliminate the infected

cells, preventing viral spread (Assarsson et al., 2008; Jameson et al., 1998; Kreijtz et al., 2008; Lee et al., 2008; Nakanishi et al., 2009).

Influenza treatment and prevention

There are currently five antiviral drugs approved by the FDA for the treatment of influenza, two M2 ion channel inhibitors, amantadine and rimantadine; and three NA inhibitors, oseltamivir, zanamivir, and peramivir. Amantadine and rimantadine, only effective against influenza A, target the M2 ion channel on the influenza virus surface, inhibiting the transport of protons to the interior of the virus, thus blocking viral uncoating (Wharton et al., 1994). Many influenza strains (>90%) are now resistant to these antivirals and they are no longer recommended as a treatment for influenza infection as of 2010/2011 (Fiore et al., 2011).

The NA inhibitors, oseltamivir, marketed as Tamiflu, zanamivir, and peramivir, are effective against influenza A and B. They target the NA glycoprotein on the viral surface and prevent the release of newly formed virus and therefore viral spread (Carnell et al., 2015; Choung U Kim et al., 1997; Itzstein et al., 1993; Pooran Chand et al., 2001; WHO, 1980; 2014a). During the 2007-2008 influenza season, resistance to oseltamivir increased (Sheu et al., 2008; Tamerius et al., 2011). However, the oseltamivir resistant H1N1 was replaced in 2009 with the oseltamivir sensitive A(H1N1)pdm09 virus, which has a much lower resistance rate, ~3% (Cox and Subbarao, 1999; Okomo-Adhiambo et al., 2015; Takashita et al., 2015).

The current preventative measure for influenza is a strain-specific vaccine which must be updated annually due to the antigenic drift of the virus (Centers for Disease Control and Prevention (CDC), 2008; Russell et al., 2008). The WHO and CDC track influenza virus strains isolated throughout the year and use this

information to recommend which strains should be included in vaccines. This decision is made ~6 months in advance of the next flu season due to vaccine manufacturing constraints (Russell et al., 2008). This can lead to mismatch between the influenza strains used in the vaccine and circulating strains, which can result in a lower efficacy of the vaccine (de Jong et al., 2000a; Jin et al., 2005).

There are two types of influenza vaccines, inactivated and live attenuated. The most commonly used influenza vaccine is the trivalent inactivated vaccine, containing one each A/H1N1, A/H3N2, and Influenza B strain (Cox et al., 2004). Alternatively, there is a cold-adapted live-attenuated quadrivalent vaccine, containing one each A/H1N1, A/H3N2, and two influenza B strains (Beyer et al., 2002; Palese and Shaw, 2007). This vaccine also offers the advantage of eliciting cellular and mucosal immunity (Beyer et al., 2002; Bouvier and Palese, 2008; Hoft et al., 2011).

Antigenic drift and shift

Influenza can escape the humoral immune system through a phenomenon known as antigenic drift. This occurs when influenza accumulates point mutants in antibody-binding sites, thus allowing influenza variants to evade the influenza-specific antibody response (de Jong et al., 2000b; Rambaut et al., 2008; Smith et al., 2004).

Antigenic shift occurs when two or more influenza strains infect the same cell and reassort to produce an antigenically distinct virus. Swine are considered influenza “mixing vessels” because their respiratory epithelium contains both human and avian type influenza receptors, from which re-assorted virus can emerge (Figure I-8) (Ma et al., 2008).

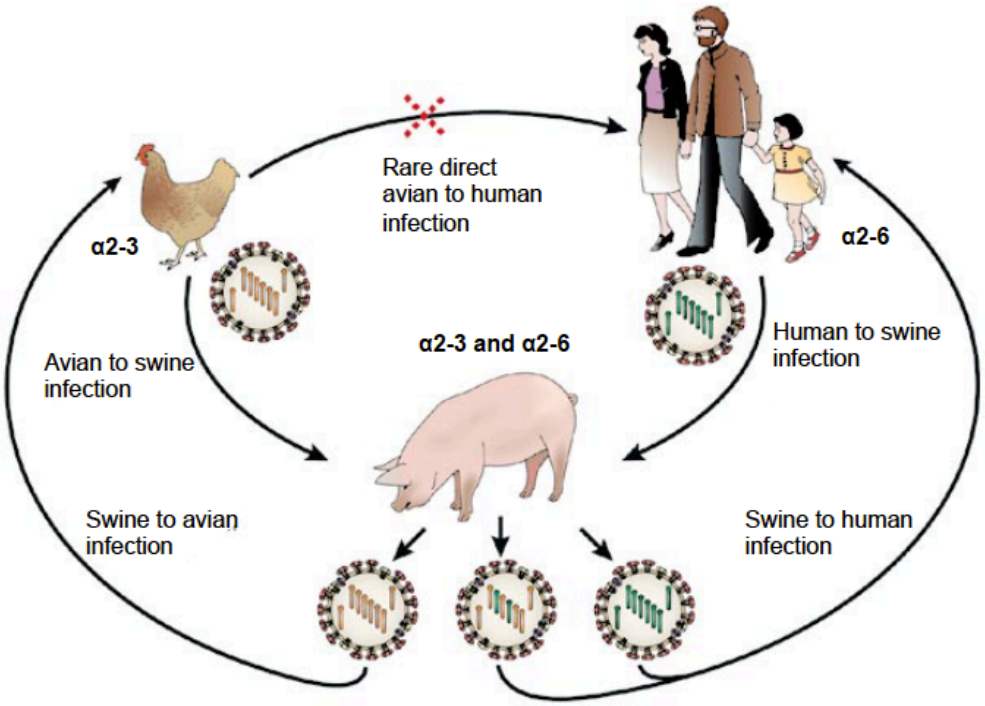

Figure I-8. Influenza antigenic shift. Human and avian-type influenza viruses can infect pigs, which have both types of influenza receptors (human, α2,6-SA and avian, α 2,3-SA). Influenza virus gene segments can reassort in pigs, an influenza "mixing vessel", resulting in intact human, avian, or a novel virus. If the novel virus is functional, a new pandemic strain may emerge. Figure adapted from (Stevens et al., 2006b).

Influenza pandemics and circulating strains

There have been four influenza pandemics since the beginning of the last century, the 1918 H1N1 Spanish Flu, 1957 H2N2 Asian Flu, 1968 H3N2 Hong Kong Flu, and 2009 H1N1 Swine Flu, which were caused by genetic reassortment of the influenza virus (Figure I-9). Additionally, all of these viruses acquired the capacity to cause illness and transmit efficiently in the immunologically naïve human population, important features of a pandemic virus (Poland et al., 2007).

The 1918 H1N1 Spanish Flu, the result of a novel H1N1 influenza virus, is estimated to have killed 50-100 million people, most by secondary bacterial pneumonia (Banerjee et al., 2013; Johnson and Mueller, 2002; Taubenberger et al., 2001). This was followed by the 1957 H2N2 Asian Flu which resulted in the death of ~2 million people and introduced H2N2 influenza into the human population. This virus was a result of a reassortment event between human and avian influenza viruses; it contained HA, NA, and PB1 genes of avian origin (Colman, 1994; Kawaoka et al., 1989; Schäfer et al., 1993; Scholtissek et al., 1978b). This was followed by the 1968 H3N2 Hong Kong Flu which caused ~1 million deaths. This virus contained the HA and PB1 genes from Eurasian avian influenza viruses (Connor et al., 1994; Kawaoka et al., 1989; Scholtissek et al., 1978b). In 1977 H1N1 influenza was re-introduced into the human population when a 1950s-like virus was accidently released from a Russian lab, resulting in the Russian flu (Kendal et al., 1978; Scholtissek et al., 1978a; Webster et al., 1992). This virus predominantly affected children (under 25), as those over 25 had pre-existing immunity (Kilbourne, 2006).

In 2009, a new strain of H1N1 emerged in Mexico and spread rapidly, causing the 2009 H1N1 Swine Flu Pandemic (A(H1N1)pmd09).

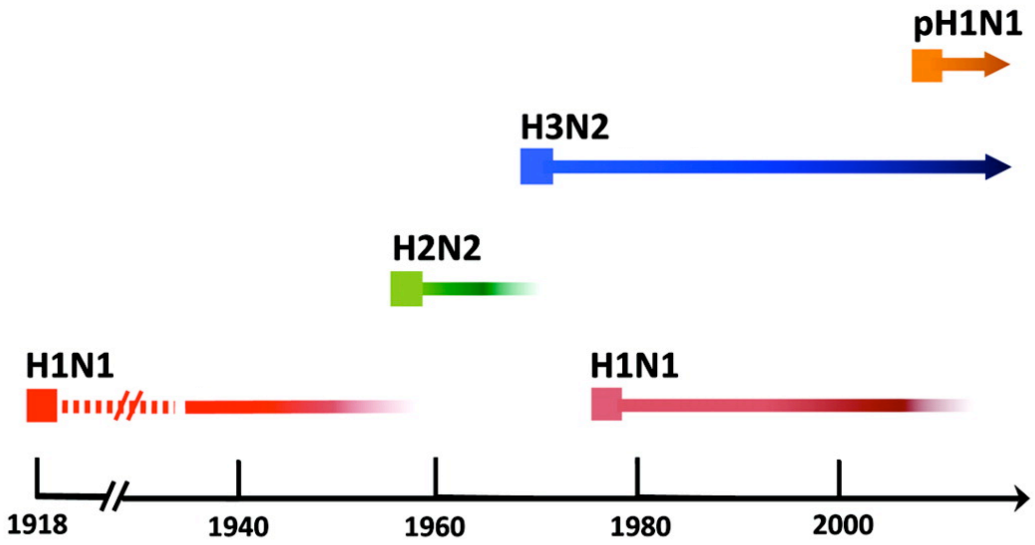

Figure I-9. Timeline of Influenza pandemics and circulating strains. H1N1 (red) circulated in the human population beginning with the 1918 H1N1 Spanish Flu. It was replaced by H2N2 (green) during the 1957 Hong Kong Flu. In 1968 the H3N2 Asian Flu (blue) began circulating in the human population. In 1977, H1N1 (pink) was reintroduced into the human population with the Russian Flu, and circulated along with H3N2. In 2009 the H1N1 Swine Flu (orange) occurred, this virus replaced the previously circulating H1N1 strains. Figure adapted from (Palese and Wang, 2011; Weis et al., 1988).

This virus was the result of genes from a Eurasian avian virus (NA (N1) and M) reassorting with a known triple reassortant virus, containing genes of North American avian virus origin (PB2 and PA); H3N2 virus origin (PB1); and classic swine virus origin (HA (H1), NP, and NS) (Dawood et al., 2009; Garten et al., 2009; Smith et al., 2009).

Avian influenza

Avian influenza viruses can be transmitted from wild waterfowl, the natural reservoir of the influenza A virus, to domestic poultry through the fecal oral route (Webster et al., 1992). Avian influenza in domestic poultry and the culling of poultry has had a large economic impact throughout the world.

There have been isolated cases of direct transmission of avian influenza to humans; avian influenza viruses including H7N7, H5N1, H9N2, H7N9, H10N8, H6N1, H7N3, and H7N2 have been isolated from humans (Chen et al., 2014; Claas et al., 1998; Fouchier et al., 2004; Gao et al., 2013; Koopmans et al., 2004; Ostrowsky et al., 2012; Tweed et al., 2004; Yuan et al., 2013). These viruses are not currently transmissible in humans, however they do meet the other criteria for a pandemic virus; novel viruses to which the human population has little to no preexisting immunity, and the ability to cause illness in humans (Poland et al., 2007).

H5N1

The first reported human case of H5N1 influenza virus occurred in Hong Kong in 1997 (Claas et al., 1998; Class et al., 1998; Subbarao et al., 1998). Since 1997, H5N1 has spread infecting ~850 people and resulting in a 50% mortality rate

(WHO, 2016). The virus is usually transmitted to humans by close contact with infected poultry or with a contaminated environment (Ungchusak et al., 2005). The virus is not currently transmissible between humans, in part due to the receptor specificity of the virus, but clusters of human cases have been reported (Kandun et al., 2006; Ungchusak et al., 2005; Wang et al., 2008).

H5N1 causes a slightly different disease than the currently circulating seasonal H1N1 and H3N2 viruses. The incubation period for H5N1 is longer (2-8 days) and it attacks the lower respiratory system, as opposed to the upper respiratory system in seasonal influenza infections. H5N1 begins with symptoms similar to seasonal influenza including, fever, cough, sore throat, nasal congestion, followed by diarrhea and vomiting. However, it then progresses to pneumonia, respiratory failure, multiple organ failure, and death (WHO, 2014b).

Pandemic potential and respiratory droplet transmissible H5N1

As stated above, the three elements needed for a pandemic are a novel virus, the capacity to transmit efficiently in humans, and the ability to cause illness in humans. H5N1 is a novel virus capable of causing illness in humans. And recent studies have shown few mutations are necessary for airborne transmission of the virus in ferrets (Herfst et al., 2012; Imai et al., 2012).

In these studies two different H5N1 strains were serially passaged in ferrets, and the groups were able to isolate respiratory droplet transmissible (*rdt*) H5N1 virus. The H5 mutants from A/Vietnam/1203/2004 (N158D, N224K, Q226L and T318I, H3 numbering; VN/1203) and A/Indonesia/05/2005 (H110Y, T160A, Q226L and G228S) indicated that very few mutations in HA are necessary for airborne transmission (Herfst et al., 2012; Imai et al., 2012). While these mutations did not change the preference of the HAs to human-type receptors, as seen in

pandemic influenza strains (1918, 1956, 1968, 2009), the affinity for human type receptors was slightly increased (de Vries et al., 2014; Xiong et al., 2013; Zhang et al., 2013).

Further studies have identified alterations in the H5 RBS necessary to change receptor preference, they are similar to those in the *rdt* VN/1203 strain, mutation of residues in the 220 loop (K224, Q226), removal of a glycosylation site at 158, extension in 190 helix, and deletion of 133a in the 130 loop (Tharakaraman et al., 2013; Zhu et al., 2015). This again indicates few mutations are needed to change the receptor specificity of the virus. However, it has also been shown that several mutations in the polymerase proteins, PA, PB1, and PB2, nucleoprotein, and nuclear export protein are needed to enhance viral replication in mammals (Mänz et al., 2013).

Neutralizing antibodies against influenza

Antibodies that bind influenza HA, NA, NP, and M2 have been isolated (Cretescu et al., 1978; Gerhard, 1976; Potter and Oxford, 1979). However, only anti-HA and NA antibodies are neutralizing (Couch and Kasel, 1983; Epstein et al., 1993). The antibodies can be involved in non-neutralizing functions, including complement-mediated lysis, phagocytosis, and antibody-dependent cell cytotoxicity (ADCC) (Hashimoto et al., 1983; Huber et al., 2001; Jegaskanda et al., 2013; O'Brien et al., 2011).

Neutralizing NA antibodies prevent the release of the new virus, therefore preventing the spread of the virus (Couch et al., 1974; Kilbourne et al., 1968; Powers et al., 1996). While, neutralizing HA antibodies bind either to the head or stem domain of HA, and prevent attachment, viral membrane fusion, release of

virion progeny from infected cells, or promote ADCC. Many neutralizing HA antibodies have been structurally characterized using X-ray crystallography, these antibodies will be discussed further.

Antibodies that recognize the HA head

The main target of antibodies elicited following vaccination is the immunedominant HA head domain. Five antigenic regions have been described using mouse monoclonal antibodies for the H1 (Sa, Sb, Ca1, Ca2, and Cb) and H3 (A-E) subtypes (Caton et al., 1982; Wiley et al., 1981). These sites are hypervariable and accumulate mutations that help avoid detection by the immune system. In contrast, the RBS, surrounded by the 130-loop, 150-loop, 190-helix, and 220-loop, is highly conserved. The footprint of an antibody is typically larger than the RBS; therefore antibody will also contact the hypervariable regions surrounding the RBS, which can lead to antibody escape mutants.

There are two groups of structurally characterized antibodies that bind outside the RBS. The first blocks receptor binding, either due to proximity of the epitope to the RBS (Thornburg et al., 2016) or by blocking receptor binding with the antibody Fc by steric hindrance (Xiong et al., 2015). The second group binds epitopes below the RBS and blocks viral membrane fusion (Iba et al., 2014; Zhu et al., 2013) (Figure I-10, H5M9).

Two groups of structurally characterized antibodies block attachment through interactions with the RBS. The first group of antibodies inserts CDRH3, which contains an aspartic acid, into the RBS and molecularly mimics the interactions between the HA RBS and the carboxylate group of the influenza receptor, sialic acid (Barbey-Martin et al., 2002; Bizebard et al., 1995; Hong et al., 2013; Lee et al., 2014; Schmidt et al., 2013; Whittle et al., 2011; Xu et al., 2010;

Zuo et al., 2015). This trend suggests the presence of the aspartic acid mimicking the carboxylate group in sialic acid is indicative of a broadly neutralizing antibody (Lee et al., 2014).

The second group of antibodies directed against the RBS contains hydrophobic residues in the H-CDR inserted into the hydrophobic pocket of the RBS, formed by the conserved Trp 153 and Leu 194, which interact with the acetimide moiety of SA (Figure I-10) (Corti et al., 2011; Ekiert et al., 2012; Lee et al., 2012; Xu et al., 2013). This group includes the antibodies 2G1 and 8M2, which insert CDRH2 into the HA RBS mediated by hydrophobic interactions (Xu et al., 2013). Both 2G1 and 8M2 are encoded by IGHV1-69, which encodes a hydrophobic CDRH2, and insert the germ line encoded Phe154 into the RBS, forming hydrophobic contacts with the hydrophobic floor of the RBS.

For some HA RBS-directed antibodies, the affinity of the Fab for HA is enhanced through avidity (Ekiert et al., 2012; Hong et al., 2013; Lee et al., 2012). The Fabs of these broadly neutralizing antibodies have intermediate affinity to accommodate the variability around the RBS, which is rescued by binding of the full-length IgG.

Antibodies that recognize the HA stem

Antibodies that neutralize influenza through interactions with the HA stem domain do so by inhibiting the HA pH-induced conformational change that occurs in the endosome, block host proteases from cleaving HA0, prevent viral egress, or promote ADCC (Corti et al., 2011; DiLillo et al., 2014; Dreyfus et al., 2012; Ekiert et al., 2011). The first HA stem binding antibody, C179, was identified in 1993 as a murine antibody and neutralizes H1, H2, H5, and H6 viruses (Dreyfus et al., 2013; Okuno et al., 1993).

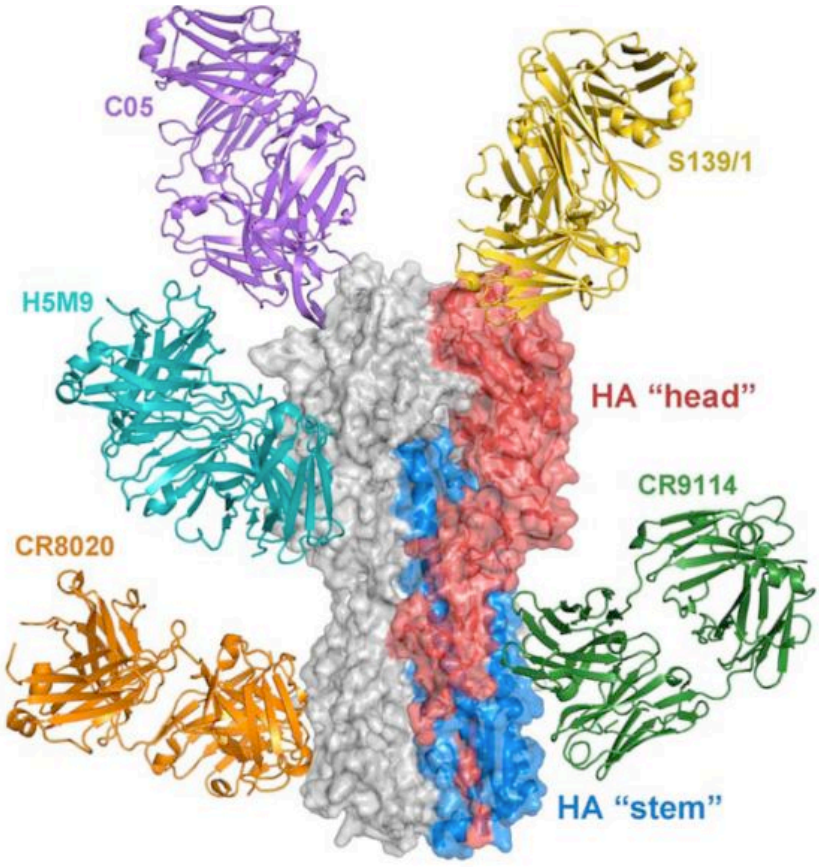

Figure 1-10. Broadly neutralizing antibodies bound to influenza HA. Broadly neutralizing influenza antibodies modeled onto A/Hong Kong/1/1968 (H3N2) HA shown as a surface model with one protomer colored for clarity; HA1, red; HA2, blue. Figure from (Lee and Wilson, 2015)

The HA stem binding antibodies can be organized by the HA group they neutralize, Group 1 HAs (Dreyfus et al., 2013; Ekiert et al., 2009; Sui et al., 2009), Group 2 HAs (Ekiert et al., 2011; Friesen et al., 2014), and pan-Influenza A and B (Corti et al., 2011; Dreyfus et al., 2012). A number of HA stem directed antibodies use the VH1-69 gene segment, which encodes a hydrophobic CDRH2 that inserts into a hydrophobic pocket on the HA stem (Dreyfus et al., 2012; Ekiert et al., 2009; Sui et al., 2009).

The highly conserved epitopes on the HA stem domain which are essential for fusion are an attractive target for structure-based vaccine design.

H5N1 specific antibodies

H5N1-specific antibodies were isolated from subjects in a phase I clinical trial of an experimental H5N1 vaccine, containing the HA and NA glycoproteins from A/Vietnam/1203/2004 (H5N1) influenza strain (Bernstein et al., 2008; Thornburg et al., 2013). The antibodies were characterized by testing the ability of the antibodies to bind 7 H5s from different H5N1 strains, hemagglutination inhibition activity, and capacity to neutralize VN/1203 H5N1 influenza (Table I-1). We were interested in structurally characterizing an antibody that binds the H5 head domain, and chose H5.3 to study further.

Table I-1. Binding of human mAbs to HAs from different H5N1 virus *wt* field strains.

Domain/ mAb		EC_{50} for binding to HA of indicated H5N1 strain (ng/ml)							Neut IC_{50} (µg/ml)
		Wild-type H5N1 field strain							
		VN/ 1203	Indo	Anhui	Egypt	BHG	HK/ 156	HK/ 213	VN/ 1203
Head	H5.2	106	325	143	22	1140	14	157	0.07
	H5.3	17	10,000	2,780	>	>	18	>	0.02
	H5.9	200	1,800	376	178	16	22	61	0.04
	H5.13	660	19,900	119	16	>	63	>	0.04
	H5.31	44	>	83	201	>	28	>	0.2
Stem	H5.7	79	156	134	12,800	518	109	275	5
n.d.	H5.36	31	34	32	36	37	27	53	2.5

Field strain HAs used were from A/Vietnam/1203/2004, clade 1.1 (“VN/1203”), A/Indonesia/05/2005, clade 2.1.3.2 (“Indo”), A/Anhui/1/2005, clade 2.3.4 (“Anhui”), A/Egypt/3300-NAMRU3/2008 (“Egypt”), A/bar-headed goose/Qinghai/1A/2005, clade 2.2.1.1 (“BHG”), A/Hong Kong/156/1997, clade 0 (“HK/156”), A/HK/213/2003, clade 0
(“HK/213”).

> indicates a value of ≥ 50,000 was assigned when the curve did not reach a maximum within the limits of the assay.

n.d. indicates domain not determined because of complex results in the functional mapping experiments.

Table adapted from (Thornburg et al., 2013).

Research Objective

Since 2003, ~850 people have been infected with H5N1, through direct or indirect contact with infected poultry, resulting in a ~50% mortality rate (WHO, 2016). Currently this virus cannot be directly transmitted between humans, though it is a novel virus, capable of causing illness in the immunologically naïve human population, meeting two of the three elements for a pandemic virus (Poland et al., 2007). Recent studies have shown very few mutations may be necessary for efficient human-to-human transmission of the virus (Herfst et al., 2012; Imai et al., 2012). The current best method for prevention of influenza pandemics is vaccination. The antibody H5.3 was isolated from a subject in an experimental H5N1 vaccine trial and characterized as a potent and specific antibody (Thornburg et al., 2013). My goal for this project was to determine molecular mechanism H5.3 uses to neutralize H5N1 influenza and examine the affinity maturation of H5.3.

I have shown H5.3 neutralizes H5N1 by binding an epitope on H5 encompassing the highly conserved RBS and polymorphic residues on the periphery, indicating the breadth and potency of the antibody conflict due to variability outside the RBS. I have shown H5.3 binds respiratory droplet transmission VN/1203 H5 in the same manner as it binds wild type HA, indicating receptor specificity may not be critically important for vaccine development. I have shown H5.3 and other H5-specific antibodies isolated from the experimental H5N1 vaccine trial have fewer somatic mutations than broadly neutralizing influenza antibodies, suggesting the vaccine elicited a naïve B cell response. Finally I have demonstrated the H5.3 somatic mutations do not have large effect on increasing the affinity of H5.3 for H5 and do not stabilize the protein conformation, as it

remains flexible after affinity maturation, indicating the somatic mutations may have another function.

CHAPTER II

EXPRESSION AND PURIFICATION OF A/VIETNAM/1203/2004 H5 HEAD DOMAIN FROM *ESCHERICHIA COLI* INTO ITS NATIVE IMMUNOGENIC STRUCTURE

Introduction

Influenza is a worldwide health concern, causing the death of between 250,000-500,000 people each year (WHO, 2014a). Influenza pandemics occur when a novel influenza virus acquires the ability to transmit efficiently and cause illness in the immunologically naïve human population (Poland et al., 2007). Since 2003, there have been ~850 humans cases of the avian influenza virus, H5N1, instances of direct transmission from birds to humans, resulting in a ~50% mortality rate (WHO, 2016). This virus cannot currently be transmitted efficiently between humans, due in part to the receptor specificity of the virus.

The surface glycoprotein hemagglutinin (HA) is responsible for attachment and entry of the virus into the host cell. The HA globular head domain is the primary target of the humoral immune response and contains the conformation-specific antigenic sites (Caton et al., 1982; Stevens et al., 2006a; Wiley et al., 1981).

HAs for structural studies are typically produced using mammalian cell culture or baculovirus infected insect cell expression. These methods offer the advantages of properly folding the protein and the ability to add post-translational modifications (i.e., glycosylation). However, these methods can also lead to heterogeneous glycosylation. An alternative method is the cheaper and faster bacterial expression of HA, and although the protein is not soluble, it can be

refolded. Bacterially-expressed HA head domain can be properly folded, bind conformation specific monoclonal antibodies, and is capable of eliciting an immune response in mice and ferrets (Aguilar-Yáñez et al., 2010; Biesova et al., 2009; Chiu et al., 2009; Song et al., 2008b). Immunogenic viral proteins from other viruses, including rotavirus, vaccinia, and orthopoxvirus, have been successfully purified from bacteria, are able to bind human monoclonal antibodies (mAbs), used as a vaccine, and elicited an immune response in mice (Aiyegbo et al., 2013a; 2013b; Berhanu et al., 2008; Fang et al., 2006).

Here, I present the expression and purification of the A/Vietnam/1203/2004 (H5N1) (VN/1203) H5 head domain (H5hd) in bacteria. I have shown the H5hd folds properly, binds VN/1203 H5-specific mAbs, and have identified a set of H5hd constructs that will be useful in future crystallization studies. Additionally, I have determined the x-ray crystallographic structure of one these Fabs, H5.3.

Materials and Methods

Cloning H5 head domain into pET28a

The VN/1203 H5 head domain was subcloned into the pET28a expression vector with an N-terminal 6x-His tag and a thrombin cleavage site. Additional H5 head domain constructs were generated in pET28a by PCR-based mutagenesis and verified by nucleotide sequencing.

HA expression and purification

The plasmid was transformed into BL21 (DE3) *E. coli* cells. The proteins were expressed in BL21 (DE3) cells grown in LB medium at 37 °C to an optical density (at 600 nm) of 0.6 and were induced with 0.1 mM isopropyl β-D-

thiogalactopyranoside for 12 h at 20 °C. Bacteria were harvested by centrifugation and lysed with a French press in 1xPBS with ~1 µg/mL hen egg white lysozyme, ~1 µg/mL DNase I, 10 µg/mL leupeptin, 1 mM PMSF, and 0.7 µg/mL pepstatin. The lysate was clarified by centrifugation and the insoluble fraction was resuspended in 8 M urea, 50 mM Tris, pH 8, and purified by Co-NTA affinity using TALON resin. The protein was refolded overnight by rapid dilution (10 mL into 200 mL) into 1 M arginine, 10 mM Tris, pH 7.5, 0.5 mM reduced glutathione, 0.05 mM oxidized glutathione, followed by dialysis against 150 mM NaCl, 10 mM Tris, pH 7.5, for 24 h, and centrifugal concentration. The 6x-His tag was removed using thrombin, followed by gel filtration on a 24-mL Superdex 200 (GE Healthcare) column. The final protein yield is ~20 mg/L.

H5.3 Fab purification

The variable regions of the H5.3 Fab were subcloned into Lonza Ig expression vectors (already containing constant regions). Protein was expressed by transient transfection of 293F cells (Invitrogen) according to the manufacturer's instructions, with the exception that polyethyleneimine was used as the transfection reagent as previously described (Durocher et al., 2002), instead of 293Fectin. Cells were grown for 7 days then harvested by centrifugation at 2500 x g. Supernatant was passed through a 0.45 µm membrane. The clarified supernatant was applied to a HiTrap Protein G HP column (GE Healthcare) and buffer exchanged 2x with DPBS using an Amicon Ultra centrifugal concentrator with a 10 kilodalton cutoff membrane (Millipore).

Gel filtration assays

Fab and H5hd were mixed together and incubated on ice for 20 min. The complex was then loaded onto a 24 mL Superdex S200 column (GE Healthcare) maintained in 150 mM NaCl, 10 mM Tris, pH 7.5.

Crystallization, data collection, and structure determination

H5.3 Fab crystals were grown by vapor diffusion of 21 mg/mL protein against a reservoir of 24% PEG 1500 and 20% glycerol. Crystals were frozen directly from the crystallization drops. Diffraction data were collected from single crystals at 100K at sector LS-CAT 21-ID-G at the Advance Photon Source (Argonne, IL). Data were indexed, integrated and scaled with HKL2000 (Otwinowski and Minor, 1997). Data collection statistics are given in Table II-1. Molecular replacement was performed with Molrep (Vagin and Teplyakov, 1997) by iteratively searching a library of ~250 Fab fragments. The best solution, obtained with PDB 1FGW, was identified based on the Contrast score. Side chains of this oriented model that differed from the H5.3 sequence were trimmed to alanine, and the resulting oriented model was refined in Phenix (Adams et al., 2002). Refinement included rigid body refinement of the individual domains, simulated annealing, positional, individual B-factor, and TLS. Loops were rebuilt and side chains added in COOT (Emsley and Cowtan, 2004) using simulated annealing composite omit maps (Brünger et al., 1997) generated by Phenix (Adams et al., 2002). TLS refinement (Painter and Merritt, 2006) was incorporated in the final rounds of refinement using TLS groups identified using Phenix. The refined model consists of amino acids 5-211 of the light chain, 2-223 of the heavy chain, and 188 water molecules. The final R_{factor} is 17.23%, the R_{free} is 20.31% for data between 50 and 2.25 Å. Additional data and model statistics are given in

Table II-1. The structure has been deposited in the Protein Data Bank under accession code 4GSD.

Iodoacetamide assay

The iodoacetamide assay was performed on all H5hd constructs as described in (Pecorari, 1999). Briefly, 50 mM of iodoacetamide was added to 50 mg of each H5hd construct for 15 min. LDS-PAGE sample buffer was added to stop the reaction, samples were boiled for 1 min and loaded on 12% SDS-PAGE gel. Additional controls included H5hd + sample buffer and H5hd + sample buffer + DTT. Gels were stained with SimplyBlue SafeStain and the presence of disulfide bridge species was analyzed.

Fab deglycosylation assay

The Fab deglycosylation assay was performed using PNGase F (New England BioLabs) according to manufacturer's instructions. Briefly, 20 mg of Fab was mixed with GlycoBuffer and incubated at 100°C for 10 min. GlycoBuffer, NP-40, and PNGase F were then added and the reaction was incubated at 37°C for 1 hr. LDS-PAGE sample buffer was added to each reaction, they were boiled for 10 min, and loaded on a 4-20% SDS-PAGE with control Fabs that were not exposed to PNGase F, and stained with SimplyBlue SafeStain to detect mobility shifts.

Results

Cloning, expression, purification, and refolding of VN/1203 H5hd

The initial 25 kD construct I expressed and purified, H5hd-P1, contained residues 54-268 (H3 numbering), based on the structure of the H5 ectodomain

(Figure II-1A) (Stevens et al., 2006a). It was subcloned into the pET28a expression vector, with an N-terminal 6x-His tag, under a T7 promoter (Figure II-1B). The plasmid was transformed into BL21 (DE3) *E. coli* cells, grown in LB medium at 37°C, induced with 100 mM IPTG, and grown overnight at 20°C. The bacteria was harvested by centrifugation and lysed using a French Press. The insoluble fraction was separated by centrifugation and the inclusion bodies were resuspended in 8 M Urea. The solubilized H5hd-P1 was purified by Co-NTA affinity using TALON resin in 8 M Urea, yielding ~100 mg/L of very pure H5hd-P1 (Figure II-1C).

I then refolded the protein in a 10:1 reduced to oxidized glutathione redox buffer in 1M Arginine and dialyzed the protein to remove excess Urea and Arginine. The final yield of H5hd-P1 was ~20 mg/L.

H5hd-P1 binds to human monoclonal antibodies

I verified the conformational integrity of H5hd-P1 by testing binding to VN/1203 H5-specific human monoclonal antibodies (mAbs; H5.2, H5.3, H5.13, H5.9) using gel filtration. The mAbs were isolated from subjects in an H5N1 vaccine trial, using a vaccine containing the HA and NA glycoproteins from VN/1203 H5N1. These mAbs have been characterized to bind the VN/1203 H5 head domain using a hemagglutination inhibition assay (Thornburg et al., 2013).

I mixed 100 mg of Fab with 100 µg H5hd-P1 together, when run over gel filtration the H5hd-P1 with H5.2 or H5.3 mixtures co-eluted at a faster retention time indicating complex formation (Figure II-2). However, I did not detect complex formation between H5hd-P1 and the H5.9 and H5.13 Fabs indicating that H5.9 and H5.13 recognize features not present in H5hd-P1.

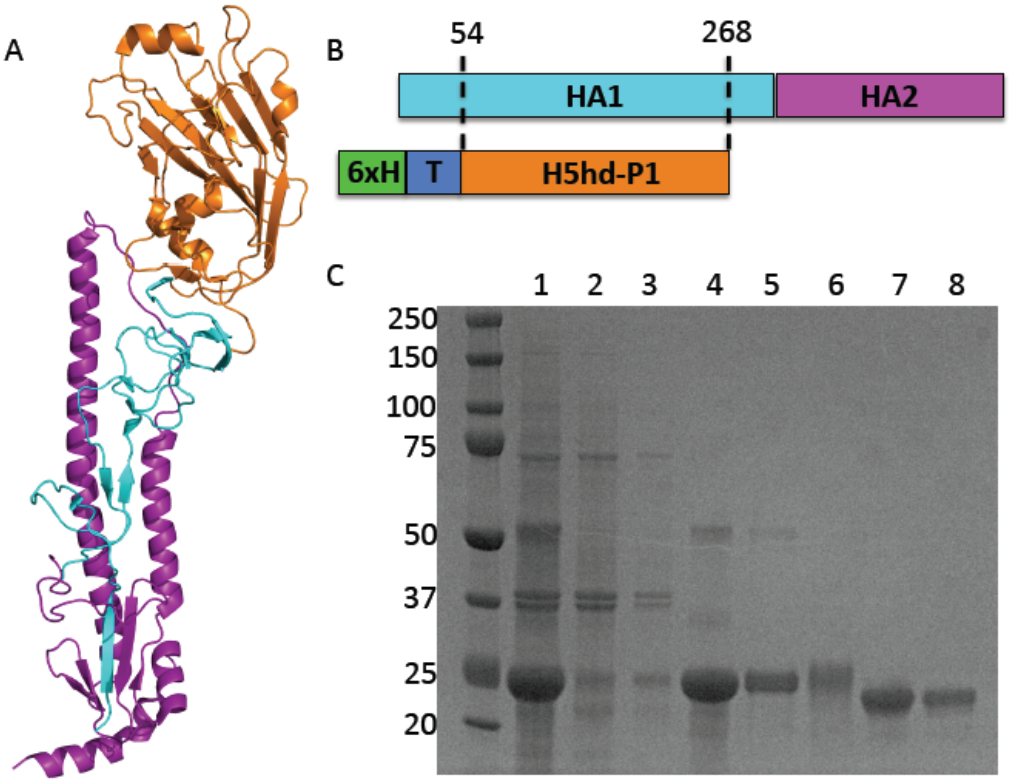

Figure II-1. H5hd construct and purification. (A) One protomer of the HA trimer with the H5hd_P1 construct highlighted in orange. Cyan, HA1; Magenta, HA2. PDB ID: 2FK0 (B) Schematic representation of H5hd-P1 construct, HA1 residues 54-268, with an N-terminal 6x His tag (6xH, green) and thrombin cleavage sequence (T, blue). (C) SDS-PAGE gel with samples from each step of the purification process, H5hd-P1 ~25kD. (1) resuspended inclusion bodies; (2) flowthrough, (3) wash, and (4) elution steps from affinity purification on Co-NTA TALON resin; (5) refolded H5hd; (6) dialyzed H5hd; (7) H5hd with 6x-His tag removed; (8) H5hd after gel filtration.

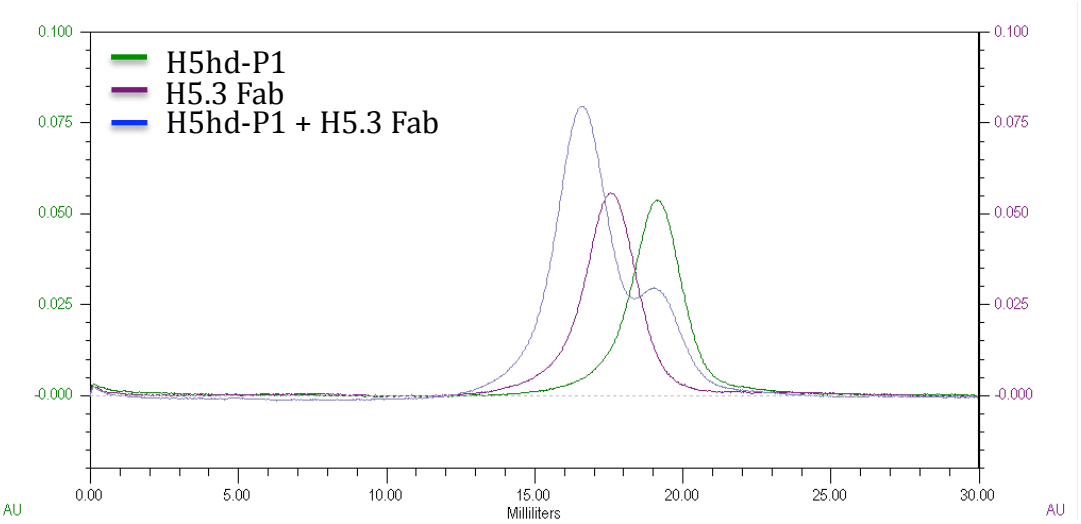

Figure II-2. H5.3 Fab binds H5hd-P1 by gel filtration. Gel filtration chromatogram showing H5hd-P1 and H5.3 Fab co-eluted, resulting in a shift when they are mixed together (blue) compared to when they are separate (H5hd-P1, green; H5.3 Fab, purple). AU, absorbance units.

Crystal Structure of H5.3 Fab

After determining H5hd-P1 is folded into its native immunogenic state, I focused my attention on determining the molecular mechanism of neutralization used by H5.3. H5.3 was chosen because it is a potent and specific neutralizing and antibody (Thornburg et al., 2013).

The recombinantly expressed H5.3 Fab H5hd-P1 complex was isolated using gel filtration, put into crystal trays, and produced crystals in many conditions. We harvested and collected diffraction data on many crystals, however we were not able to determine the structure of the H5.3 Fab H5hd-P1 complex.

All of the crystals contained only the H5.3 Fab. I have determined the x-ray crystallographic structure of the H5.3 Fab alone to 2.25 Å (PDB ID code 4GSD) (Figure II-3). Refinement and data quality statistics given in Table II-1. There is one copy of the Fab in the asymmetric unit (ASU) and it was well ordered.

New H5 head domain constructs

While I was working to obtain crystals of the H5.3 Fab H5hd-P1 complex, structures of bacterially expressed HA head domain alone (DuBois et al., 2010) and in complex with a Fab (Hong et al., 2013) were published. These structures were used as models to change the length of the current H5hd construct. The N- and C-termini of H5hd were shortened and/or lengthened (Figure II-4A). The most notable difference is the additional residues on the C-terminus of H5hd-P5 adds a disulfide bond to the construct (Stevens et al., 2006a).

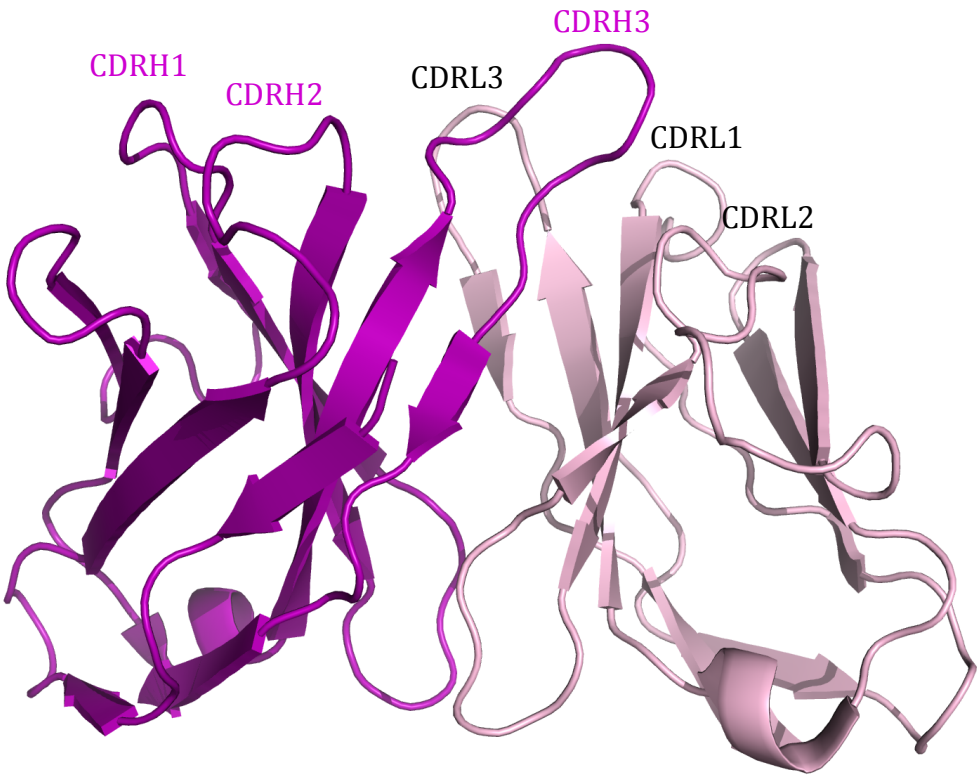

Figure II-3. Structure of H5.3 Fab. The Fv of the H5.3 Fab, with each CDR labeled. HC, magenta; LC, light pink.

Table II-1. Data collection, phasing, and refinement statistics.

Data collection	
Space group	$P6_1$
Cell dimensions	
a, b, c (Å)	150.43, 150.43, 70.517
Wavelength	0.97856
Resolution (Å)	50-2.25
Completeness (%)	50-2.25 Å: 99.7 (100)
Redundancy	50-2.25 Å: 4.4 (4.4)
I/sigmaI	50-2.25 Å: 18.3 (2.6)
Refinement	
Resolution (Å)	2.25 Å
No. reflections	43,167
No. reflections free set	2,173
R_{work} / R_{free} %	17.23/20.31
R.m.s deviations	
Bond lengths (Å)	0.008
Bond angles (°)	1.136
Ramachandran Plot	98.6% of residues in favored regions. 0 outliers.

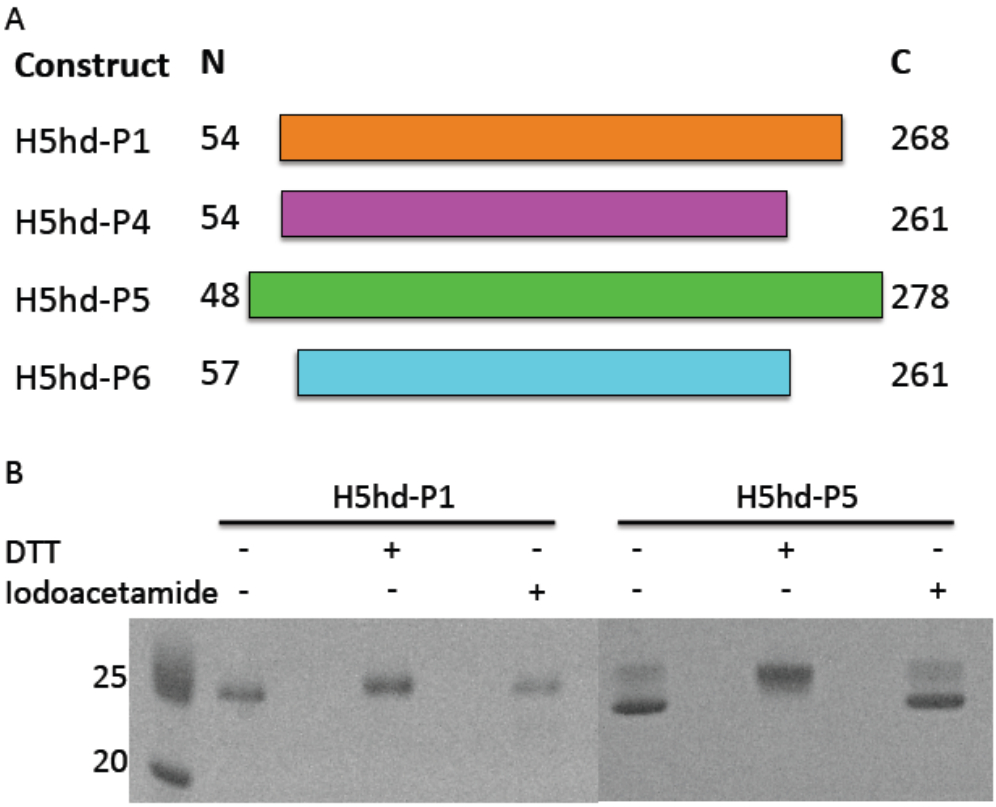

Figure II-4. H5hd constructs and Iodoacetamide assay. (A) Schematic representation of the additional H5hd constructs. (B) SDS-PAGE gels from Iodoacetamide Assays. H5hd-P1 runs as one band with and without Iodoacetamide, while H5hd-P5 runs as two bands without DTT or Iodoacetamide, indicating the disulfide bond is not always formed.

I used an iodoacetamide assay to determine if the new H5hd constructs were folded properly by assessing disulfide bond formation, as described in (Pecorari, 1999). In this assay each H5hd construct was incubated with iodoacetamide, which covalently bonds to free thiol groups on cysteine, preventing disulfide bond formation, and the reaction was then run on an SDS-PAGE gel. I found H5hd-P5 + iodoacetamide resulted in two bands (Figure II-4B). As the other constructs are present as one species, it is the additional disulfide added by the additional residues in H5hd-P5 that is not formed. This indicates the additional disulfide bond in the H5hd-P5 construct is not always formed under oxidizing conditions. Based on this information I discontinued the use of H5hd-P5.

To further characterize the new constructs I used gel filtration to show H5hd-P4 and -P6 were able to bind H5.3 Fab. Both of these constructs were chosen for inclusion in future H5.3 Fab H5hd crystallization trials.

Discussion

The results suggest the bacterially expressed H5hd refolds into its native immunogenic conformation to bind VN/1203 H5-specific human mAbs. Additionally I have determined the x-ray crystallographic structure of one mAb, H5.3, capable of binding H5hd. And I have identified H5hd constructs that may be more appropriate for H5.3 Fab H5hd complex crystallization.

I have identified a protocol for the purification and refolding of an HA head domain, involving resuspension of the insoluble H5hd in urea, affinity purification using Co-NTA in 8M urea, followed by refolding in 1M arginine in a redox buffer overnight. While previously published methods involve resuspension of inclusion bodies in different buffers, such as guanidine, or refolding the protein on the affinity

column (Aguilar-Yáñez et al., 2010; Chiu et al., 2009; DuBois et al., 2010); expressing a full-length HA1 construct (Biesova et al., 2009); or expressing an HA1-flagellin fusion construct (Song et al., 2008b).

Similar to other bacterially expressed HAs, H5hd, described here, binds HA-specific mAbs, indicating correct folding and the RBS and conformational epitopes presented correctly.

The inability to crystallize the H5.3 Fab H5hd complex using reagents described here resulted in efforts, described in chapter III, to focus on alternate sources for the H5.3 antibody. However, as described in this Chapter I have determined the structure of the H5.3 Fab alone and other HA head domain constructs expressed in bacalovirus (Ekiert et al., 2012; Schmidt et al., 2013) and bacteria (Hong et al., 2013) have been successfully crystallized in complex with a Fab. The modifications I made to the H5hd construct will lead to a stable, homogenous protein better suited for crystallization. This H5.3 Fab structure in combination with the new H5hd constructs will assist in our plans to determine the crystal structure of the H5.3 Fab H5hd complex.

All of the attempts made to produce crystals containing both recombinantly expressed H5.3 Fab (rH5.3 Fab) and H5hd-P1 were unsuccessful. However, in Chapter III, I described the structure of hybridoma produced H5.3 Fab (hH5.3 Fab) H5hd-P6 complex. As the difference between the H5hd constructs is only 10 residues and I determined the structure of unliganded H5.3 Fab, it does not seem likely the H5hd construct hindered complex crystallization.

It seems more likely the rH5.3 Fab impeded efforts to crystallize the complex for three possible reasons. (1) All of the diffraction data I collected from crystals grown in conditions containing rH5.3 Fab H5hd-P1 were in the same space group. Therefore it is possible crystal contacts in rH5.3 Fab precluded

complex crystallization. CDRH3 is “inserted” into a “pocket” on the LC constant region of a neighboring molecule (Figure II-5). However, the sequence differences between rH5.3 and hH5.3 LC constant regions are not involved in this interaction; there are four total amino acid differences in the constant regions, three in the HC (rH5.3-hH5.3, V132S, P228L, K230T) and one in the LC (R113G).

(2) There is a large difference in the elbow angles between the variable and constant regions of the unliganded rH5.3 Fab and liganded hH5.3 Fab structures (Figure II-6). This highlights the general flexibility of this region. Also studies have shown lambda light chains are more flexible due to an insertion in the switch region, making them one residue longer than kappa light chains (Stanfield et al., 2006).

(3) Fabs expressed in 293F cells run at different molecular weights (Figure II-7A). In order to test if this disparity is due to glycosylation differences, I performed a deglycosylation assay, and found the variances in molecular weight were caused by differences in glycosylation (Figure II-7B). The differences in glycosylation may have prevented complex crystallization by disrupting the interaction between rH5.3 Fab and H5hd-P1.

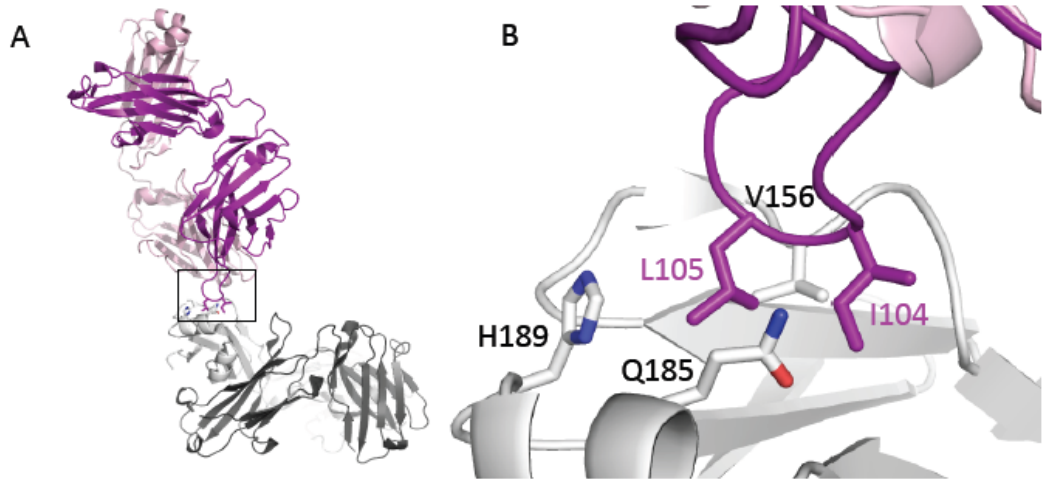

Figure II-5. Crystal contacts in rH5.3 Fab structure. (A) Two symmetry mates in the rH5.3 Fab structure. LC, light pink, white; HC, purple, grey. (B) Enlarged view of area outlined in the box in A. The CDRH3 of one copy packed against the LC constant region of another rH5.3 Fab molecule. Residues involved are labeled. Black, LC residues; magenta, HC residues.

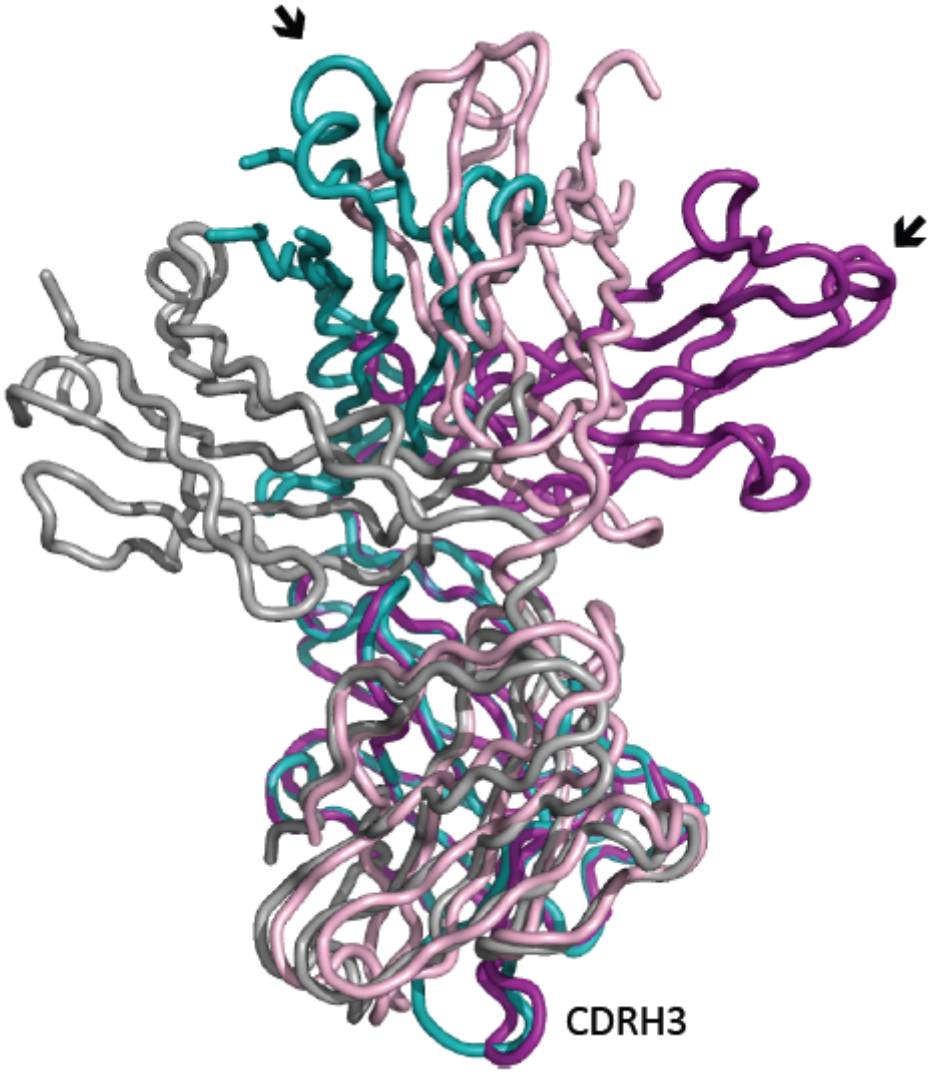

Figure II-6. Comparison of the orientation of rH5.3 and hH5.3 constant regions. Structural alignment of the Fv regions of rH5.3 and hH5.3, highlighting the flexibility of the elbow region. Arrows are pointing to the same location in each HC, T200, ~43Å apart. rH5.3, HC, purple; LC, light pink. Bound hH5.3, HC, teal; LC, grey.

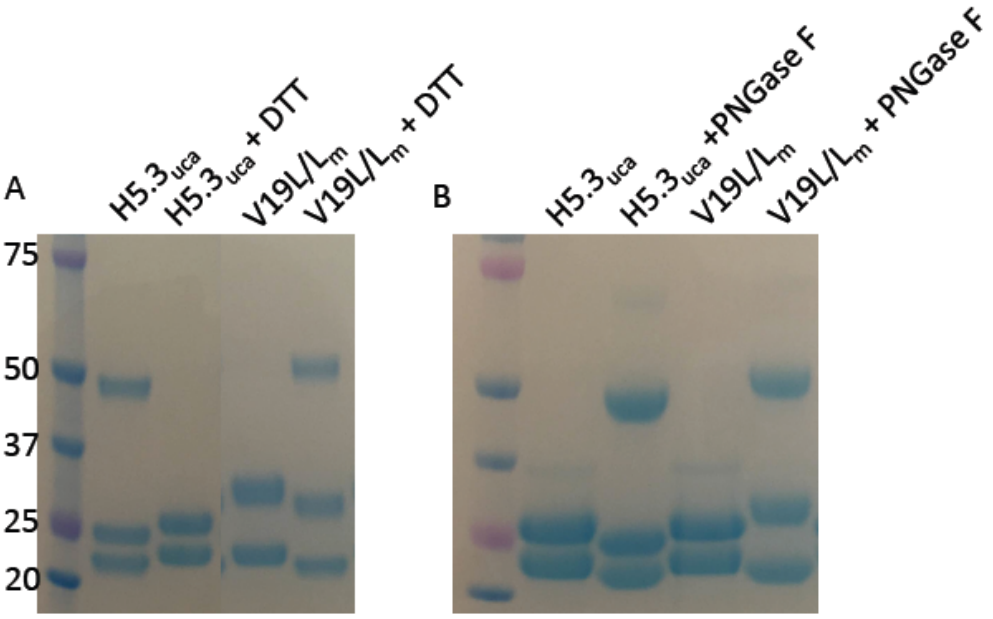

Figure II-7. Recombinant Fab expressed in 293F is differentially glycosylated. SDS-PAGE gels showing Fabs produced in 293F with and without DTT (A) and with and without PNGase F (B) showing difference in glycosylation due to expression in 293F cells. $H5.3_{uca}$, H5.3 unmutated common ancestor; $V19L/L_m$, H5.3 with V19L mutation in HC and mature LC. Standards are the same on each gel, kD. In (B) lanes without PNGase F do not have DTT; lanes with PNGase F have DTT.

CHAPTER III

VACCINE-ELICITED ANTIBODY THAT NEUTRALIZES H5N1 INFLUENZA AND VARIANTS BINDS THE RECEPTOR SITE AND POLYMORPHIC SITES

Introduction

Influenza remains a major public health concern because seasonal influenza infects 600 million to 1.1 billion people annually, resulting in 3–5 million cases of severe disease, and 250,000–500,000 deaths (WHO, 2014a). Antigenic drift of circulating seasonal influenza viruses necessitates an international vaccine effort to reduce the impact on human health. A critical feature of the seasonal vaccine is that it stimulates an already primed immune system to diversify memory B cells to recognize closely related, but antigenically distinct, influenza glycoproteins (hemagglutinins). Influenza pandemics arise when hemagglutinins to which no preexisting adaptive immunity exists acquire the capacity to infect humans. The four influenza pandemics of the 20th century, caused by novel influenza strains infecting the immunologically naive human population, resulted in 50–100 million deaths (Garten et al., 2009; Kilbourne, 2006; Lambert and Fauci, 2010; WHO, 2014a). Influenza A immunity is principally mediated by the antibody response to the viral glycoprotein, hemagglutinin (HA) (Skehel and Wiley, 2000). HA is expressed as a preprotein, HA0, assembled as a trimer on the viral envelope, and cleaved by host proteases into HA1 and HA2. HA1 is a largely globular domain responsible for receptor binding, and HA2 is a rod-shaped helical bundle responsible for membrane fusion (Fig. III-1A) (Skehel and Wiley, 2000). There are 18 genetically distinct subtypes of influenza A HA (H1–H18), of which only H1 and H3 currently circulate among humans (Knossow and Skehel, 2006;

Laursen and Wilson, 2013; Nobusawa et al., 1991; WHO, 2014a; Zhou et al., 2013).

Despite the widespread presence of H5N1 influenza viruses in wild birds, the virus is not currently transmissible within the human population. Human-to-human transmission is inefficient and is partially restricted by the receptor specificity of the virus; human-type HAs preferentially recognize α2,6-linked sialic acid whereas avian-type HAs prefer α2,3-linked sialic acid (Couceiro et al., 1993; Shinya et al., 2006; WHO, 2014a; Yamada et al., 2006). However, there have been >600 human cases of H5N1 infection since 2003, resulting from the direct transmission of the virus from birds to humans, associated with an ~60% mortality rate. There is the potential for a significant pandemic if H5 viruses develop the ability to spread efficiently between humans, which would necessitate specificity for α2,6-linked sialic acid (Garten et al., 2009; Kilbourne, 2006; Lambert and Fauci, 2010; WHO, 2014c; 2014b).

Receptor binding occurs in a shallow depression on the HA globular head domain, the edges of which are formed by four structural elements, the 190 helix and the 130, 150, and 220 loops (Fig. III-1B), and the receptor binding site (RBS) base, which includes invariant hydrophobic residues Tyr98, Trp153, and Leu194 (Skehel and Wiley, 2000; Weis et al., 1988; Xu et al., 2013). Receptor specificity is critically influenced by position 226 on HA; Gln226-containing H3 strains are specific for α2,3 sialic acid linkages, and Leu226-containing H3 strains are specific for α2,6 sialic acid linkages (Rogers et al., 1983; Skehel and Wiley, 2000).

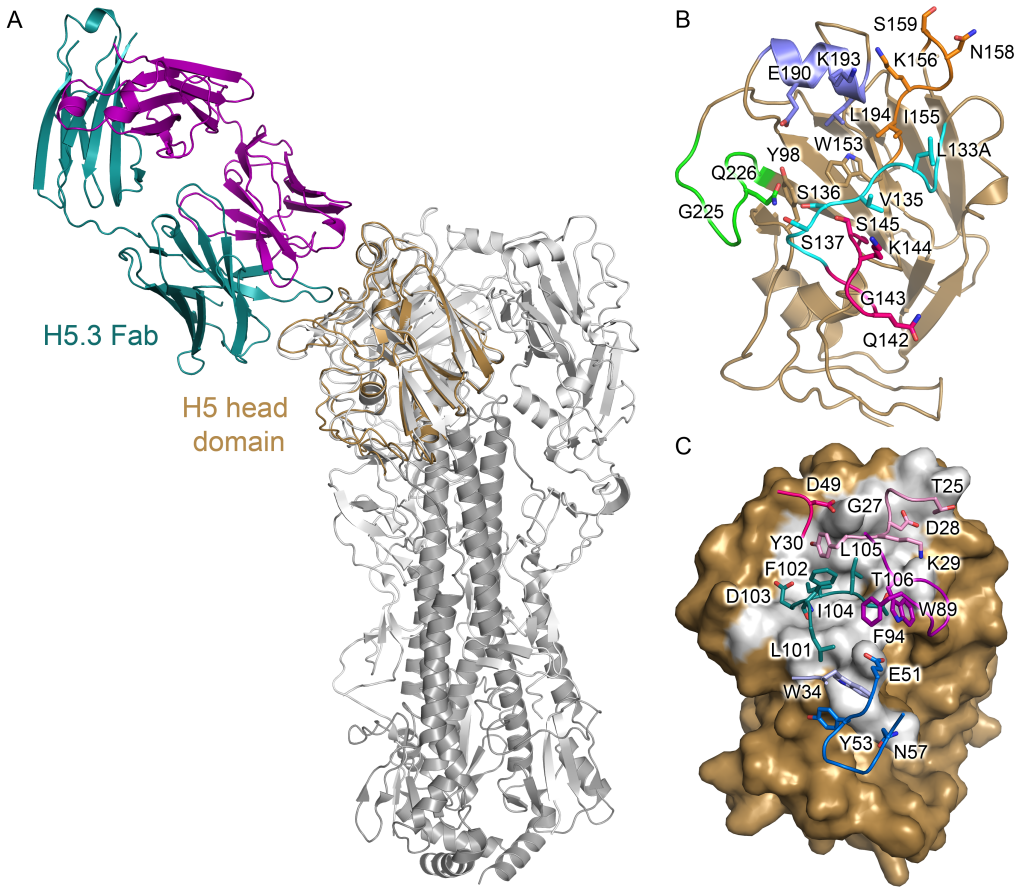

Figure III-1. Human monoclonal antibody H5.3 recognizes the H5 receptor-binding site. (A) H5.3-wt_H5hd complex overlaid on the VN/1203 H5 trimer (PDB ID code 2FK0) showing H5hd in gold, the H5.3 light chain in purple, the H5.3 heavy chain in teal, and the H5 trimer (2FK0) in gray. (B) A cartoon diagram of H5hd showing HA residues contacted by H5.3 as sticks. The structural elements of the RBS are highlighted: the 130 loop is cyan, the 140 loop is pink, the 150 loop is orange, the 190 helix is blue, and the 220 loop is green. Trp153 forms the base and denotes the approximate center of the receptor-binding site. (C) A surface representation of H5hd in the same orientation as in B, with the solvent inaccessible interface shown in gray. H5.3 contact residues are labeled and shown as sticks and colored by CDR, with CDRH1 in light blue, CDRH2 in blue, CDRH3 in teal, CDRL1 in light pink, CDRL2 in dark pink, and CDRL3 in purple.

In H5 strains, Leu226 enhances binding to α2,6-linked sialic acid receptors, but H5 viruses isolated from humans contain mutations at other sites that also promote use of α2,6-linked sialic acid receptors (Xiong et al., 2013; 2014; Yamada et al., 2006).

Recent influenza pandemics have been caused by the acquisition of mutations that change the receptor preference to α2,6 sialic acid linkages, and recent studies with multiply passaged laboratory strains indicated that only a small number of mutations are necessary to introduce preference for α2,6 linkages into H5 strains (Connor et al., 1994; Herfst et al., 2012; Imai et al., 2012; Knossow and Skehel, 2006; Laursen and Wilson, 2013; Matrosovich et al., 2000; Nobusawa et al., 1991; WHO, 2014b; Xiong et al., 2013; Zhang et al., 2013; Zhou et al., 2013). These viruses, termed respiratory droplet transmissible (*rdt*), typically have three mutations in or near the receptor binding site on HA (Herfst et al., 2012; Imai et al., 2012).

The most frequent potent neutralizing antibody response to HA arises from antibodies that target the RBS and prevent virus attachment (Skehel et al., 1982). Recent studies indicate that among RBS-directed antibodies, broad neutralization (across multiple isolates within a subtype or across subtypes) is achieved by insertion of a single complementary determining region (CDR) into the RBS to inhibit receptor binding (Laursen and Wilson, 2013). These broadly neutralizing antibodies (bnAbs) target conserved amino acids within the RBS and simultaneously avoid polymorphic sites on the ridges of the RBS. BnAbs may be relatively rare in human repertoires, and, as a consequence, current seasonal vaccine efforts focus on developing or boosting strain-specific responses to three or four currently circulating (“seasonal”) variants (Lambert and Fauci, 2010). Such strategies do not directly address the threat posed by noncirculating viruses with

pandemic potential, such as H5 strains that circulate widely in wild bird populations and sporadically infect humans where they acquire mutations that enhance binding to human receptors (Xiong et al., 2014). Instead, H5N1 vaccines against "prepandemic" strains have been developed commercially for future use in the case of a pandemic, illustrating that a prepandemic immunization program is feasible (Belshe et al., 2014; Treanor, 2014).

The immune response against H5N1 vaccines in healthy adults is less robust than for most seasonal influenza strains, typically resulting in a response restricted to the strain used in the vaccine and to closely related variants (Belshe et al., 2011; Nicholson et al., 2001; Treanor et al., 2001; 2006). Notwithstanding this observation, a recent study described panel of human anti-H5 antibodies induced in response to vaccination of volunteers with an experimental H5N1 subunit vaccine (Thornburg et al., 2013). Here, I describe the structure and characterization of a human monoclonal antibody, H5.3, bound to A/Vietnam/1203/2004 (VN/1203) H5 and to two H5 *rdt* variants. H5.3 is an RBS-directed antibody that recapitulates many of the electrostatic interactions of the natural receptor, sialic acid, as well as forming additional interactions to the periphery of the RBS that provide specificity. H5.3 is potent and specific despite containing only 11 mutations from its unmutated common ancestor (UCA) and maintaining the structural flexibility typically associated with unmutated antibodies, as evidenced by significant rearrangement of CDRH3 and CDRL3. The structures determined here offer a chemical explanation for the evident trade-off between breadth and potency, and the germ-line characteristics highlight the role of lightly mutated antibodies in neutralization of new viral strains.

Material and Methods

Expression and Purification of H5.3 Fab

The H5.3 hybridoma cell line was generated as previously reported (Thornburg et al., 2016). Briefly, the H5.3 expressing hybridoma cell line was grown in serum-free medium (Life Tech), and H5.3 IgG was purified from the supernatant using Protein G resin. Purified full-length antibody was digested with papain, and H5.3 Fab fragments were purified using Protein A resin. The Fab was concentrated and stored at −80 °C until needed.

Expression and Purification of HA

The proteins were expressed in BL21 (DE3) cells grown in LB medium at 37 °C to an optical density (at 600 nm) of 0.6 and were induced with 0.1 mM isopropyl β-D-thiogalactopyranoside for 12 h at 20 °C. Bacteria were harvested by centrifugation and lysed with a French press in PBS with ~1 μg/mL hen egg white lysozyme, ~1 μg/mL DNase I, 10 μg/mL leupeptin, 1 mM PMSF, and 0.7 μg/mL pepstatin. The lysate was clarified by centrifugation, and the insoluble fraction was resuspended in 8 M urea, 50 mM Tris, pH 8, and purified by Co-NTA affinity using TALON resin. The protein was refolded overnight by rapid dilution (10 mL into 200 mL) into 1 M arginine, 10 mM Tris, pH 7.5, 0.5 mM reduced glutathione, 0.05 mM oxidized glutathione, followed by dialysis against 150 mM NaCl, 10 mM Tris, pH 7.5, for 24 h, and centrifugal concentration. The 6x-His tag was removed using thrombin, followed by gel filtration on a 24-mL Superdex 200 (GE Healthcare) column. Biotinylated H5hd was prepared the same as H5hd, with the following modifications: a BirA tag (GGGLNDIFEAQKIEQHE) was introduced at the carboxyl

terminus by PCR, and the purified, refolded protein was labeled with *Escherichia coli* biotin ligase following standard protocols (Howarth and Ting, 2008).

Crystallization

The H5.3 Fab was mixed with excess H5hd, and the complex was isolated by gel filtration on a Superdex 200 column maintained in 150 mM NaCl, 10 mM Tris, pH 7.5. The complex was concentrated to ~10 mg/mL and immediately used for crystallization trials in sitting drop vapor diffusion trays. H5.3-H5hd crystals were grown from a reservoir containing 100 mM Hepes, pH 7.5, 20% (wt/vol) PEG 10,000. H5.3-H5hd_*rdt*_In crystals were grown from 200 mM ammonium sulfate, 100 mM Hepes, pH 7.5, 25% (wt/vol) PEG 3350. H5.3-H5hd_*rdt*_Vn crystals were grown from 200 mM sodium malonate, pH 7, 20% (wt/vol) PEG 3350. After 3–10 d, crystals were cryoprotected with a solution containing the reservoir solution with 2% (wt/ vol) additional PEG and 15% (wt/vol) glycerol, harvested onto nylon loops, and flash cooled in liquid nitrogen.

Data Collection and Structure Determination

Diffraction data were collected from single crystals at 100 K at LS-CAT Sector 21 at the Advance Photon Source (Argonne, IL). Data were indexed, integrated, and scaled with either HKL2000 (H5.3-H5hd and H5.3- H5hd_*rdt*_Vn) or XDS and Scala as called from xia2 (H5.3- H5hd_*rdt*_In) (Evans, 2006; Kabsch, 2010a; 2010b; Otwinowski and Minor, 1997; Sauter et al., 2004; Winter, 2010). Data collection statistics are given in Table III-1. Molecular replacement was performed with Molrep (Vagin and Teplyakov, 1997) by iteratively searching a library of Fab fragments. A solution, obtained with PDB ID code 1IGI, was used in

Phaser (McCoy et al., 2005) to locate the head domain of 2FK0. The variable and constant domains of H5.3 (PDB ID code 4GSD) were aligned individually to the molecular replacement solution, and residues that differed between the recombinant H5.3 structure (the initial structure of H5.3 was determined using a recombinant protein) and the hybridoma-derived H5.3 were mutated to alanine, and the resulting model was refined in Phenix (Adams et al., 2002). The sequence of H5.3 variable regions has been described (Thornburg et al., 2013). Germline gene-encoded antibody constant region sequences IGLC1*02 and IGHG1*03 were used for the light or heavy chain constant regions, respectively. An additional two residues, observed at the amino terminus of the light chain in all structures, were modeled as Y and E. Refinement included rigid body refinement of the individual domains, simulated annealing, positional refinement, individual B-factor refinement, and translation/libration/screw (TLS) refinement. Loops were rebuilt and side chains added in COOT (Emsley and Cowtan, 2004) using simulated annealing composite omit maps (Brünger et al., 1997) generated by Phenix (Adams et al., 2002). TLS refinement (Painter and Merritt, 2006) was incorporated in the final rounds of refinement using TLS groups identified using Phenix. N-linked glycans were placed in the final rounds of refinement. Data and model statistics are given in Table III-1. The structures have been deposited in the Protein Data Bank under accession codes 4XNM (H5.3-H5hd), 4XNQ (H5.3-H5hd_*rdt*_Vn), and 4XRC (H5.3-H5hd_*rdt*_In).

Biosensor Assays

Affinity measurements were performed using Fab fragments and biotinylated H5hd on an Octet interferometry instrument (ForteBio) with streptavidin biosensors (Fortebio 18-5019). HA and Fab were diluted in 1× kinetics

buffer (Forte bio, 18-5032) with PBS. Fabs were diluted to 100 nM, 50 nM, 25 nM, 12.5 nm, 7.5 nM, and 3.6 nM. Tips were equilibrated in 1× kinetics buffer for 60 s, HA was immobilized on biosensors for 120 s, baselines were established in 1× kinetics buffer for 60 s, and dilutions of H5.3 Fab were used for 180-s association curves, and 180-s 1× kinetic buffer dissociation curves. The data were analyzed with ForteBio data analysis software version 7.1. Briefly, the y-axis was aligned to baseline, and data were processed with Savitzky–Galay filtering. Affinities were calculated by doing curve fits of association and dissociations with a 1:1 binding model and local fitting of the full curves. All R^2 were greater than 0.98 and X^2 were less than 0.25.

Results

Structure of H5.3:H5hd Complexes

As described in Chapter II, I was unable to determine the structure of the H5.3 Fab H5hd complex using recombinantly expressed H5.3 Fab. I determined the crystal structure of a human monoclonal antibody Fab, H5.3, in complex with VN/1203 H5 head domain (H5hd, PDB ID code 4XNM) to 2.5 Å, using H5.3 Fab produced in hybridoma cells and digested with papain (Fig. III-1). I also determined the structures of H5.3 in complex with H5hd containing the *rdt* mutations from the Kawaoka (H5hd_*rdt*_Vn, PDB ID code 4XNQ) and Fouchier (H5hd_*rdt*_In, PDB ID code 4XRC) laboratory strains to 2.15 Å and 2.74 Å, respectively (Xiong et al., 2013; Zhang et al., 2013). Refinement and data quality statistics are given in Table III-1.

Table III-1 Data collection, phasing, and refinement statistics

	H5.3-H5hd	H5.3-H5hd-Vietnam	H5.3-H5hd-Indonesia
Data collection			
Space group	C2	C2	C2
Cell dimensions			
a, *b*, *c* (Å)	250.9, 51.4, 127.2	250.4, 51.2, 127.7	248.4, 51.1, 127.6
a, b, g (°)	90.0, 99.8, 90.0	90.0, 100.2, 90.0	90.0, 99.9, 90.0
Wavelength	0.97856	1.00394	0. 97856
Resolution (Å)[a]	2.5 (2.59-2.51)	2.15 (2.19-2.15)	2.74 (2.81-2.74)
R_{sym} [a,b]	10.9% (66%)	4.8 (60.0)	8.5 (59.8)
I / sI [a]	14.2 (1.7)	26.2 (2.4)	14.5 (2.2)
Completeness (%)[a]	97.6 (94.3)	96.9 (91.9)	99.8 (99.8)
Redundancy[a]	4.9 (3.7)	4.0(3.9)	5.1 (4.5)
Refinement			
Resolution(Å)[a]	50-2.51 (2.57-2.51)	50-2.0 (2.05-2.0)	50-2.74 (2.81-2.74)
No. reflections [a]	53,874 (3,221)	97,220 (3,778)	42,101 (2,847)
R_{work} / R_{free} [c,d]	21.4/24.6	19.7/21.1	19.7/25.1
No. atoms			
Protein	9,644	9,614	9,704
Ligand/Glycans	38	38	38
Water	85	415	102
B-factors (Å^2)			
Protein	85.8	59.7	69.2
Ligand/Glycans	110.5	87.0	107.4
Water	64.9	54.0	51.3
R.m.s deviations			
Bond lengths (Å)	0.003	0.003	0.002
Bond angles (°)	0.7	0.8	0.8
Ramachandran			
Outliers	0.08%	0.08%	0.16%
Allowed	2.27%	1.9%	1.9%
Favored	97.7%	98.1%	97.9%

[a]Parenthesis indicate outer-shell statistics .

[b]*R*sym = $\sum hkl \sum i |Ihkl,i - \langle Ihkl \rangle| / \sum hk \sum i\ Ihkl,i$ $Ihkl,i$ is the scaled intensity of the *i*th measurement of reflection *h*, *k*, *l*,.

$\langle Ihkl \rangle$ is the average intensity for reflection *I*, and *N* is the number of observations of *I.*

[c]*R*cryst = $\sum hkl\ |Fo - Fc| / \sum hkl\ |Fo|$, where *Fo* and *Fc* are the observed and calculated structure factors.

[d]*R*free was calculated as for *R*cryst, but using 5% of data, randomly chosen and excluded from refinement.

In all cases, the asymmetric unit (ASU) contained two copies of the H5.3–H5hd complex (rmsd of 0.51, 0.52, and 0.63 Å between main chain atoms of the H5hd and antibody variable regions for the two copies of *wt*, *rdt*_Vn, and *rdt*_In, respectively). Both copies of the H5.3 Fab in the ASU were well ordered in all crystals, except for residues 138–145 in the heavy chain constant region.

The H5hd, which was expressed in bacteria, was well resolved throughout the structure, except for one loop: residues 78–90 in chain C of the *wt*_H5hd, 79–82A in chain C of H5hd_*rdt*_In, and 77–82 in chain C of H5hd_*rdt*_Vn.With the exception of the poorly ordered loop, the rmsd between main chain atoms of H5hd and the trimeric ectodomain (PDB file2FK0) (Stevens et al., 2006a) was 0.76 Å. An additional loop, described below, is disordered in the H5hd_*rdt*_Vn structure.
H5.3 forms an extensive interface with H5hd, using all six CDR loops and burying ~808 $Å^2$ on H5hd and ~795 $Å^2$ on H5.3 (Fig. III-1 B and C). The interface is roughly centered on the H5 RBS. CDRH3 inserts into the highly conserved RBS, and CDRs L1, L2, L3, H1, and H2 contact variable residues on the periphery of the RBS, including the 130 loop, 150 loop, 220 loop, and 190 helix. CDRs L1 and L2 interact with the 190 helix on the rim of the RBS; and CDRs H1 and H2 interact with the 140 loop of H5hd (Fig. III-1C). The interface (~800 $Å^2$ per partner) is slightly smaller than a typical protein–protein interface, yet H5.3 is, to our knowledge, the most potent human antibody described for H5N1 strains, with a viral neutralization IC_{50} of 0.02 µg/mL and a Kd of 5 nM (for recombinant H5.3 Fab binding to recombinant HA from strain VN/1203) (Fig. III-2) (Jones and Thornton, 1996; Thornburg et al., 2013). CDRH3 is critical for this interaction, and mutations to CDRH3 abolish binding (Fig. III-2). As described in the section Recognition of H5 RDT Variants, the HA *rdt* mutations are largely outside the contact interface.

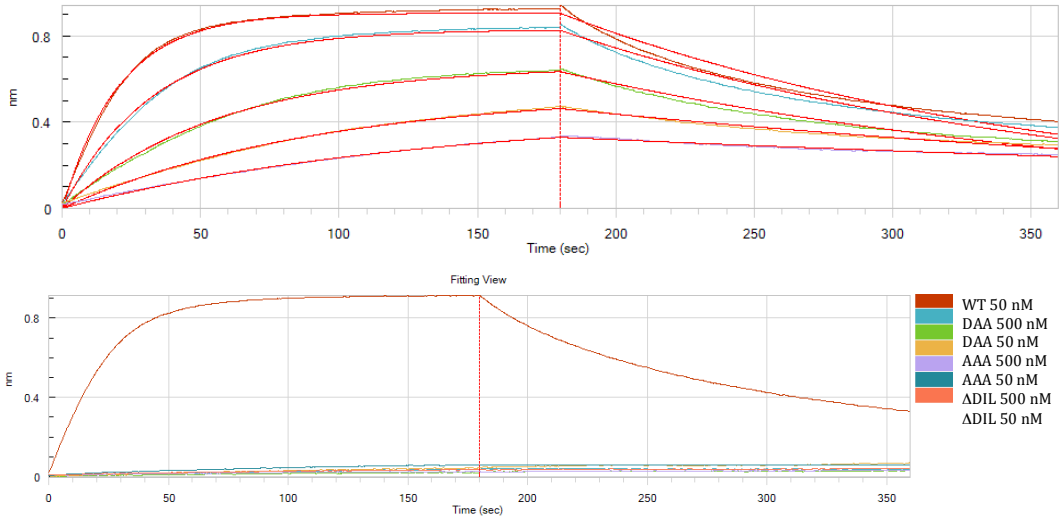

Figure III-2. H5.3-H5hd affinities. Measured on an Octet interferometry instrument. (A) These data were fit with a 1:1 binding mode, yielding apparent Kd = 8 nM. The Fab concentrations tested in this experiment were 100 nM, 50 nM, 25 nM, 12.5 nm, 7.5 nM, and 3.6 nM. (B) The WT Fab concentration tested in this experiment was 50 nM. Mutant Fabs were tested at 500 nM and 50 nM. The affinity of all mutant Fabs was bellow the limit of detection. Mutants were made in the tip of CDRH3 (D103, I104, L105). The WT residues D103/I104/L105 (DIL) insert into the receptor-binding site and are essential for binding.

Comparison with the Receptor and Other RBS-Directed Antibodies

Because the H5.3 CDRH3 inserts into the RBS, I compared the H5.3–H5hd complexes with the structure of the avian receptor analog (α2,3-SLN; 3′-sialyl-N-acetyllactosamine) bound to A/Vietnam/1194/2004 H5 (PDB ID code 4BGY) (Xiong et al., 2013) and to influenza HA-antibody complexes that similarly project CDRH3 into the RBS (PDB ID codes 3SM5, 4HKX, 4M5Z, 4O5I, 2VIR, and 1KEN) (Barbey-Martin et al., 2002; Bizebard et al., 1995; Hong et al., 2013; Lee et al., 2014; Schmidt et al., 2013; Whittle et al., 2011) (Fig. III-3). H5.3 hydrogen bonding (H-bonding) interactions replace sialic acid hydrogen bonding in the H5.3–H5hd complex (Fig. III-3 A and B), much as has been seen in other receptor mimetic antibodies, with the difference that H5.3 uses, exclusively, main chain H-bonding residues.

In H5.3, the backbone amide of Leu105 accepts a hydrogen bond from the carbonyl oxygen of HA1 Val135. The carbonyl oxygen of H5.3 Asp103 donates hydrogen bonds to the side chain hydroxyl of Ser136 and the backbone amide nitrogen of Ser137 in HA1 (Fig. III-3A). In the receptor analog, the carbonyl oxygen of Val135 accepts a hydrogen bond from the amide of the acetamide group of sialic acid, essentially the same as the interaction between H5 Val135 and H5.3 Leu105. The carboxylate group of sialic acid accepts hydrogen bonds from the side chain hydroxyl of Ser136 and the backbone amide of Ser137, similar to the interaction between these residues and the H5.3 Asp103 main chain carbonyl oxygen (Fig. III-3). In addition to this direct readout of the receptor hydrogen-bonding network, Ile104 from H5.3 contacts the hydrophobic RBS floor formed by HA1 Tyr98, Trp153, and Leu194 (Fig. III-3A).

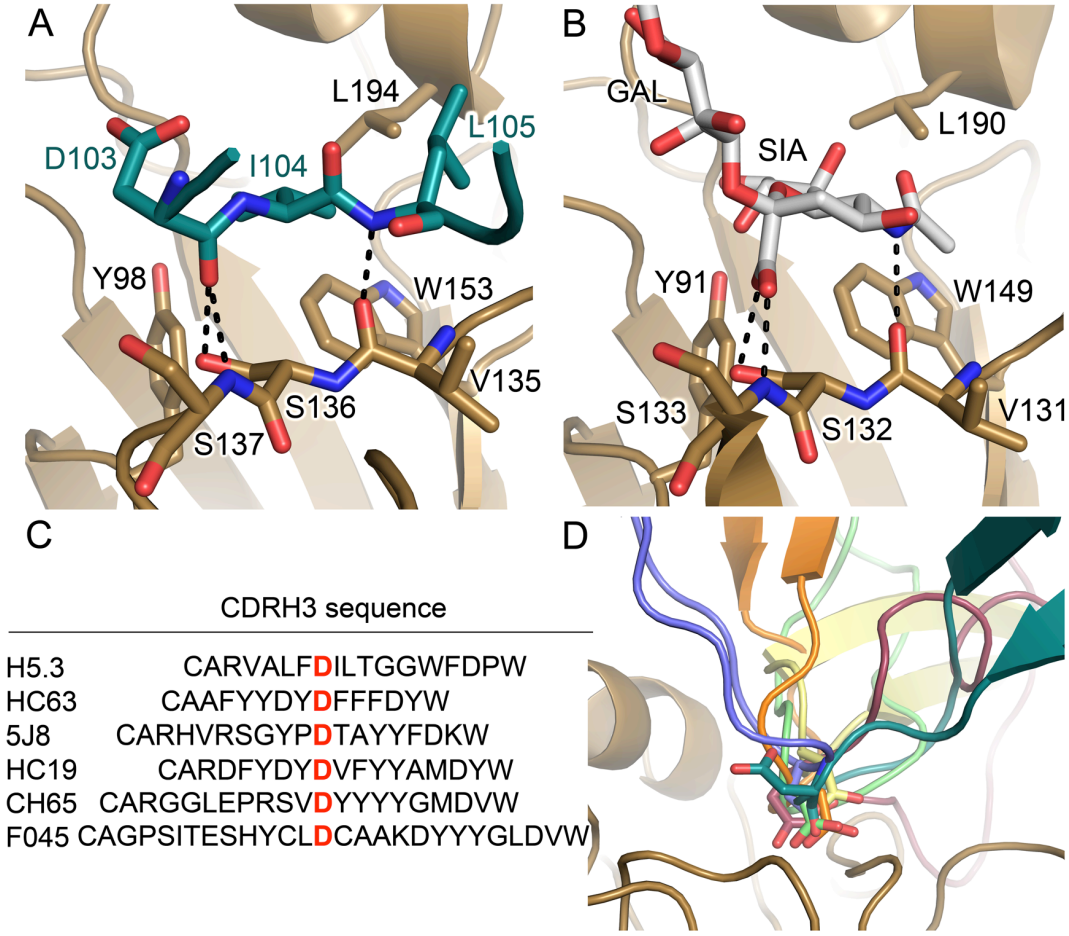

Figure III-3. H5.3 binds to the HA receptor binding site. (A and B) The CDRH3 of H5.3 (teal) is inserted into the HA (gold) receptor binding site and binds in the same location as the α2,3 sialoglycan receptor analog (PDB ID code 4BGY). The backbone of H5.3 CDRH3 forms the same pattern of hydrogen bonds with H5 as does sialic acid. Hydrogen bonds are shown as dashed black lines. (C) Sequence alignment of HA receptor-binding site targeting antibodies, highlighting the Asp at the tip of CDRH3 that often mimics the carboxylate of sialic acid. F045-092 is abbreviated as F045. (D) The Asp at the tip of the H5.3 CDRH3 (teal) is oriented away from the RBS, unlike the Asp at the tips of CDRH3 in HC63 (blue, 1KEN), 5J8 (orange, 4M5Z), HC19 (gray, 2VIR), CH65 (3SM5, green), F045-092 (4O5I, burgundy), which are inserted into the receptor binding site, mimicking the carboxylate group of sialic acid.

H5.3 recapitulates the hydrogen-bonding scheme of the α2,3-SLN receptor using only main chain antibody features. In this regard, H5.3 differs substantially from other examples of CDRH3-based RBS-directed antibodies, which use an Asp side chain to form the contacts made by the carboxylic acid of the receptor. Notably, H5.3 possesses an Asp (Asp103) on the tip of CDRH3, but this functional group is pointed away from the RBS and does not form similar contacts to the carboxylic acid in sialic acid (Fig. III-3D).

Recognition of H5 RDT Variants

H5.3 has been shown to bind H5 *rdt* variants presented in the VN/1203 background as efficiently as *wt* VN/1203 (Thornburg et al., 2013). To understand how an RBS-directed antibody is able to accommodate both human and avian receptor binding sites, I determined the structures of H5.3 in complex with two H5 *rdt* variants. Each H5N1 *rdt* virus contains three mutations in or near the RBS: Asn158Asp, Asn224Lys, Gln226Leu (H5hd_*rdt*_Vn) in the VN/1203 H5 (Imai et al., 2012) and Thr160Ala, Gln226Leu, Gly228Ser (H5hd_*rdt*_In) in the A/Indonesia/05/2005 H5 (Herfst et al., 2012). I introduced both sets of *rdt* mutations into the VN/1203 background and determined the structures of each H5 *rdt* variant in complex with H5.3 Fab to 2.15 Å and 2.74 Å, for H5.3-H5hd_*rdt*_Vn and H5.3-H5hd_*rdt*_In, respectively. Overall, both *rdt* complex structures align well with the H5.3–H5hd complex structure, and H5.3 binds the variants in the same orientation as it binds H5hd (Fig. III-4).

The most significant difference among these structures is that the 220 loop (residues 219–226 in one copy and 218–226 in the other copy in the crystallographic ASU) is disordered in H5hd_*rdt*_Vn (Fig. III-4A).

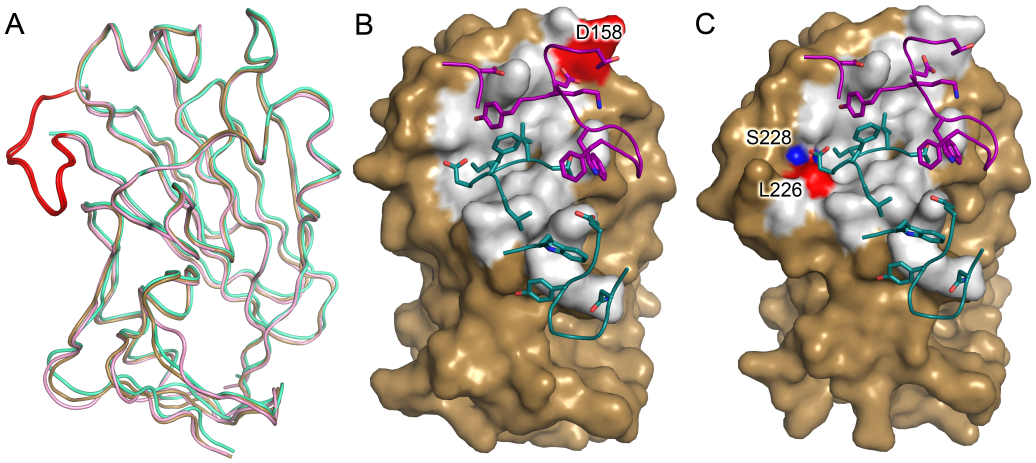

Figure III-4. Comparison of H5.3 interfaces in H5hd-*rdt* complexes. (A) Overlay of *wt*_H5hd (gold), H5hd_*rdt*_Vn (green), and H5hd_*rdt*_In (light pink). The 220 loop is highlighted in red in the *wt*_H5hd and H5hd_*rdt*_In structures; the 220 loop is not visible in the H5hd_r*dt*_Vn structure. The surface rendering of H5 is rotated 20° relative to A and highlights the solvent inaccessible interface of H5.3 on H5hd_*rdt*_Vn (B) and H5hd_*rdt*_In (C). The *rdt* residues in the H5.3 interface are highlighted in red. The *rdt* residue not in the interface is highlighted in blue (T160A in H5hd_*rdt*_In is not visible in this view of the structure). The CDR loops of H5.3 are shown as loops, with the residues involved in the interface highlighted as sticks, with the heavy chain in teal and the light chain in purple.

The 220 loop forms one rim of the receptor-binding site and contains two of the three *rdt* residues in H5hd_*rdt*_Vn (Asn224Lys and Gln226Leu). The loop is part of the H5.3-H5hd interface, as judged by solvent accessibility, although it makes only a single contact (a van der Waals contact in the H5.3-H5hd structure and a hydrogen bond in the H5.3-H5hd_*rdt*_In structure). The disorder is likely dependent on both the presence of the H5hd_*rdt*_Vn mutations and the loss of intersubunit contacts to the adjacent HA1 protomer (Fig. III-5). Despite forming a rim of the RBS, and dictating receptor use, the 220 loop is not important for H5.3 binding.

Binding Determinants Outside the Receptor-Binding Site

In addition to contacts between the H5.3 CDRH3 and H5, H5.3 forms important interactions with the 190 helix and 140 loop, elements that form the extreme edges of the RBS (Fig. III-6). The 140 loop is recognized by residues from CDRs H1 and H2, and residues from CDRs L1 and L2 recognize the 190 helix. The 140 loop and 190 helix are sites of sequence divergence between H5 strains, and H5.3 forms highly sequence-specific interactions with two sites of polymorphism: Lys193 and Lys144. These sites are critical for dictating binding specificity of H5.3, which shows a strong preference for Lys at these positions (Fig. III-6). The combination of CDRH3 inserting into the RBS and binding invariant residues on H5, and sequence-specific interactions with the variable periphery of the RBS, combine to produce an extremely potent and specific neutralizing antibody.

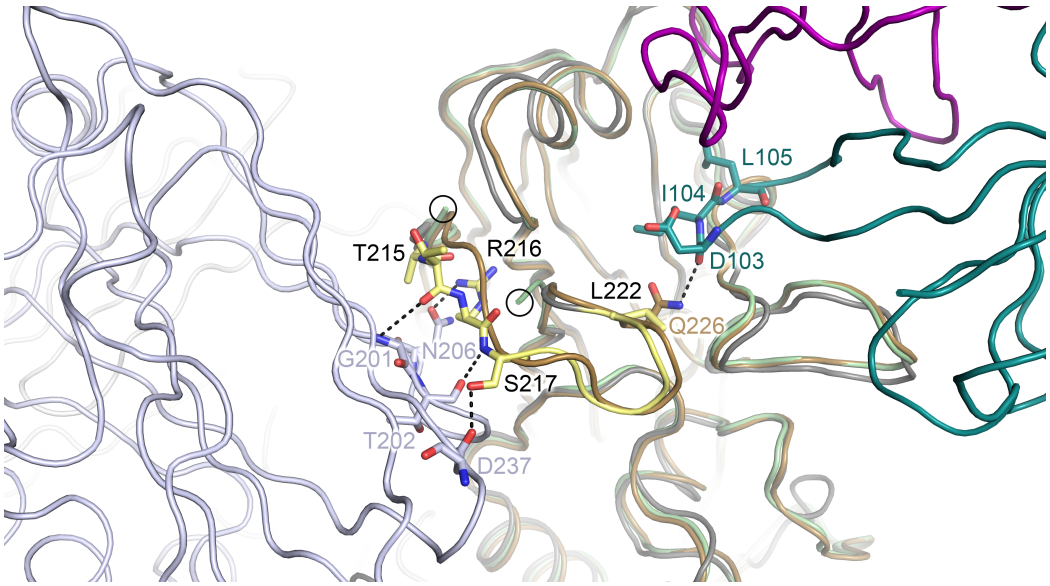

Figure III-5. The loss of trimer contacts and the Gln226→Leu mutation contribute to destabilize the 220 loop in the H5.3-H5hd_*rdt*_Vn structure. In gray, with the 220 loop highlighted in yellow, is the trimeric VN/1203 *rdt* H5 ectodomain (PDB ID code 4BH2). Intersubunit H-bonds are shown as dotted lines between the 220 loop (yellow) and a neighboring protomer (blue-gray). These interactions are lost in monomeric head domain constructs. Additionally, the loss of the hydrogen bond between Gln226 and Asp103 likely further destabilizes the 220 loop. In the figure, the H5.3-H5hd_*rdt*_Vn structure (H5hd_*rdt*_Vn in light green, H5.3 heavy chain in teal, H5.3 light chain in purple) is aligned to both *wt*_H5hd (gold) and a protomer of the VN/1203 *rdt* trimeric H5 ectodomain (PDB ID code 4BH2) protomer (gray). Additional H5 ectodomain protomers are shown as blue-gray (front, left) and light gray (back, left). The last structured residues in the 220 loop from the H5.3-H5hd_*rdt*_Vn structure are circled.

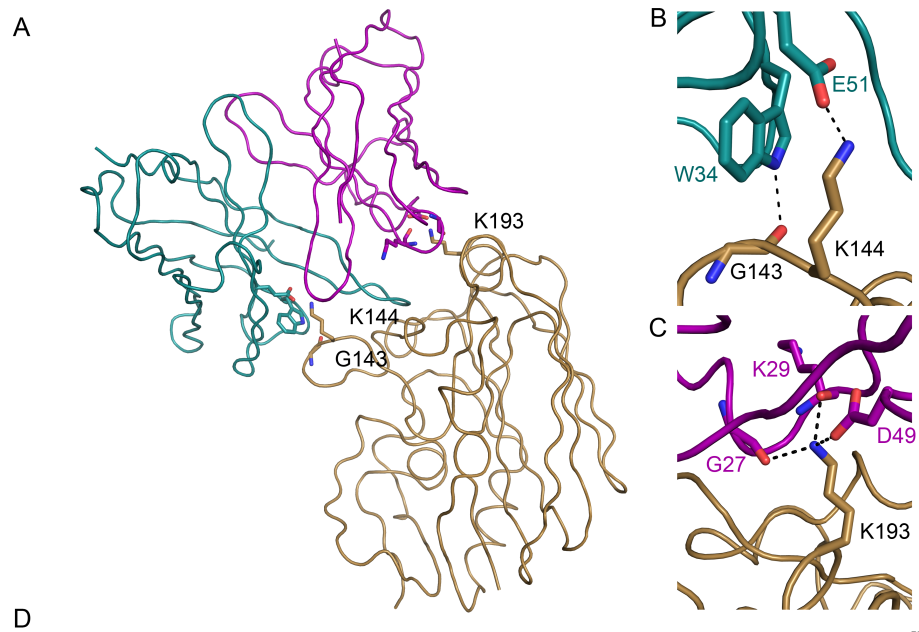

D

	144*	150	160	170	180	193*	H5.3 EC50 (ng/mL)
VN/1203	YQG**K**SSFFRNVVWLIKKNSTYPTIKRSYNNTNQEDLLVLWGIHHPNDAAEQT**K**LYQNPTT						17
H5_rdt_Vn	YQG**K**SSFFRNVVWLIKKDSTYPTIKRSYNNTNQEDLLVLWGIHHPNDAAEQT**K**LYQNPTT						19
H5_rdt_In	YQG**K**SSFFRNVVWLIKKNSAYPTIKRSYNNTNQEDLLVLWGIHHPNDAAEQT**K**LYQNPTT						16
Indo	YLG**S**PSFFRNVVWLIKKNSTYPTIKKSYNNTNQEDLLVLWGIHHPNDAAEQT**R**LYQNPTT						10,000
Indo rdt	YLG**S**PSFFRNVVWLIKKNSAYPTIKKSYNNTNQEDLLVLWGIHHPNDAAEQT**R**LYQNPTT						>
Anhui	YQG**T**PSFFRNVVWLIKKNNTYPTIKRSYNNTNQEDLLILWGIHHSNDAAEQT**K**LYQNPTT						2,780
Egypt	YQG**R**SSFFRNVVWLIKKDNAYPTIKISYNNTNQEDLLVLWGIHHPNDAAEQT**R**LYQNPTT						>
BHG	YQG**R**SSFFRNVVWLIKKNNAYPTIKRSYNNTNQEDLLVLWGIHHPNDAAEQT**R**LYQNPTT						>
HK 156	YLG**R**SSFFRNVVWLIKKNSAYPTIKRSYNNTNQEDLLVLWGIHHPNDAAEQT**K**LYQNPTT						18
HK 213	YQG**K**SSFFRNVVWLIKKNNAYPTIKRSYNNTNQEDLLVLWGIHHPNDAAEQT**R**LYQNPTT						>

Figure III-6. H5.3 forms critical interactions with polymorphic residues on the extreme edges of the interface. H5hd is shown in gold, the H5.3 light chain is shown in purple, and the H5.3 heavy chain is shown in teal. (A) Lys144 and Lys193 form two extreme edges of the H5.3-H5hd interface and are recognized exclusively by heavy chain and light chain residues, respectively. (B) Lys144 and Gly143 are recognized by Glu51 and Trp34 of the H5.3 heavy chain. (C) Lys193 makes three specific interactions with residues in the H5.3 light chain, two with the backbone carbonyls of Gly27 and Lys29 and a salt bridge to Asp49. (D) A sequence alignment of multiple H5N1 strains with ELISA EC_{50} values (taken from ref. (Thornburg et al., 2013)) reveals the preference for Lys or Arg at 144 and the requirement for Lys at position 193. Strains shown in D are as follows: VN (A/Vietnam/1203/2004), *rdt*_Vn (VN/1203 N158D, N224K, Q226L), *rdt*_In (VN/1203 T160A, Q226L, G228A), Indo (A/Indonesia/05/ 2005), In *rdt* (Indo T160A, Q226L, G228S), Anhui (A/Anhui/1/2005), Egypt (A/ Egypt/3300-NAMRU3/2008), BHG (A/bar-headed goose/Qinghai/1A/2005), HK 156 (A/Hong Kong/156/1997), and HK 213 (A/HK/213/2003).

Conformational Flexibility in H5.3 CDRs

H5.3 was isolated from an H5N1 vaccine trial participant (~3 months after immunization), rather than a repeatedly infected or immunized volunteer, and is not highly mutated. H5.3 differs at 11 sites (4 in the heavy chain and 7 in the light chain) from its UCA. The low number of somatic mutations is consistent with the response expected after initial exposure to a new antigen and is representative of the antibodies isolated from the H5N1 vaccine trial. Six of the nine H5 antibodies isolated and characterized from this trial were specific for only H5 (Thornburg et al., 2013). The H5-specific antibodies have significantly fewer somatic mutations than bnAbs ($P = 0.008$), which are reactive against strains to which most people have numerous exposures. The H5-specific antibodies have an average of 12.3 ± 5 mutations from the UCA compared with 21.6 ± 7 mutations for bnAbs (Table III-2). Of the 11 mutations in H5.3, none contact H5hd (Fig. III-7).

The low number of somatic mutations in H5.3 results in an antibody that is not optimally configured for antigen binding. Comparison of the previously described (in Chapter II) structure of the H5.3 Fab alone (PDB ID code 4GSD) (Thornburg et al., 2013) with the conformation of H5.3 observed in the H5hd complexes reveals large conformational changes upon binding (Fig. III-8). Most critically, the tip of CDRH3 is rotated ~90° compared with the unliganded structure. This reorientation of CDRH3 is required to position the H5.3 H-bond donors such that they recapitulate the H-bonding pattern of sialic acid. The liganded structure of CDRH3 would clash with the unliganded structure of CDRL3, causing CDRL3 to shift away from its unliganded position by ~5 Å. This shift causes CDRL3 to pack against the C' strand of the heavy chain. Although this reorganization shifts CDRL3 away from H5, CDRL1 and L2 shift ~1 Å closer to H5.

Table III-2. Somatic mutations in H5-specific and Abs and bnAbs.

H5 Specific Antibodies					Broadly Neutralizing Antibodies				
		Number of Variable Domain Mutations^					Number of Variable Domain Mutations^		
Antibody	epitope*	Heavy Chain	Light Chain	Total	Antibody	epitope*	Heavy Chain	Light Chain	Total
H5.2	head	10	8	18	CH65	head	12	6	18
H5.3	head	4	7	11	CH67	head	10	9	19
H5.7	stem	5	2	7	C05	head	22	14	36
H5.13	head	4	2	6	CR6261	stem	15	3	18
H5.16	n.d.	9	7	16	CR8020	stem	13	8	21
H5.24	n.d.	6	10	16	FI6	stem	14	9	23
					CR9114	stem	17	12	29
					F045-092	head	13	9	22
					H5.9	n.d.	16	11	27
					H5.31	head	9	7	16
					H5.36	n.d	2	7	9
			Average	12.3					21.6
			Standard Deviation	5.1					7.2

n.d., not determined (due to complex results in competition binding experiments).
^ Number of amino acid mutations.
*Epitope determination for these antibodies has been published (Laursen and Wilson, 2013; Lee et al., 2014; Thornburg et al., 2013; Whittle et al., 2011).

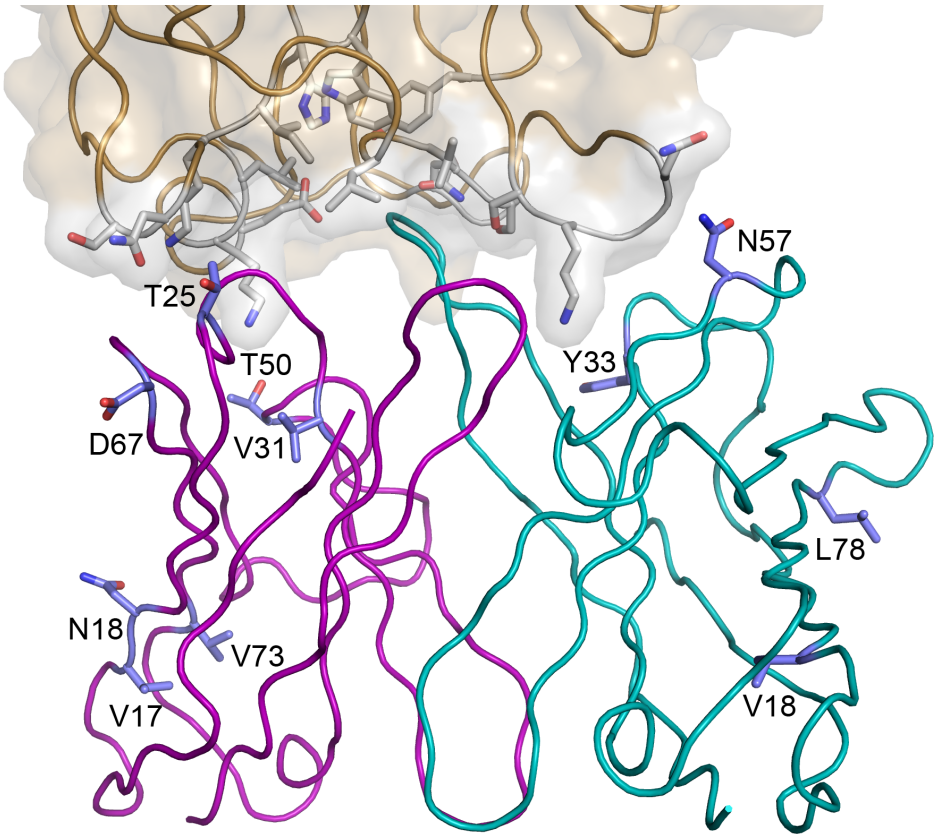

Figure III-7. Location of H5.3 mutations from UCA relative to the interface with H5. There are 11 mutations in H5.3 (4 in the heavy chain and 7 in the light chain) compared to its UCA, none of which are involved in the H5.3-H5 interface. H5.3 light chain in purple, heavy chain in teal, residues mutated from the H5.3 UCA shown as blue sticks, H5hd in gold, H5 residues involved in the interface shown as blue sticks.

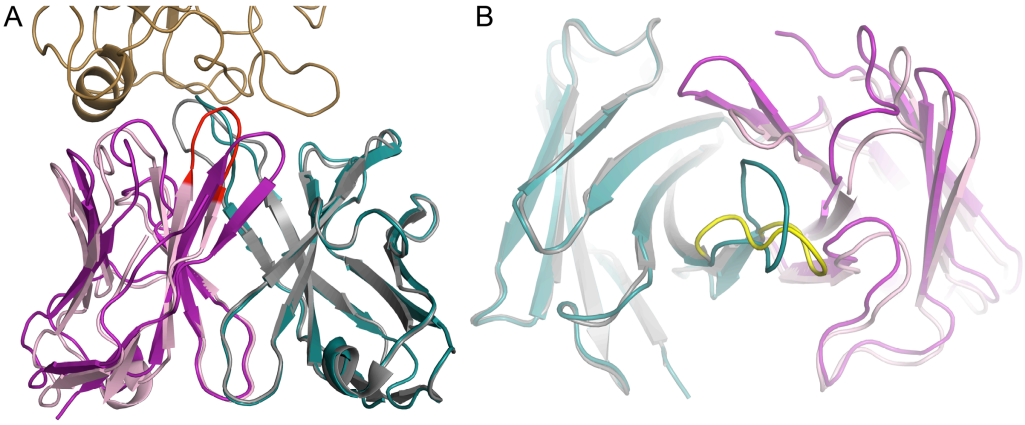

Figure III-8. H5.3 retains germline flexibility. (A) An overlay of the free and bound structures of H5.3 shows the conformational reorganization associated with antigen binding. The bound H5.3 heavy chain is shown in teal, the free heavy chain is shown in gray, the bound light chain is shown in purple, the free light chain is shown in light pink, the tip of CDRL3 of the free light chain is highlighted in red, and the head domain is shown in gold. (B) View from the receptor-binding site. The heavy chain CDR3 is rotated ~90°, the light chain CDR3 is shifted ~5 Å. The free CDRH3 is highlighted in yellow.

Discussion

H5N1 influenza A viruses are not currently transmissible between humans, in part due to the receptor specificity of the virus. However, when humans are infected through contact with infected birds, the mortality rate is ~60%, which is unusually high for an influenza infection (WHO, 2014c). In this study, I show that a highly potent human antibody against H5 that also recognizes *rdt* variants shares many structural features with other anti-HA antibodies. H5.3 is an RBS-directed antibody that inserts CDRH3 into the RBS and recapitulates the H-bonding pattern between HA and the sialic acid receptor. H5.3 is able to bind H5 *rdt* variants, indicating that mutations that alter receptor preference are not necessarily escape mutants for RBS targeted antibodies.

Unlike HA-specific bnAbs, H5.3 forms critical interactions with residues on the extreme edges of the HA head domain. These interactions are formed between H5.3 heavy chain residues and H5 Lys144, as well as H5.3 light chain residues and H5 Lys193. Lys144 and Lys193 are sites of diversity within H5 strains and are critical for the high potency and specificity of H5.3. The combination of RBS-directed CDRH3 and peripheral interactions to polymorphic residues enables H5.3 to tightly bind H5 *rdt* variants, and indicates that antibodies produced in response to an appropriate H5 vaccine challenge can reasonably be expected to neutralize human transmissible influenza strains.

H5.3 undergoes a conformational change upon binding to H5 that is, to our knowledge, unprecedented among affinity-matured antibodies (Fig. III-7). The critical binding determinants on CDRH3 rotate ~90° from their positions in the unliganded structure (Fig. 5). Additionally, CDRL3 moves ~5 Å to avoid steric

clashes with H5hd. The rotation of CDRH3 emphasizes the difficulty of predicting binding mode, even within a family of structurally similar proteins. Conformational flexibility is typically a characteristic of unmutated, rather than affinity-matured, antibodies, yet the lack of a preformed combining site in H5.3 and large conformational change associated with binding indicate that H5.3 has retained some of the flexibility present in germline gene-encoded antibodies (Schmidt et al., 2013; Thorpe and Brooks, 2007; Wedemayer et al., 1997; Willis et al., 2013). H5.3 differs from its UCA by only 11 mutations and is therefore substantially less mutated than most influenza bnAbs (Table III-2), and, of these mutations, none directly contact H5 (Fig. III-7).

Among the structurally characterized antibodies that use CDRH3 to recapitulate the H-bonding pattern of sialic acid, all except H5.3 use an aspartic acid from CDRH3 to mimic the carboxylate group of sialic acid. In H5.3, a main chain carbonyl makes interactions with HA that are similar to those made by the carboxylate group of sialic acid, illustrating an additional way to recognize a conserved feature of the RBS.

The potency of H5.3 comes from binding energy derived from interactions between the RBS and CDRH3, as well from key interactions outside the RBS (to Lys144 and Lys193). In H5.3, potency comes at the expense of breadth because Lys144 and Lys193 are polymorphic sites in H5N1 strains. H5.3 was isolated from the blood of a healthy donor who had participated, ~3 months earlier, in a clinical trial of an experimental H5N1 vaccine (Belshe et al., 2014; Thornburg et al., 2013). The structural and sequence analysis presented here indicate that H5.3 is lightly mutated and flexible, consistent with an antibody that is not optimally matured. Of the nine human monoclonal antibodies isolated against H5, the six that are specific

for only H5 have, on average, fewer mutations than bnAbs (Table III-2). BnAbs have significantly more mutations and likely arise through stimulation of memory B cells. In general, the presence of reactive memory B cells correlates with the ability to produce a bnAb response (Bentebibel et al., 2013; Crotty, 2014; Dogan et al., 2009; Pallikkuth et al., 2012). It seems that, for both influenza and HIV, bnAbs require significantly more somatic mutation than seems common in vaccine-induced antibodies in otherwise antigen-naive humans (Kepler et al., 2014; Klein et al., 2013), suggesting that bnAbs might be elicited by repeated immunization against multiple strains, rather than fortuitous gene use. H5.3 is illustrative of the lack of breadth typical of vaccine-induced antibodies, and our results indicate that breadth and potency directly conflict in H5.3 interactions. The H5.3 interactions with Lys144 and Lys193 prevent tight binding to variant H5 strains that do not contain these residues, yet H5.3 is extremely potent against VN/1203 (Thornburg et al., 2013), indicating it was likely strongly selected for, and expanded, in germinal centers during affinity maturation.

H5.3 was elicited by a VN/1203 H5N1 experimental vaccine and is representative of the type of antibodies an H5-naive person is likely to produce. Subsequent infection or immunization with a variant strain would likely be an effective route to generate broadly reactive anti-H5 antibodies. Such strategies are known to be effective within influenza subtypes (Belshe et al., 2014; Mulligan et al., 2014; Suguitan et al., 2011). Our structural understanding of H5.3 supports the hypothesis that repeated challenge through immunization or infection is an effective strategy to enhance universal binding determinants, such as a CDRH3 loop that effectively binds conserved features of the RBS, similar to the natural receptor, while minimizing strain specific interactions. Achieving a universal flu

vaccine may require methods to develop and maintain a memory B-cell population that has already expanded multiple times against diverse antigens.

CHAPTER IV

GERMLINE ENCODED ANTIBODY BINDS A/VIETNAM/1203/2004 H5 WITH HIGH AFFINITY

Introduction

Seasonal influenza remains a worldwide health concern, causing the death of 250,000-500,000 people each year (WHO, 2014a). In addition, there have been four influenza pandemics since the beginning of the 20th century, killing 50-100 million people, caused by novel influenza viruses to which the human population had little to no pre-existing immunity (Garten et al., 2009; Kilbourne, 2006). For an influenza pandemic to occur, the virus must be novel, be able to cause disease in humans, and transmit efficiently through the immunologically naïve human population (Poland et al., 2007). Since 2003, there have been ~850 human cases of the novel H5N1 influenza virus usually caused by direct or indirect contact with infected poultry, resulting in a ~50% mortality rate (Ungchusak et al., 2005; WHO, 2016). Currently, this virus is not transmissible in humans due, in part, to the receptor specificity of the virus, however recent studies have shown that very few mutations may be required for efficient human-to-human transmission of the virus (Herfst et al., 2012; Imai et al., 2012).

The influenza humoral immune response is directed against the immunodominant hemagglutinin (HA) head domain (van de Sandt et al., 2012). Following natural influenza infection or vaccination, naïve and memory B cells can be stimulated to undergo multiple rounds of somatic hypermutation and clonal

selection, increasing antibody titers (De Silva and Klein, 2015; Victora and Nussenzweig, 2012).

Currently, the best prevention against influenza is a yearly vaccine, which comes with many limitations, including the need for annual vaccination due to the antigenic drift of the virus, possible mismatch between the vaccine and circulating strains, and a long (6-8 month) production time (Carrat and Flahault, 2007; Lambert and Fauci, 2010). In contrast, a universal flu vaccine would provide protection against many circulating seasonal and novel influenza strains (Burton et al., 2012; Krammer and Palese, 2015).

The discovery and structural characterization of broadly neutralizing antibodies has led to a renewed interest in rational vaccine design (Burton et al., 2012). Molecular structures have enhanced our understanding of the mechanism of neutralization and have spurred new efforts in vaccine design. Alternative methods for influenza vaccine design are being explored, including the use of subunit vaccines focusing on the HA head or stem domains (Bommakanti et al., 2010; Khurana et al., 2010; Lu et al., 2014; Song et al., 2008a). The goal of one method, used in HIV vaccine design, termed germline-targeting, is to develop novel antigens that faithfully elicit a desired germline precursor B-cell to begin the process of affinity maturation (Dosenovic et al., 2015; Jardine et al., 2016; 2015).

The relatively new ability to study human antibody antigen interactions and structures presents the opportunity to use structural information for rational vaccine design. This will require diverse methods, but will likely include the use of structural and biochemical data to design better vaccine immunogens, with the goal of eliciting more broadly neutralizing antibodies.

I previously described the functional and structural characterization of H5.3, an antibody elicited in response to an experimental H5N1 vaccine, containing the

HA and NA glycoproteins from the A/Vietnam/1203/2004 (H5N1) (VN/1203) influenza strain in Chapters II and III (Thornburg et al., 2013). Here, I describe the immunogenic origin, effect of somatic mutations on affinity, and structure of the unmutated common ancestor (UCA) of the H5.3 ($H5.3_{uca}$) antibody. I determined the x-ray crystallographic structure of $H5.3_{uca}$, which highlights the inherent flexibility of H5.3, an intrinsic feature of this antibody in both the mature and UCA forms. I also show individual UCA mutations do not have a cumulative effect on increasing the affinity of mature H5.3 ($H5.3_{m}$) for H5hd. Most strikingly, the UCA mutations only increase affinity by 10-fold; consistent with the idea that affinity maturation is not needed for a potent anti-H5 antibody response.

Materials and Methods

Site-directed mutagenesis

The QuikChange II XL kit (Agilent) was used to generate H5.3 Fab constructs that possessed point mutations in the antibody coding sequence of the plasmids encoding the H5.3 Fab light and heavy chains. Mutagenesis was performed according to the manufacturer's instructions. The introduction of the intended mutation was confirmed by nucleotide sequence determination.

Expression and Purification of H5.3 Fabs

Protein was expressed by transient transfection of 293F cells (Invitrogen) according to the manufacturer's instructions, with the exception that polyethyleneimine was used as the transfection reagent as previously described (Durocher et al., 2002), instead of 293Fectin. Cells were grown for 7 days then harvested by centrifugation at 2500 x g. Supernatant was passed through a 0.45

μm membrane. The clarified supernatant was applied to a HiTrap Protein G HP column (GE Healthcare) and buffer exchanged 2x with DPBS using an Amicon Ultra centrifugal concentrator with a 10 kilodalton cutoff membrane (Millipore).

Expression and purification of HA

The proteins were expressed in BL21 (DE3) cells grown in LB medium at 37 °C to an optical density (at 600 nm) of 0.6 and were induced with 0.1 mM isopropyl β-D-thiogalactopyranoside for 12 h at 20 °C. Bacteria were harvested by centrifugation and lysed with a French press in PBS with ~1 μg/mL hen egg white lysozyme, ~1 μg/mL DNase I, 10 μg/mL leupeptin, 1 mM PMSF, and 0.7 μg/mL pepstatin. The lysate was clarified by centrifugation, and the insoluble fraction was resuspended in 8 M urea, 50 mM Tris, pH 8, and purified by Co-NTA affinity using TALON resin. The protein was refolded overnight by rapid dilution (10 mL into 200 mL) into 1 M arginine, 10 mM Tris, pH 7.5, 0.5 mM reduced glutathione, 0.05 mM oxidized glutathione, followed by dialysis against 150 mM NaCl, 10 mM Tris, pH 7.5, for 24 h, and centrifugal concentration. The 6x-His tag was removed using thrombin, followed by gel filtration on a 24-mL Superdex 200 (GE Healthcare) column. Biotinylated H5hd was prepared the same as H5hd, with the following modifications: a BirA tag (GGGLNDIFEAQKIEQHE) was introduced at the carboxyl terminus by PCR, and the purified, refolded protein was labeled with *Escherichia coli* biotin ligase following standard protocols (Howarth and Ting, 2008).

Biosensor Assays

Affinity measurements were performed using Fab fragments and biotinylated H5hd on an Octet interferometry instrument (ForteBio) with

streptavidin biosensors (Fortebio 18-5019). HA and Fab were diluted in 1X kinetics buffer (Fortebio, 18-5032) with PBS. Fabs were diluted to 2 μM, 1 μM, 500 nM, 250 nM, 125 nM, 75 nM, 37.5 nM; or 500 nM, 250 nM, 125 nM, 75 nM, 37.5 nM, 18.75 nM, 9.375 nM. Tips were equilibrated in 1X kinetics buffer for 60 s, HA was immobilized on biosensors for 60 s, baselines were established in 1X kinetics buffer for 60 s, and dilutions of H5.3 Fab mutants were used for 180 s association curves, and 180 s 1X kinetic buffer dissociation curves. The data were analyzed with ForteBio data analysis software version 7.1. Briefly, the y-axis was aligned to baseline, and data were processed with Savitzky–Galay filtering. Affinities were calculated by doing curve fits of association and dissociations with a 1:1 binding model and global fitting.

Crystallization, data collection, and structure determination

$H5.3_{uca}$ Fab crystals were grown by vapor diffusion of 10 mg/mL protein against a reservoir containing 24% PEG 1500 and 20% glycerol. Crystals were frozen directly from crystallization drops. Diffraction data were collected from single crystals at 100K at sector LS-CAT 21-ID-F at the Advanced Photon Source (Argonne, IL). Data were indexed, integrated, and scaled using HKL2000 (Otwinowski and Minor, 1997). Data collection statistics are given in Table IV-2. Molecular replacement solution for the antibody constant region was obtained with PDB code ID 4GSD, and with PDB code ID 4XRC for the variable region using Phaser (McCoy et al., 2005). Initially the constant regions were identified and used to find the variable regions in a Fourier search. Residues that differed between the $H5.3_{m}$ and $H5.3_{uca}$ structures were mutated to correct residue in $H5.3_{uca}$ and the resulting model was refined in Phenix (Adams et al., 2002). Refinement included rigid body refinement of the individual domains, simulated annealing, positional

refinement, individual B-factor refinement, and translation/libration/screw (TLS) refinement. Loops were rebuilt and side chains added in COOT (Emsley and Cowtan, 2004) using simulated annealing composite omit maps (Brünger et al., 1997) generated by Phenix (Adams et al., 2002). TLS refinement (Painter and Merritt, 2006) was incorporated in the final rounds of refinement using TLS groups identified using Phenix.

Results

Somatic mutations in H5.3

The H5.3 antibody was isolated from a subject in an experimental H5N1 vaccine trial, containing the HA and NA glycoproteins from the VN/1203 H5N1 influenza strain (Thornburg et al., 2013). In Chapters II and III, I described the structures of the unliganded and liganded (in complex with VN/1203 H5hd) $H5.3_m$ Fab structures. Based on structural alignments of the $H5.3_m$ Fab structures, I determined H5.3 undergoes a conformational change in order to bind H5, involving a ~90° rotation of CDRH3, 5Å shift of CDRL3 away from H5, and ~1Å shift of CDRL1 and L2 closer to H5 (Figure III-8). However, as emphasized by further crystallization studies, described in Effects of Somatic Mutations on H5 structure section, I have shown H5.3 is an inherently flexible antibody.

The IMGT tool was used to determine the V_H and V_L genes that encode H5.3 (Thornburg et al., 2013). The analysis indicated the heavy chain is encoded by the IGHV4-4*02, IGHD3-9*01, and IGHJ5*02 genes; and the light chain is encoded by IGLV3-1*01 and IGLJ1*01. Sequence comparison indicates there are 4 and 7 somatic mutations in the heavy and light chains, respectively, all of which are in the V gene regions (Figure IV-1). The heavy chain mutations are: L18(V),

N33(Y), S57(N), and Q78(L) (Figure IV-1A). The light chain mutations are: A17(V), S18(N), L25(T), A31(V), S50(T), N67(D), and I73(V) (Figure IV-1B). The structure of the H5.3 Fab H5hd complex, described in Chapter III, shows none of the somatic mutations are involved in the antibody antigen interface (Figure III-7). Interestingly, one somatic mutation in the light chain, S18(N) adds a putative glycosylation site in the antibody.

The critical H5.3 residues at the H5.3 H5 interface are those on the tip of CDRH3, which are involved in recapitulating the interaction between H5 and the influenza receptor, sialic acid. As described in Chapter III, deletion or mutation (to alanine) of these residues, D103, I104, and L105, eliminates H5.3-H5 binding. These residues are all encoded by IGHD3*9-01.

Effect of somatic mutations on H5.3 affinity for VN/1203 H5

In order to determine the effect of the somatic mutations on the affinity of H5.3 for VN/1203 H5, a fully UCA light chain (L_{uca}), heavy chain (H_{uca}), and single revertants of each somatic mutant in the $H5.3_m$ background were generated. The $H_{uca}L_{uca}$, $H_{uca}L_m$, H_mL_{uca}, and single reversion mutants with H_m or L_m were expressed and purified.

I determined the affinities of the H5.3 UCA mutants for biotinylated VN/1203 H5hd using biolayer interferometry (Table IV-1). The fully reverted $H_{uca}L_{uca}$ had a binding affinity of 30 nM, while H_mL_m had a binding affinity of 3.2 nM, only a ~10-fold increase over $H_{uca}L_{uca}$. Comparison of the affinities of $H_{uca}L_m$ (10.6 nM) and H_mL_{uca} (10.7 nM) indicates both chains contribute equally to binding. Additionally, the affinity of each revertant for VN/1203 H5hd was close to the range of affinities for $H5.3_{uca}$ and $H5.3_m$, 4.3-20 nM. This suggests the somatic mutations do not have an additive effect in increasing the affinity of H5.3 for H5.

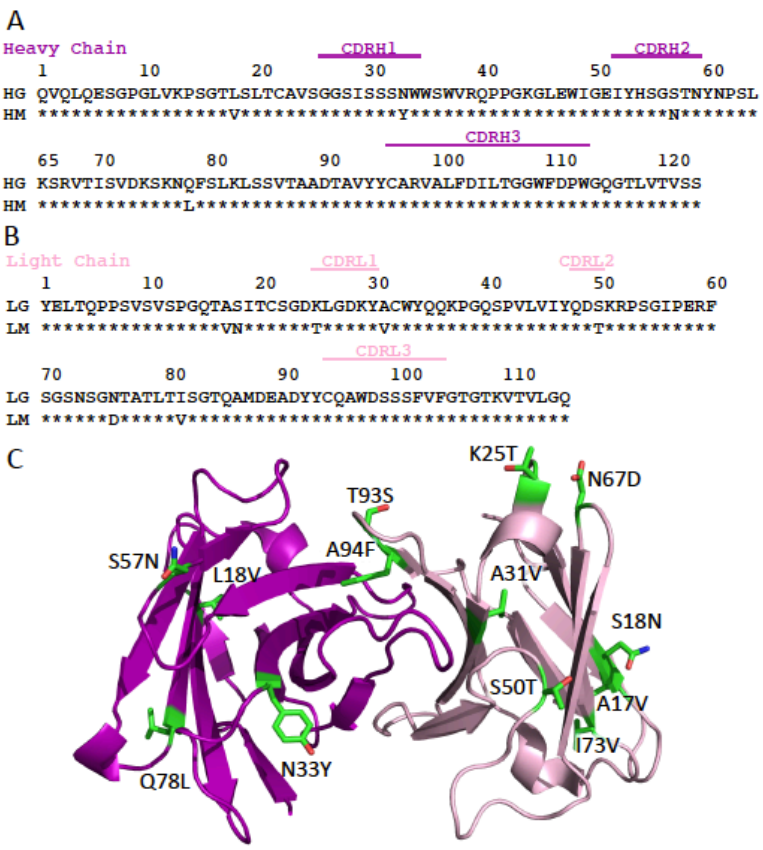

Figure IV-1. H5.3 somatic mutations. Alignment of H5.3 inferred unmutated common ancestor sequence with affinity-matured sequence. (A) There are four mutations between the H5.3$_{uca}$ (HG) and H5.3$_{m}$ (HM) heavy chain sequences. (B) There are seven mutations between the H5.3$_{uca}$ (LG) and H5.3$_{m}$ (LM) light chain sequences. (C) Crystal structure of the unliganded H5.3$_{m}$ structure with the locations of the somatic mutations in green. There are two addition mutated residues (T93(S) and A94(F)) highlighted on the LC, as these seemed to be ambiguous and were included in the H5.3$_{uca}$ Fab used for crystallization. HC, purple; LC, light chain.

Table IV-1. Affinities of H5.3 mutants for VN/1203 H5hd.

Fab	Affinity (nM)
$H5.3_{uca}$	30.2 ± 0.3
$H5.3_{m}$	3.2 ± 0.2
H_mL_{uca}	10.7 ± 0.1
H_{uca}/L_m	10.6 ± 0.1
$V18L/L_m$	12.7 ± 0.2
$Y33N/L_m$	13.9 ± 0.2
$N57S/L_m$	20 ± 0.3
$L78Q/L_m$	15 ± 0.3
H_m /V17A	15.9 ± 0.1
H_m/N18S	4.3 ± 0.5
H_m/T25K	11.7 ± 0.1
H_m/V31A	5.4 ± 0.5
H_m/T50S	9.5 ± 0.1
H_m/D67N	10.9 ± 0.1
H_m/V73I	4.8 ± 0.5

Effect of somatic mutations on H5.3 structure

In order to understand how the somatic mutations alter the H5.3 structure, I determined the X-ray crystallographic structure of the $H5.3_{uca}$ Fab to 2.1 Å. Refinement and data quality statistics are given in Table IV-2. There are two copies of the Fab in the crystallographic asymmetric unit (ASU), with an RMSD between the main chain atoms of 0.224 Å (variable region) and 0.257 Å (constant region). Both copies of the Fab are well ordered.

The most significant difference between the two copies of $H5.3_{uca}$ in the ASU is CDRH3, which adopts different conformations in each copy (Figure IV-2). The CDRH3 of Copy A is packed against the LC constant region of the next copy A (Figure IV-3), while copy B CDRH3 is packed against the LC constant region of the next copy B on one side and solvent exposed on the other (Figure IV-4). Although the CDRH3s are in different conformations due to crystal packing, this also highlights the inherent flexibility of the H5.3 CDRH3.

As previously described, in Chapter III, I initially concluded $H5.3_m$ is not optimally configured to bind H5, and must undergo a large conformational change, yielding structures of $H5.3_m$ in two different conformations. However, further structural studies with the $H5.3_{uca}$ have shown H5.3 is an inherently flexible antibody. In order to highlight the flexibility of the antibody, Figure IV-5 shows the structural alignment of $H5.3_{uca}$ with liganded and unliganded $H5.3_m$ (Figure IV-5 A and B, respectively). The comparison of these structures emphasizes the flexibility of the antibody, especially the conformation of CDRH3. Although, the CDRH3s of $H5.3_{uca}$ and $H5.3_m$ have the same sequence, they crystallized in different conformations, again stressing the inherent flexibility of the H5.3 CDRH3 (Figure IV-5C).

Table IV-2. Data collection, phasing, and refinement statistics.

Data collection	
Space group	C2
Cell dimensions	
a, b, c (Å)	114.53, 83.52, 109.49
α, β, γ (°)	90.00, 117.15, 90.00
Wavelength	0.97872
Resolution (Å)	50-1.95
Completeness (%)*^	50-1.95: 95.7 (68.8) 50-2.1: 99.8 (97.6)
Redundancy*^	50-1.95: 4.0 (2.9) 50-2.1: 4.2 (3.7)
I/sigmal*^	50-1.95: 17.0 (2.4)
Refinement	
Resolution (Å)*	50-1.95Å (50-2.1Å)
No. reflections	62,125
No. reflections free set	1,993
R_{work} / R_{free} % $^{\$,\#}$	21.44/24.51
No. atoms	
Protein	6381
Water	789
B factors (Å^2)	
Protein	30.4
Water	37.0
R.m.s deviations	
Bond lengths (Å)	0.002
Bond angles (°)	0.599
Ramachandran Plot	98% of residues in favored regions. 0 outliers.

* Parentheses indicate outer-shell statistics.
^ Statistics given on the first line is for data used in refinement. Statistics given on the second line is for the correct structure resolution, 2.1 Å.
$^{\$}$ $R_{cryst} = \Sigma hkl \left| Fo - Fc \right| / \Sigma hkl \left| Fo \right|$, where Fo and Fc are the observed and calculated structure factors.
$^{\#}$ R_{free} was calculated as for R_{cryst}, but using 5% of data, randomly chosen and excluded from refinement.

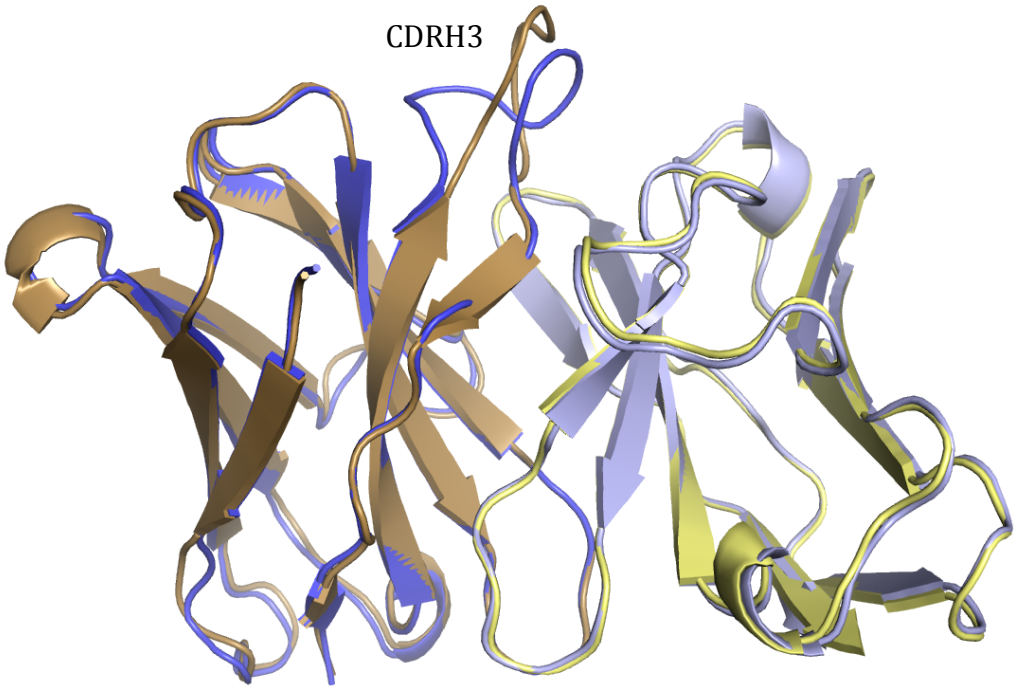

Figure IV-2. Alignment of H5.3$_{uca}$ copies A and B. Structural alignment of H5.3$_{uca}$ Fv regions. Overall, the structures are very similar with the exception of the CDRH3 conformation. Copy A: HC, blue; LC, light blue. Copy B: HC, sand; LC, light yellow.

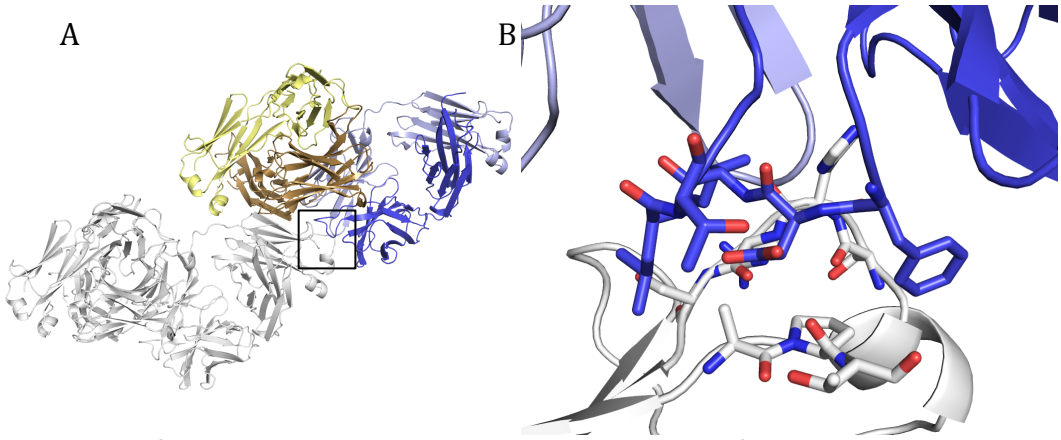

Figure IV-3. Crystal contacts involving H5.3$_{uca}$ copy A CDRH3. (A) The H5.3$_{uca}$ Fab ASU consists of copy A (HC, blue; LC, light blue) and copy B (HC, sand; LC, yellow). A neighboring symmetry mate is shown in white. (B) Close-up view of black box in (A). The copy A CDRH3 is packed against the LC constant region of the next copy A Fab.

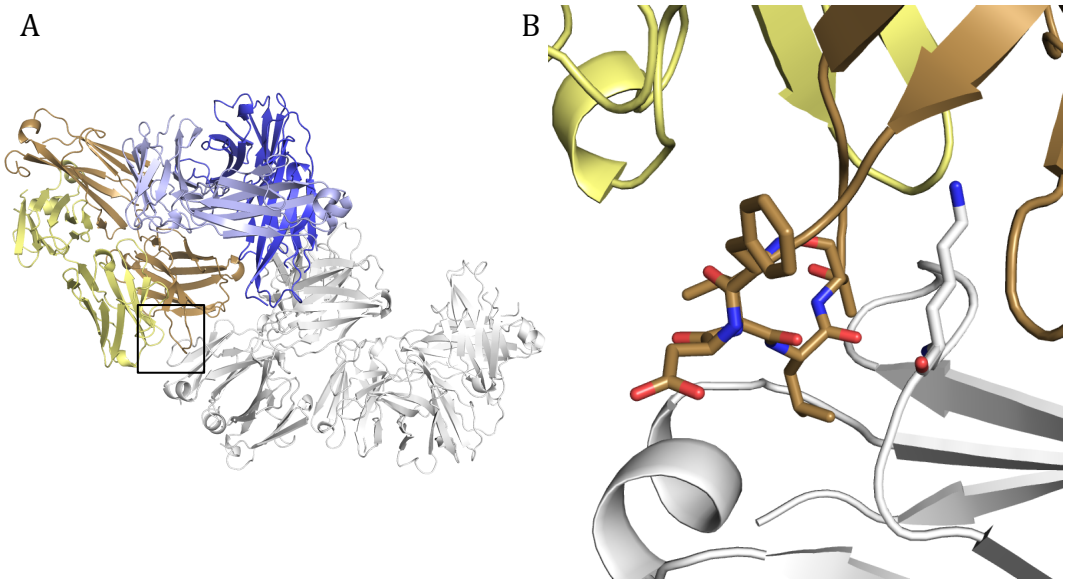

Figure IV-4. Crystal contacts involving H5.3$_{uca}$ copy B CDRH3. (A) The H5.3$_{uca}$ Fab ASU consists of copy A (HC, blue; LC, light blue) and copy B (HC, sand; LC, yellow). A neighboring symmetry mate is shown in white. (B) Close-up view of black box in (A). Half of the copy B CDRH3 is packed against the LC constant region of the next copy B Fab and half is solvent exposed.

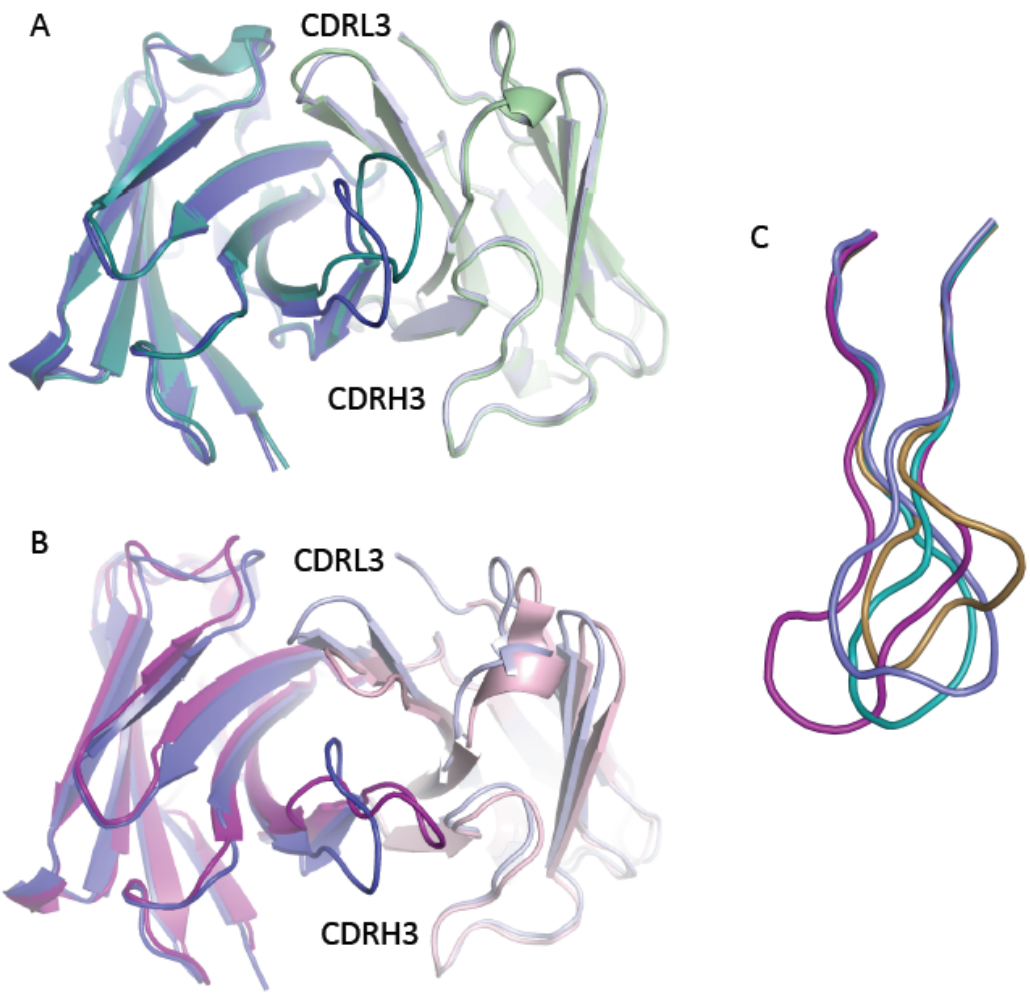

Figure IV-5. Comparison of H5.3$_{uca}$ and H5.3$_{m}$ highlights the inherent flexibility of the antibody. (A) H5.3$_{uca}$ copy A (HC, blue; LC, light blue) aligned to liganded H5.3$_{m}$ (HC; teal, LC, light green). (B) H5.3$_{uca}$ copy A aligned to unliganded H5.3$_{m}$ (HC, purple; LC, light pink). (C) The CDRH3s in H5.3$_{uca}$ copy A (blue) and copy B (sand), and liganded (teal) and unliganded H5.3$_{m}$ (purple) crystallized in different conformation.

Discussion

In this Chapter I have shown H5.3 has a low number of somatic mutations and affinity maturation did not have a large effect on the affinity of H5.3 for VN/1203 H5hd. In addition, I have demonstrated the H5.3 is a flexible antibody as evidenced by the structural alignments of the $H5.3_{uca}$ Fab, and liganded and unliganded $H5.3_{m}$ Fab structures, indicating affinity maturation does not preconfigure the antibody-combining site.

As described in Chapter III, H5.3 has a lower number of somatic mutations compared to most broadly neutralizing influenza antibodies, indicating H5.3 was a vaccine-elicited antibody (Winarski et al., 2015). The high number of somatic mutations in broadly neutralizing antibodies typically results from repeat vaccinations or infections (Kepler et al., 2014; Klein et al., 2013; Schmidt et al., 2015). Although some broadly neutralizing antibodies with a low number of somatic mutations have been identified (Prabakaran et al., 2015).

Affinity maturation did not have a large effect on increasing the affinity of H5.3 for VN/1203 H5hd. Other studies have characterized UCA antibodies capable of binding VSV, HCMV, and HIV (Alam et al., 2011; Kalinke et al., 1996; 2000; McLean et al., 2005),and UCA mouse antibodies capable of neutralizing VSV and influenza (IgM) (Harada et al., 2003; Kalinke et al., 1996; 2000). This may indicate that the common view that germline-encoded antibodies have a lower affinity for antigen, which is increased during affinity maturation, needs to be reconsidered. In support of this view is a recent observation that pharmacological disruption of affinity maturation increases antibody breadth (Keating et al., 2013).

The $H5.3_{uca}$ structure shows CDRH3 crystallized in two different conformations, highlighting the inherent flexibility of CDRH3, an intrinsic property

of germline-specified CDRH3 sequences (Babor and Kortemme, 2009). Germline-specified CDRH3 flexibility has been described for another influenza UCA antibody that after undergoing affinity maturation is preconfigured for antigen binding (Schmidt et al., 2013; Whittle et al., 2011). In contrast, the H5.3 CDRH3 and the entire $H5.3_m$ Fab remains flexible after affinity maturation. Other antibodies have been described that display varying degrees of conformational flexibility after affinity maturation, similar to H5.3 (Bhat et al., 1990; Herron et al., 1991; Stanfield et al., 1993).

Taken together these data indicate affinity maturation has a small effect on increasing the affinity of H5.3 for H5 and does not preconfigure the antibody-combining site, though H5.3 is a potent neutralizing antibody. Therefore the H5.3 germline may be an appropriate target for a germline-targeting immunogen, similar to what is being done in HIV vaccine research (Dosenovic et al., 2015; Jardine et al., 2015; 2016).

CHAPTER V

SUMMARY AND FUTURE DIRECTIONS

Summary

Influenza is a worldwide health concern causing the death of 250,000-500,000 people each year (WHO, 2014a). There have been four influenza pandemics since the beginning of the 20th century caused by novel influenza viruses, which have resulted in 50-100 million deaths (Garten et al., 2009; Kilbourne, 2006). A new pandemic could be caused by zoonotic transfer of novel influenza viruses to the immunologically naïve human population. H5N1 continues to evolve and cause disease in poultry and sporadically results in direct transmission of the virus to humans. Since 2003, there have been ~850 human cases of H5N1 influenza with a 50% mortality rate (WHO, 2016). Recently, two labs have serially passaged two different H5N1 strains in ferrets and isolated virus capable of respiratory droplet transmission in ferrets, indicating few mutations maybe necessary for efficient transmission in humans (Herfst et al., 2012; Imai et al., 2012). The most effective method of preventing an influenza pandemic is vaccination. The research presented here examines the molecular neutralization mechanism and the inferred unmutated common ancestor of the potent and specific vaccine-elicited anti-H5N1 antibody, H5.3.

The first goal of my project, presented in Chapters II and III, was to determine the molecular mechanism used by H5.3 to neutralize H5N1 influenza virus. It had been shown H5.3 recognized the HA head domain (Thornburg et al., 2013), and for this reason we elected to develop an H5 head domain construct that

could be expressed in bacteria, a fast, cost effective system that yields large amounts of protein. Using X-ray crystallography, I showed that H5.3 potently neutralizes VN/1203 H5N1 through interactions with the HA head domain (Thornburg et al., 2013; Winarski et al., 2015).

In Chapter II, I describe the purification of bacterially expressed H5hd. The protein forms inclusion bodies, which are resuspended 8M Urea, purified using affinity chromatography, and refolded in 1M Arginine under redox conditions. The protein is further purified by dialysis to remove excess urea and arginine and size exclusion chromatography. I demonstrated H5hd binds H5.3 and H5.2 Fabs, H5-specific HA-head domain directed antibodies, using gel filtration, indicating the protein is properly folded.

During my initial attempts to crystallize the H5hd H5.3 Fab complex, I determined the structure of the H5.3 Fab alone to 2.25 Å. In order to obtain a structure of the complex, I expressed and purified three additional H5hd constructs, varying the length of the N- and C- termini. I demonstrated three of the four constructs, H5hd-P1, -P4, and –P6, bound H5.3, indicating they were properly folded. One construct, H5hd-P5, did not form all the necessary disulfides bonds, as seen in an iodoacetamide assay, indicating this construct was unsuitable for bacterial expression and crystallization.

As described in Chapter III, I determined the structure of the H5.3 Fab H5hd complex to 2.5 Å. The complex structure was determined using the H5hd-P6 construct and H5.3 Fab expressed in hybridoma cells and digested with papain. This structure shows all six H5.3 CDRs contact H5 and the epitope on H5 includes both the receptor binding site and critical contacts on periphery. The CDRH3 of H5.3 is inserted in the RBS, and the residues on the tip, Asp, Ile, and Leu, recapitulate the interactions between H5 and the influenza receptor, SA, thus

blocking receptor binding. Other HA RBS directed antibodies use a similar mode of binding the RBS, though the orientation of the Asp on CDRH3 is different. In other HA RBS directed antibodies, the Asp side chain mimics the SA carboxylate group interactions with HA, where as the Asp backbone carbonyl of H5.3 recapitulates those interactions. The observation that a main chain carbonyl can substitute for the carboxylate further complicates the prediction of binding modes.

I demonstrated H5.3 binds H5 *rdt* variants in the same manner as *wt* by determining the structures of H5.3 Fab in complex with H5hd_*rdt*_Vn and H5hd_*rdt*_In to 2.15 Å and 2.74 Å, respectively. This indicates HA receptor specificity may not be critically important for H5N1 vaccine development.

Structural alignment of liganded and unliganded H5.3 Fab implied H5.3 had to undergo a conformational change in order to bind H5, including a ~90° rotation of CDRH3, ~5Å shift of CDRL3, and ~1 Å shift of CDRL2 and –L3 closer to H5. However, further structural studies, described in Chapter IV, indicate H5.3 is an inherently flexible antibody. This indicates that unlike many other affinity-matured antibodies, H5.3 maintains flexibility, characteristic of unmutated Abs and is not preconfigured for antigen binding. H5.3 is a lightly mutated antibody, containing 11 mutations from its inferred unmutated common ancestor. We analyzed the number of amino acid changes resulting from somatic mutation in H5-specific and broadly neutralizing influenza antibodies, and found H5-specific Abs have a lower average number of mutations than bnAbs. We interpret this to mean bnAbs arise from repeated stimulation of memory B cells through repeated exposure to multiple influenza strains.

In Chapter IV, I examined how affinity maturation affected H5.3 in terms of binding and structural conformation. Mature H5.3 ($H5.3_m$) has 11 somatic mutations from its inferred unmutated common ancestor ($H5.3_{uca}$), four in the HC

and seven in the LC. All of the mutations are confined to areas encoded by the V gene and none contact H5. I demonstrated the affinity maturation did not have a large effect on the affinity of $H5.3_m$ for VN/1203 H5. This indicates the common view that germline-encoded antibodies have lower affinity for antigen, which is increased during affinity maturation should be reconsidered.

In order to determine the effect of affinity maturation on the $H5.3_m$ structure, I determined the crystal structure of the $H5.3_{uca}$ Fab to 2.1 Å. Structural alignment of $H5.3_{uca}$ with liganded and unliganded $H5.3_m$ highlighted the inherent flexibility of the antibody. This emphasizes that flexibility typically associated with unmutated antibodies is maintained in $H5.3_m$.

Collectively, the findings presented here show how an H5N1 specific antibody recognizes and binds HA. And examines the small role of affinity maturation in a vaccine-elicited H5-specific antibody.

Future Directions

Examining the breadth of H5.3

H5.3 has been characterized as a potent and specific anti-H5N1 antibody, binding to 4 out of the 7 tested H5s from different H5N1 field strains (Thornburg et al., 2013). The structure of the H5.3 Fab VN/1203 H5hd complex, presented in Chapter III, revealed the H5.3 epitope on H5 encompasses the RBS along with critical interactions on the periphery. The peripheral interactions, specifically K193, dictate the ability of H5.3 to bind different H5s and mutation of this residue to Ser or Arg eliminates or severely hinders binding (Thornburg et al., 2013). Further assessment of the breadth of this antibody with an expanded panel of H5s would present a sharper portrait of antibody breadth and identify additional binding

determinants for H5.3. These experiments, completed using ELISA or biolayer interferometry, could help inform on the accuracy of predicting the ability of an antibody to bind HA based on sequence.

As described in Chapter IV, affinity maturation did not have large effect on the affinity of $H5.3_m$ for VN/1203 H5hd. The binding breadth of $H5.3_{uca}$ could be tested against a panel of H5s from different H5N1 field strains. This would indicate if the H5.3 germline would be appropriate target for a H5N1 vaccine development, similar to studies using germline-targeting immunogens to produce broadly neutralizing HIV antibodies (Jardine et al., 2016; 2013; McGuire et al., 2013).

Utilization of the H5 purification method for other bacterially expressed HA head domains

In Chapter II, I outlined a novel method for H5 head domain purification. The fast, cost effective method yields a large quantity of properly folded protein (~20mg/L). This purification method could be applied to other bacterially expressed HA head domain constructs. Although these proteins would lack glycosylation, and therefore not be appropriate for primary binding characterizations, they would be useful for crystallization and affinity studies.

Determination of the role of the H5.3 somatic mutations

In Chapter IV, I showed the $H5.3_{uca}$ is able to bind H5hd with high affinity (~30 nM), however it is not currently known if $H5.3_{uca}$ is capable of neutralizing VN/1203 H5N1 virus or if the somatic mutations affect how H5.3 binds H5hd. The ability of $H5.3_{uca}$ to neutralize VN/1203 H5N1 will be determined using a microneutralization assay, as I have already demonstrated $H5.3_{uca}$ binds VN/1203 H5hd. Studies have characterized mouse UCA antibodies that are capable of

binding and neutralizing viruses (Harada et al., 2003; Kalinke et al., 1996; 2000). This experiment will determine if $H5.3_{uca}$, a germline-encoded antibody is capable of neutralizing VN/1203 H5N1. To determine how the somatic mutations affect H5.3 binding to H5, the structure of the $H5.3_{uca}$ Fab H5hd complex could be determined. I have already obtained crystals from trays containing the $H5.3_{uca}$ Fab H5hd complex (Figure V-1). This structure would inform if the somatic mutations affect the interaction between the antibody and H5 and provide further insight into the effect of affinity maturation on H5.3.

The data presented in Chapter IV shows the somatic mutations in H5.3 do not contact H5, do not preconfigure the antibody-combining site, and only have a small effect on increasing the affinity of H5.3 for H5. Therefore, these mutations may be involved in increasing the stability or decreasing the polyspecificity of the antibody. Studies have shown some of the somatic mutations not involved in increasing the affinity of the antibody for the antigen are involved in increasing the thermodynamic stability of the antibody (Sun et al., 2013; Wang et al., 2013). A ThermoFluor assay could be used to determine if the somatic mutations increase the stability of the antibody. In order to determine if the somatic mutations decrease the polyspecificity of the antibody, $H5.3_{uca}$ will be tested to determine if it is an autoreactive antibody. Taken together these data will indicate the role of the H5.3 somatic mutations.

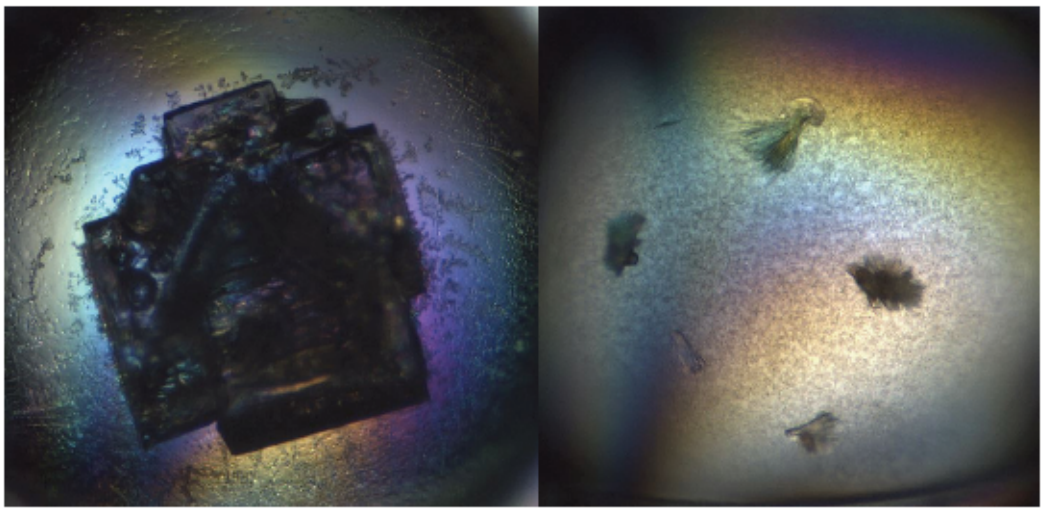

Figure V-1. Crystallization of H5.3$_{uca}$ H5hd complex. The panels above show crystals formed in wells containing the H5.3$_{uca}$ Fab H5hd complex.

Examination of H5.3 flexibility using X-ray crystallography

As outlined in Chapters III and IV, H5.3 is a flexible antibody and maintains its flexibility after affinity maturation, as evidenced by the liganded and unliganded $H5.3_m$ and $H5.3_{uca}$ structures. Other flexible antibodies have been described, with varying degrees of flexibility, involving small movements of CDR positions, large conformational changes in the CDR loops, changes in the orientations of the HC and LC variable domains relative to each other, or a combination of the three (Bhat et al., 1990; Herron et al., 1991; Käiväräinen et al., 1981; Rini et al., 1992; Stanfield et al., 1993).

In order to further examine the flexibility of H5.3 and ensure the conformation of unliganded $H5.3_m$ was not a crystal-packing artifact, I determined an additional structure of unliganded $H5.3_m$ in a different space group. The initial unliganded structure was determined using recombinant H5.3 Fab (rH5.3) expressed in 293F cells. However, the complex structure was obtained from crystals containing H5.3 Fab produced by hybridoma cells and digested with papain (hH5.3). As the rH5.3 Fab only crystallized in one crystal-packing conformation in many different conditions, I used the hH5.3 Fab for this set of crystallization studies.

I have determined the structure of unliganded hH5.3 Fab to 3.4 Å in the $P6_3$ space group, different from the $P6_1$ space group of rH5.3 Fab. Refinement and data statistics for the unrefined structure are given in Table V-1. While these two structures have different crystal contacts (Figure II-5, V-2), they are overall very similar with an RMSD of 0.27 Å between main chain atoms. This confirms the structure of unliganded rH5.3 Fab was not due to crystal contacts.

Table V-1. Data collection, phasing, and refinement

Data collection	
Space group	$P6_3$
Cell dimensions	
a, b, c (Å)	149.85, 149.85, 72.69
α, β, γ (°)	90, 90, 120
Wavelength	0.97856
Resolution (Å)*	3.40 (3.49-3.40)
Completeness (%)*	99.8 (99.7)
Redundancy*	15.2 (14.6)
I/sigmal*	23.6 (3.8)
Refinement	
Resolution (Å)	3.40
No. reflections	12,766
No. reflections free set	701
R_{work} / R_{free} % $^{\$,\#}$	44.93/46.37
No. atoms	
Protein	3,211
Water	0
R.m.s deviations	
Bond lengths (Å)	0.016
Bond angles (°)	1.642
Ramachandran Plot	93.41% favored 0.71% outliers

* Parentheses indicate outer-shell statistics.

$^{\$}$ $R_{cryst} = \Sigma hkl \left| Fo - Fc \right| / \Sigma hkl \left| Fo \right|$, where Fo and Fc are the observed and calculated structure factors.

$^{\#}$ R_{free} was calculated as for R_{cryst}, but using 5% of data, randomly chosen and excluded from refinement.

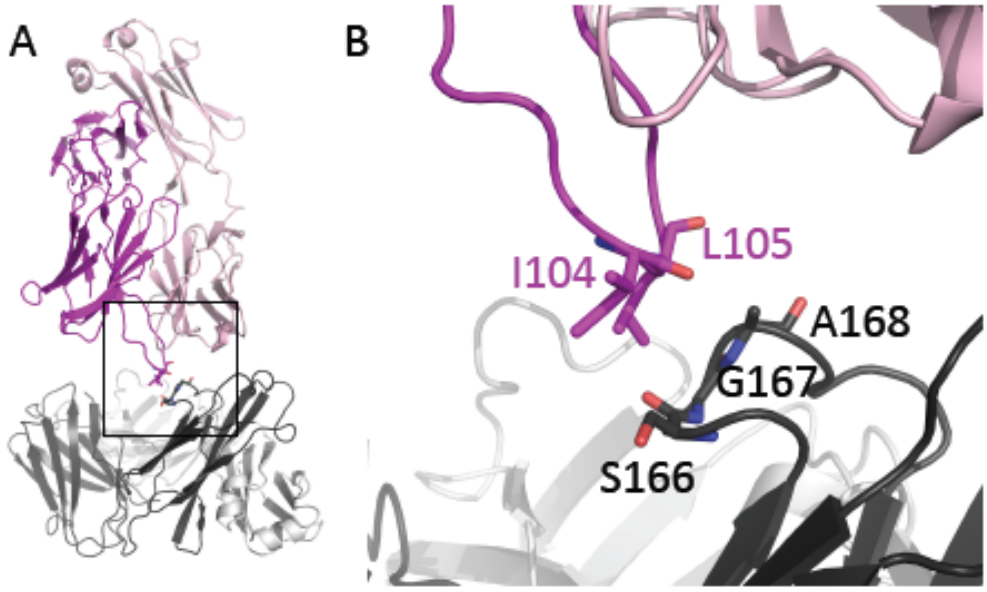

Figure V-2. Crystal contacts in hH5.3 structure. (A) Two symmetry mates in the hH5.3 Fab structure. LC, light pink, white; HC, purple, dark grey. (B) Enlarged view of area outlined in the box in A. The CDRH3 of one copy packed against the HC constant region of another hH5.3 Fab molecule. Residues involved are labeled. Black, HC residues; magenta, HC residues.

Examination of H5.3 flexibility using NMR

The three H5.3 crystal structures described in Chapters II, III, and IV, liganded and unliganded $H5.3_m$ and $H5.3_{uca}$, have demonstrated the inherent flexibility of H5.3. All of these structures were determined using x-ray crystallography, a method that freezes the protein in a single conformation. In order to further characterize the flexibility of H5.3, methods that can provide information on protein dynamics, such as NMR or molecular dynamics, could be used. NMR has been successfully used to study the flexibility of other antibodies (Wilson and Stanfield, 1994). This would provide further insight into the flexibility exhibited by H5.3.

Does H5.3 flexibility confer an advantage?

In order to determine if the flexibility of H5.3 is advantageous for the antibody, computational structural biology methods could be used to "lock" the antibody in the liganded conformation. The antibody construct could then be synthesized, expressed, purified, and tested to determine its conformation using NMR. The "locked" antibody would then be tested and compared with $H5.3_m$ in terms of neutralization and binding breadth.

Analysis of H5.3 gene usage

The experiments completed in Chapter IV, showed $H5.3_{uca}$ binds VN/1203 H5hd, a novel human pathogen. Deep sequencing data of the antibody repertoire of H5-naïve subjects will be analyzed in order to determine the frequency of this specific gene recombination. The results from this analysis will indicate if this gene rearrangement occurs at the statistically expected frequency.

Analysis of novel influenza-specific neutralizing antibody lineages

A key observation presented in Chapter III is broadly neutralizing antibodies (bnAbs) are more heavily mutated than specific Abs. Other studies have shown influenza antibodies with high levels of somatic mutations are indicative of an antibody recall response and prior immune history can shape the antibody response to antigens with shared homology, such as HA (Li et al., 2013; Schmidt et al., 2015; Tan et al., 2015; Wrammert et al., 2011).

In order to better understand the pathway to a broadly neutralizing antibody, the lineages of broadly neutralizing antibody lineages and antibodies against novel influenza viruses could be examined. This type of experiments has been carried out for bnAbs against HIV and influenza, but more research is necessary (Schmidt et al., 2015; Wu et al., 2015). The breadth, affinity, and footprint of the antibody on the antigen could then be tested for these lineages. I would expect as the antibody acquires more somatic mutations the breadth and affinity would increase, while the size of the footprint would decrease. H5.3 has been characterized as potent and specific antibody; the footprint of the antibody on H5 is 810 $Å^2$. This is on the high end of size of footprints of broadly neutralizing influenza antibodies, which range from 490 $Å^2$ - 820 $Å^2$ (Lee et al., 2014). The small footprint of the bnAbs on HA is because these antibodies interact with the highly conserved regions on HA and avoid contact with polymorphic residues. These experiments would provide more insight on the development of anti-influenza antibodies.

These studies could also inform the best method to elicit antibodies to novel influenza viruses, either through germline-targeting to recruit naïve B cells or activating memory B cells using a specific immunogen (Dosenovic et al., 2015; Jardine et al., 2015; 2016).

REFERENCES

Adams, P.D., Grosse-Kunstleve, R.W., Hung, L.W., Ioerger, T.R., McCoy, A.J., Moriarty, N.W., Read, R.J., Sacchettini, J.C., Sauter, N.K., and Terwilliger, T.C. (2002). PHENIX: building new software for automated crystallographic structure determination. Acta Crystallogr. D Biol. Crystallogr. *58*, 1948–1954.

Aguilar-Yáñez, J.M., Portillo-Lara, R., Mendoza-Ochoa, G.I., García-Echauri, S.A., López-Pacheco, F., Bulnes-Abundis, D., Salgado-Gallegos, J., Lara-Mayorga, I.M., Webb-Vargas, Y., León-Angel, F.O., et al. (2010). An Influenza A/H1N1/2009 Hemagglutinin Vaccine Produced in Escherichia coli. PLoS ONE *5*, e11694.

Aiyegbo, M.S., Eli, I.M., Spiller, B.W., Williams, D.R., Kim, R., Lee, D.E., Liu, T., Li, S., Stewart, P.L., and Crowe, J.E. (2013a). Differential Accessibility of a Rotavirus VP6 Epitope in Trimers Comprising Type I, II, or III Channels as Revealed by Binding of a Human Rotavirus VP6-Specific Antibody. Journal of Virology *88*, 469–476.

Aiyegbo, M.S., Sapparapu, G., Spiller, B.W., Eli, I.M., Williams, D.R., Kim, R., Lee, D.E., Liu, T., Li, S., Woods, V.L., et al. (2013b). Human rotavirus VP6-specific antibodies mediate intracellular neutralization by binding to a quaternary structure in the transcriptional pore. PLoS ONE *8*, e61101.

Alam, S.M., Liao, H.-X., Dennison, S.M., Jaeger, F., Parks, R., Anasti, K., Foulger, A., Donathan, M., Lucas, J., Verkoczy, L., et al. (2011). Differential reactivity of germ line allelic variants of a broadly neutralizing HIV-1 antibody to a gp41 fusion intermediate conformation. Journal of Virology *85*, 11725–11731.

Assarsson, E., Bui, H.-H., Sidney, J., Zhang, Q., Glenn, J., Oseroff, C., Mbawuike, I.N., Alexander, J., Newman, M.J., Grey, H., et al. (2008). Immunomic analysis of the repertoire of T-cell specificities for influenza A virus in humans. Journal of Virology *82*, 12241–12251.

Babor, M., and Kortemme, T. (2009). Multi-constraint computational design suggests that native sequences of germline antibody H3 loops are nearly optimal for conformational flexibility. Proteins: Structure, Function, and Bioinformatics *75*, 846–858.

Banerjee, I., Yamauchi, Y., Helenius, A., and Horvath, P. (2013). High-content analysis of sequential events during the early phase of influenza A virus infection. PLoS ONE *8*, e68450–e68450.

Barbey-Martin, C., Gigant, B., Bizebard, T., Calder, L.J., Wharton, S.A., Skehel, J.J., and Knossow, M. (2002). An Antibody That Prevents the Hemagglutinin Low pH Fusogenic Transition. Virology *294*, 70–74.

Belshe, R.B., Frey, S.E., Graham, I.L., Anderson, E.L., Jackson, L.A., Spearman, P., Edupuganti, S., Mulligan, M.J., Rouphael, N., Winokur, P., et al. (2014). Immunogenicity of Avian Influenza A/Anhui/01/2005(H5N1) Vaccine With MF59 Adjuvant. Jama *312*, 1420–1428.

Belshe, R.B., Frey, S.E., Graham, I., Mulligan, M.J., Edupuganti, S., Jackson, L.A., Wald, A., Poland, G., Jacobson, R., Keyserling, H.L., et al. (2011). Safety and immunogenicity of influenza A H5 subunit vaccines: effect of vaccine schedule and antigenic variant. J. Infect. Dis. *203*, 666–673.

Bentebibel, S.-E., Lopez, S., Obermoser, G., Schmitt, N., Mueller, C., Harrod, C., Flano, E., Mejias, A., Albrecht, R.A., Blankenship, D., et al. (2013). Induction of ICOS+CXCR3+CXCR5+ TH cells correlates with antibody responses to influenza vaccination. Sci Transl Med *5*, 176ra32.

Berhanu, A., Wilson, R.L., Kirkwood-Watts, D.L., King, D.S., Warren, T.K., Lund, S.A., Brown, L.L., Krupkin, A.K., VanderMay, E., Weimers, W., et al. (2008). Vaccination of BALB/c mice with Escherichia coli-expressed vaccinia virus proteins A27L, B5R, and D8L protects mice from lethal vaccinia virus challenge. Journal of Virology *82*, 3517–3529.

Bernstein, D.I., Edwards, K.M., Dekker, C.L., Belshe, R., Talbot, H.K.B., Graham, I.L., Noah, D.L., He, F., and Hill, H. (2008). Effects of adjuvants on the safety and immunogenicity of an avian influenza H5N1 vaccine in adults. J. Infect. Dis. *197*, 667–675.

Beyer, W.E.P., Palache, A.M., de Jong, J.C., and Osterhaus, A.D.M.E. (2002). Cold-adapted live influenza vaccine versus inactivated vaccine: systemic vaccine reactions, local and systemic antibody response, and vaccine efficacy. A meta-analysis. Vaccine *20*, 1340–1353.

Bhat, T.N., Bentley, G.A., Fischmann, T.O., Boulot, G., and Poljak, R.J. (1990). Small rearrangements in structures of Fv and Fab fragments of antibody D 1.3 on antigen binding. Nature *347*, 483–485.

Biesova, Z., Miller, M.A., Schneerson, R., Shiloach, J., Green, K.Y., Robbins, J.B., and Keith, J.M. (2009). Preparation, characterization, and immunogenicity in mice of a recombinant influenza H5 hemagglutinin vaccine against the avian H5N1 A/Vietnam/1203/2004 influenza virus. Vaccine *27*, 6234–6238.

Bizebard, T., Benoit, G., Rigolet, P., Rasmussen, B., Diat, O., Bosecke, P., Wharton, S.A., Skehel, J.J., and Knossow, M. (1995). Structure of influenza virus haemagglutinin complexed with a neutralizing antibody. Nature *376*, 92–94.

Bommakanti, G., Citron, M.P., Hepler, R.W., Callahan, C., Heidecker, G.J., Najar, T.A., Lu, X., Joyce, J.G., Shiver, J.W., Casimiro, D.R., et al. (2010). Design of an HA2-based Escherichia coli expressed influenza immunogen that protects mice from pathogenic challenge. Proc Natl Acad Sci USA *107*, 13701–13706.

Bouvier, N.M., and Palese, P. (2008). The biology of influenza viruses. Vaccine *26*, D49–D53.

Brandt, V.L., and Roth, D.B. (2004). V(D)J recombination: how to tame a transposase. Immunol Rev *200*, 249–260.

Brünger, A.T., Adams, P.D., and Rice, L.M. (1997). New applications of simulated annealing in X-ray crystallography and solution NMR. Structure *5*, 325–336.

Bullough, P.A., Hughson, F.M., Skehel, J.J., and Wiley, D.C. (1994). Structure of influenza haemagglutinin at the pH of membrane fusion. Nature *371*, 37–43.

Burton, D.R., Poignard, P., Stanfield, R.L., and Wilson, I.A. (2012). Broadly neutralizing antibodies present new prospects to counter highly antigenically diverse viruses. Science *337*, 183–186.

Carnell, G.W., Ferrara, F., Grehan, K., Thompson, C.P., and Temperton, N.J. (2015). Pseudotype-based neutralization assays for influenza: a systematic analysis. Front Immunol *6*, 161.

Carr, C.M., and Kim, P.S. (1993). A spring-loaded mechanism for the conformational change of influenza hemagglutinin. Cell *73*, 823–832.

Carrat, F., and Flahault, A. (2007). Influenza vaccine: the challenge of antigenic drift. Vaccine *25*, 6852–6862.

Caton, A.J., Brownlee, G.G., Yewdell, J.W., and Gerhard, W. (1982). The antigenic structure of the influenza virus A/PR/8/34 hemagglutinin (H1 subtype). Cell *31*, 417–427.

Centers for Disease Control and Prevention (CDC) (2008). Prevention and Control of Influenza. Mmwr *57*, 1–64.

Chen, H., Yuan, H., Gao, R., Zhang, J., Wang, D., Xiong, Y., Fan, G., Yang, F., Li, X., Zhou, J., et al. (2014). Clinical and epidemiological characteristics of a fatal case of avian influenza A H10N8 virus infection: a descriptive study. Lancet *383*, 714–721.

Chen, J., Skehel, J.J., and Wiley, D.C. (1999). N-and C-terminal residues combine in the fusion-pH influenza hemagglutinin HA2 subunit to form an N cap that terminates the triple-stranded coiled coil. Proceedings of the National … *96*, 8967–8972.

Chiu, F.-F., Venkatesan, N., Wu, C.-R., Chou, A.-H., Chen, H.-W., Lian, S.-P., Liu, S.-J., Huang, C.-C., Lian, W.-C., Chong, P., et al. (2009). Biochemical and Biophysical Research Communications. Biochemical and Biophysical Research Communications *383*, 27–31.

Choung U Kim, Willard Lew, Matthew A Williams, Hongtao Liu, Lijun Zhang, S Swaminathan, Norbert Bischofberger, Ming S Chen, Dirk B Mendel, Chun Y Tai, et al. (1997). Influenza Neuraminidase Inhibitors Possessing a Novel Hydrophobic Interaction in the Enzyme Active Site: Design, Synthesis, and Structural Analysis of Carbocyclic Sialic Acid Analogues with Potent Anti-Influenza Activity. Journal of the American Chemical Society *119*, 681–690.

Claas, E.C., Osterhaus, A.D., van Beek, R., De Jong, J.C., Rimmelzwaan, G.F., Senne, D.A., Krauss, S., Shortridge, K.F., and Webster, R.G. (1998). Human influenza A H5N1 virus related to a highly pathogenic avian influenza virus. The Lancet *351*, 472–477.

Class, E.C.J., de Jong, J.C., van Beek, R., Rimmelzwaan, G.F., and Osterhaus, A.D.M.E. (1998). Human influenza virus A/HongKong/156/97 (H5N1) infection. Vaccine *16*, 977–978.

Colman, P.M. (1994). Influenza virus neuraminidase: structure, antibodies, and inhibitors. Protein Sci. *3*, 1687–1696.

Connor, R.J., Kawaoka, Y., Webster, R.G., and Paulson, J.C. (1994). Receptor specificity in human, avian, and equine H2 and H3 influenza virus isolates. Virology *205*, 17–23.

Corti, D., Voss, J., Gamblin, S.J., Codoni, G., Macagno, A., Jarrossay, D., Vachieri, S.G., Pinna, D., Minola, A., Vanzetta, F., et al. (2011). A Neutralizing Antibody Selected from Plasma Cells That Binds to Group 1 and Group 2 Influenza A Hemagglutinins. Science *333*, 850–856.

Couceiro, J.N., Paulson, J.C., and Baum, L.G. (1993). Influenza virus strains selectively recognize sialyloligosaccharides on human respiratory epithelium; the role of the host cell in selection of hemagglutinin receptor specificity. Virus Res. *29*, 155–165.

Couch, R.B., and Kasel, J.A. (1983). Immunity to influenza in man. Annu. Rev. Microbiol. *37*, 529–549.

Couch, R.B., Kasel, J.A., Gerin, J.L., Schulman, J.L., and Kilbourne, E.D. (1974). Induction of partial immunity to influenza by a neuraminidase-specific vaccine. J. Infect. Dis. *129*, 411–420.

Cox, N.J., and Subbarao, K. (1999). Influenza. Lancet *354*, 1277–1282.

Cox, R.J., Brokstad, K.A., and Ogra, P. (2004). Influenza virus: immunity and vaccination strategies. Comparison of the immune response to inactivated and live, attenuated influenza vaccines. Scand. J. Immunol. *59*, 1–15.

Cretescu, L., Beare, A.S., and Schild, G.C. (1978). Formation of antibody to matrix protein in experimental human influenza A virus infections. Infect. Immun. *22*, 322–327.

Crotty, S. (2014). T Follicular Helper Cell Differentiation, Function, and Roles in Disease. Immunity *41*, 529–542.

Dawood, F.S., Jain, S., Finelli, L., Shaw, M.W., Lindstrom, S., Garten, R.J., Gubareva, L.V., Xu, X., Bridges, C.B., and Uyeki, T.M. (2009). Emergence of a novel swine-origin influenza A (H1N1) virus in humans. N Engl J Med *360*, 2605–2615.

de Jong, J.C., Beyer, W.E., Palache, A.M., Rimmelzwaan, G.F., and Osterhaus, A.D. (2000a). Mismatch between the 1997/1998 influenza vaccine and the major epidemic A(H3N2) virus strain as the cause of an inadequate vaccine-induced antibody response to this strain in the elderly. J. Med. Virol. *61*, 94–99.

de Jong, J.C., Rimmelzwaan, G.F., Fouchier, R.A., and Osterhaus, A.D. (2000b). Influenza virus: a master of metamorphosis. J. Infect. *40*, 218–228.

De Silva, N.S., and Klein, U. (2015). Dynamics of B cells in germinal centres. Nature Reviews Immunology *15*, 137–148.

de Vries, R.P., Zhu, X., McBride, R., Rigter, A., Hanson, A., Zhong, G., Hatta, M., Xu, R., Yu, W., Kawaoka, Y., et al. (2014). Hemagglutinin receptor specificity and structural analyses of respiratory droplet-transmissible H5N1 viruses. Journal of Virology *88*, 768–773.

Deliyannis, G., Jackson, D.C., Ede, N.J., Zeng, W., Hourdakis, I., Sakabetis, E., and Brown, L.E. (2002). Induction of long-term memory CD8(+) T cells for recall of viral clearing responses against influenza virus. Journal of Virology *76*, 4212–4221.

DiLillo, D.J., Tan, G.S., Palese, P., and Ravetch, J.V. (2014). Broadly neutralizing hemagglutinin stalk-specific antibodies require FcγR interactions for protection against influenza virus in vivo. Nat Med *20*, 143–151.

Dogan, I., Bertocci, B., Vilmont, V., Delbos, F., Mégret, J., Storck, S., Reynaud, C.-A., and Weill, J.-C. (2009). Multiple layers of B cell memory with different effector functions. Nat. Immunol. *10*, 1292–1299.

Dosenovic, P., Boehmer, von, L., Escolano, A., and Jardine, J. (2015). Immunization for HIV-1 broadly neutralizing antibodies in human Ig knockin mice. Cell *161*, 1505–1515.

Dreyfus, C., Ekiert, D.C., and Wilson, I.A. (2013). Structure of a Classical Broadly Neutralizing Stem Antibody in Complex with a Pandemic H2 Influenza Virus Hemagglutinin. Journal of Virology *87*, 7149–7154.

Dreyfus, C., Laursen, N.S., Kwaks, T., Zuijdgeest, D., Khayat, R., Ekiert, D.C., Lee, J.H., Metlagel, Z., Bujny, M.V., Jongeneelen, M., et al. (2012). Highly conserved protective epitopes on influenza B viruses. Science *337*, 1343–1348.

DuBois, R.M., Aguilar-Yanez, J.M., Mendoza-Ochoa, G.I., Oropeza-Almazan, Y., Schultz-Cherry, S., Alvarez, M.M., White, S.W., and Russell, C.J. (2010). The Receptor-Binding Domain of Influenza Virus Hemagglutinin Produced in Escherichia coli Folds into Its Native, Immunogenic Structure. Journal of Virology *85*, 865–872.

Durocher, Y., Perret, S., and Kamen, A. (2002). High-level and high-throughput recombinant protein production by transient transfection of suspension-growing human 293-EBNA1 cells. Nucleic Acids Res. *30*, E9.

Eichelberger, M.C., Wang, M.L., Allan, W., Webster, R.G., and Doherty, P.C. (1991). Influenza virus RNA in the lung and lymphoid tissue of immunologically intact and CD4-depleted mice. J. Gen. Virol. *72 (Pt 7)*, 1695–1698.

Ekiert, D.C., Friesen, R.H.E., Bhabha, G., Kwaks, T., Jongeneelen, M., Yu, W., Ophorst, C., Cox, F., Korse, H.J.W.M., Brandenburg, B., et al. (2011). A Highly Conserved Neutralizing Epitope on Group 2 Influenza A Viruses. Science *333*, 843–850.

Ekiert, D.C., Bhabha, G., Elsliger, M.-A., Friesen, R.H.E., Jongeneelen, M., Throsby, M., Goudsmit, J., and Wilson, I.A. (2009). Antibody recognition of a highly conserved influenza virus epitope. Science *324*, 246–251.

Ekiert, D.C., Kashyap, A.K., Steel, J., Rubrum, A., Bhabha, G., Khayat, R., Lee, J.H., Dillon, M.A., O'Neil, R.E., Faynboym, A.M., et al. (2012). Cross-neutralization of influenza A viruses mediated by a single antibody loop. Nature *488*, 526–532.

Elhanati, Y., Sethna, Z., Marcou, Q., Callan, C.G., Mora, T., and Walczak, A.M. (2015). Inferring processes underlying B-cell repertoire diversity. Philos. Trans. R. Soc. Lond., B, Biol. Sci. *370*.

Emsley, P., and Cowtan, K. (2004). Coot: model-building tools for molecular graphics. Acta Crystallogr. D Biol. Crystallogr. *60*, 2126–2132.

Epstein, S.L., Misplon, J.A., Lawson, C.M., Subbarao, E.K., Connors, M., and Murphy, B.R. (1993). Beta 2-microglobulin-deficient mice can be protected against influenza A infection by vaccination with vaccinia-influenza recombinants expressing hemagglutinin and neuraminidase. Journal of Immunology (Baltimore, Md. : 1950) *150*, 5484–5493.

Evans, P. (2006). Scaling and assessment of data quality. Acta Crystallogr. D Biol. Crystallogr. *62*, 72–82.

Fang, M., Cheng, H., Dai, Z., Bu, Z., and Sigal, L.J. (2006). Immunization with a single extracellular enveloped virus protein produced in bacteria provides partial protection from a lethal orthopoxvirus infection in a natural host. Virology *345*, 231–243.

Fiore, A.E., Fry, A., Shay, D., Gubareva, L., Bresee, J.S., Uyeki, T.M., Centers for Disease Control and Prevention (CDC) (2011). Antiviral agents for the treatment and chemoprophylaxis of influenza --- recommendations of the Advisory Committee on Immunization Practices (ACIP). MMWR Recomm Rep *60*, 1–24.

Fouchier, R.A.M., Munster, V., Wallensten, A., Bestebroer, T.M., Herfst, S., Smith, D., Rimmelzwaan, G.F., Olsen, B., and Osterhaus, A.D.M.E. (2005). Characterization of a Novel Influenza A Virus Hemagglutinin Subtype (H16) Obtained from Black-Headed Gulls. Journal of Virology *79*, 2814–2822.

Fouchier, R.A.M., Schneeberger, P.M., Rozendaal, F.W., Broekman, J.M., Kemink, S.A.G., Munster, V., Kuiken, T., Rimmelzwaan, G.F., Schutten, M., Van Doornum, G.J.J., et al. (2004). Avian influenza A virus (H7N7) associated with human conjunctivitis and a fatal case of acute respiratory distress syndrome. Proc. Natl. Acad. Sci. U.S.a. *101*, 1356–1361.

Friesen, R.H.E., Lee, P.S., Stoop, E.J.M., Hoffman, R.M.B., Ekiert, D.C., Bhabha, G., Yu, W., Juraszek, J., Koudstaal, W., Jongeneelen, M., et al. (2014). A common solution to group 2 influenza virus neutralization. Proc. Natl. Acad. Sci. U.S.a. *111*, 445–450.

Gao, R., Cao, B., Hu, Y., Feng, Z., Wang, D., Hu, W., Chen, J., Jie, Z., Qiu, H., Xu, K., et al. (2013). Human infection with a novel avian-origin influenza A (H7N9) virus. N Engl J Med *368*, 1888–1897.

Garten, R.J., Davis, C.T., Russell, C.A., Shu, B., Lindstrom, S., Balish, A., Sessions, W.M., Xu, X., Skepner, E., Deyde, V., et al. (2009). Antigenic and Genetic Characteristics of Swine-Origin 2009 A(H1N1) Influenza Viruses Circulating in Humans. Science *325*, 197–201.

Gerhard, W. (1976). The analysis of the monoclonal immune response to influenza virus. II. The antigenicity of the viral hemagglutinin. J. Exp. Med. *144*, 985–995.

Harada, Y., Muramatsu, M., Shibata, T., Honjo, T., and Kuroda, K. (2003). Unmutated immunoglobulin M can protect mice from death by influenza virus infection. J. Exp. Med. *197*, 1779–1785.

Harrison, S.C. (2008). Viral membrane fusion. Nat Struct Mol Biol *15*, 690–698.

Hashimoto, G., Wright, P.F., and Karzon, D.T. (1983). Antibody-dependent cell-mediated cytotoxicity against influenza virus-infected cells. J. Infect. Dis. *148*, 785–794.

Herfst, S., Schrauwen, E.J.A., Linster, M., Chutinimitkul, S., de Wit, E., Munster, V.J., Sorrell, E.M., Bestebroer, T.M., Burke, D.F., Smith, D.J., et al. (2012). Airborne Transmission of Influenza A/H5N1 Virus Between Ferrets. Science *336*, 1534–1541.

Herron, J.N., He, X.M., Ballard, D.W., Blier, P.R., Pace, P.E., Bothwell, A.L., Voss, E.W., and Edmundson, A.B. (1991). An autoantibody to single-stranded DNA: comparison of the three-dimensional structures of the unliganded Fab and a deoxynucleotide-Fab complex. Proteins *11*, 159–175.

Ho, Y.-C., Wang, J.-L., Wang, J.-T., Wu, U.-I., Chang, C.-W., Wu, H.-S., Chen, C.-H., Chuang, Y.-M., and Chang, S.-C. (2009). Prognostic factors for fatal adult influenza pneumonia. Journal of Infection *58*, 439–445.

Hoft, D.F., Babusis, E., Worku, S., Spencer, C.T., Lottenbach, K., Truscott, S.M., Abate, G., Sakala, I.G., Edwards, K.M., Creech, C.B., et al. (2011). Live and inactivated influenza vaccines induce similar humoral responses, but only live vaccines induce diverse T-cell responses in young children. J. Infect. Dis. *204*, 845–853.

Holt, P.G., Strickland, D.H., Wikström, M.E., and Jahnsen, F.L. (2008). Regulation of immunological homeostasis in the respiratory tract. Nature Reviews Immunology *8*, 142–152.

Hong, M., Lee, P.S., Hoffman, R.M.B., Zhu, X., Krause, J.C., Laursen, N.S., Yoon, S.I., Song, L., Tussey, L., Crowe, J.E., et al. (2013). Antibody Recognition of the Pandemic H1N1 Influenza Virus Hemagglutinin Receptor Binding Site. Journal of Virology *87*, 12471–12480.

Howarth, M., and Ting, A.Y. (2008). Imaging proteins in live mammalian cells with biotin ligase and monovalent streptavidin. Nat Protoc *3*, 534–545.

Huber, V.C., Lynch, J.M., Bucher, D.J., Le, J., and Metzger, D.W. (2001). Fc receptor-mediated phagocytosis makes a significant contribution to clearance of influenza virus infections. Journal of Immunology (Baltimore, Md. : 1950) *166*, 7381–7388.

Iba, Y., Fujii, Y., Ohshima, N., Sumida, T., Kubota-Koketsu, R., Ikeda, M., Wakiyama, M., Shirouzu, M., Okada, J., Okuno, Y., et al. (2014). Conserved Neutralizing Epitope at Globular Head of Hemagglutinin in H3N2 Influenza Viruses. Journal of Virology *88*, 7130–7144.

Imai, M., Watanabe, T., Hatta, M., Das, S.C., Ozawa, M., Shinya, K., Zhong, G., Hanson, A., Katsura, H., Watanabe, S., et al. (2012). Experimental adaptation of an influenza H5 HA confers respiratory droplet transmission to a reassortant H5 HA/H1N1 virus in ferrets. Nature *486*, 420–428.

Itzstein, von, M., Wu, W.Y., Kok, G.B., Pegg, M.S., Dyason, J.C., Jin, B., Van Phan, T., Smythe, M.L., White, H.F., and Oliver, S.W. (1993). Rational design of potent sialidase-based inhibitors of influenza virus replication. Nature *363*, 418–423.

Jameson, J., Cruz, J., and Ennis, F.A. (1998). Human cytotoxic T-lymphocyte repertoire to influenza A viruses. Journal of Virology *72*, 8682–8689.

Jardine, J.G., Kulp, D.W., Havenar-Daughton, C., Sarkar, A., Briney, B., Sok, D., Sesterhenn, F., Ereño-Orbea, J., Kalyuzhniy, O., Deresa, I., et al. (2016). HIV-1 broadly neutralizing antibody precursor B cells revealed by germline-targeting immunogen. Science *351*, 1458–1463.

Jardine, J.G., Ota, T., Sok, D., Pauthner, M., Kulp, D.W., Kalyuzhniy, O., Skog, P.D., Thinnes, T.C., Bhullar, D., Briney, B., et al. (2015). Priming a broadly neutralizing antibody response to HIV-1 using a germline-targeting immunogen. Science *349*, 156–161.

Jardine, J., Julien, J.-P., Menis, S., Ota, T., Kalyuzhniy, O., McGuire, A., Sok, D., Huang, P.-S., MacPherson, S., Jones, M., et al. (2013). Rational HIV immunogen design to target specific germline B cell receptors. Science *340*, 711–716.

Jegaskanda, S., Job, E.R., Kramski, M., Laurie, K., Isitman, G., de Rose, R., Winnall, W.R., Stratov, I., Brooks, A.G., Reading, P.C., et al. (2013). Cross-reactive influenza-specific antibody-dependent cellular cytotoxicity antibodies in the absence of neutralizing antibodies. Journal of Immunology (Baltimore, Md. : 1950) *190*, 1837–1848.

Jin, H., Zhou, H., Liu, H., Chan, W., Adhikary, L., Mahmood, K., Lee, M.-S., and Kemble, G. (2005). Two residues in the hemagglutinin of A/Fujian/411/02-like influenza viruses are responsible for antigenic drift from A/Panama/2007/99. Virology *336*, 113–119.

Johnson, N.P.A.S., and Mueller, J. (2002). Updating the Accounts:Global Mortality of the 1918–1920 “Spanish” Influenza Pandemic. Bulletin of the History of Medicine *76*, 105–115.

Jones, S., and Thornton, J.M. (1996). Principles of protein-protein interactions. Proc Natl Acad Sci USA *93*, 13–20.

Kabsch, W. (2010a). Integration, scaling, space-group assignment and post-refinement. Acta Crystallogr. D Biol. Crystallogr. *66*, 133–144.

Kabsch, W. (2010b). XDS. Acta Crystallogr. D Biol. Crystallogr. *66*, 125–132.

Kalinke, U., Bucher, E.M., Ernst, B., Oxenius, A., and Roost, H.P. (1996). The role of somatic mutation in the generation of the protective humoral immune response against vesicular stomatitis virus. Immunity *5*, 639–652.

Kalinke, U., Oxenius, A., Lopez-Macias, C., Zinkernagel, R.M., and Hengartner, H. (2000). Virus neutralization by germ-line vs. hypermutated antibodies. Proc Natl Acad Sci USA *97*, 10126–10131.

Kandun, I.N., Wibisono, H., Sedyaningsih, E.R., Yusharmen, Hadisoedarsuno, W., Purba, W., Santoso, H., Septiawati, C., Tresnaningsih, E., Heriyanto, B., et al. (2006). Three Indonesian clusters of H5N1 virus infection in 2005. N Engl J Med *355*, 2186–2194.

Karlsson Hedestam, G.B., Fouchier, R.A.M., Phogat, S., Burton, D.R., Sodroski, J., and Wyatt, R.T. (2008). The challenges of eliciting neutralizing antibodies to HIV-1 and to influenza virus. Nat. Rev. Microbiol. *6*, 143–155.

Kawaoka, Y., Krauss, S., and Webster, R.G. (1989). Avian-to-human transmission of the PB1 gene of influenza A viruses in the 1957 and 1968 pandemics. Journal of Virology *63*, 4603–4608.

Käiväräinen, A.I., Rozhkov, S.P., Sykulev YuK, Lavrent'yev, V.V., and Franěk, F. (1981). Hapten-induced changes in pig anti-dansyl antibodies revealed by EPR spectra of spin-labelled antibodies. Immunol. Lett. *3*, 5–11.

Keating, R., Hertz, T., Wehenkel, M., Harris, T.L., Edwards, B.A., McClaren, J.L., Brown, S.A., Surman, S., Wilson, Z.S., Bradley, P., et al. (2013). The kinase mTOR modulates the antibody response to provide cross-protective immunity to lethal infection with influenza virus. Nat. Immunol. *14*, 1266–1276.

Kendal, A.P., Noble, G.R., Skehel, J.J., and Dowdle, W.R. (1978). Anitgenic similarity of influenza A (H1N1) viruses from epidemics in 1977-1978 to "Scandinavian" strains isolated in epidemics of 1950-1951. Virology *89*, 632–636.

Kepler, T.B., Liao, H.X., Alam, S.M., and Bhaskarabhatla, R. (2014). Immunoglobulin gene insertions and deletions in the affinity maturation of HIV-1 broadly reactive neutralizing antibodies. Cell Host and Microbe *16*, 304–313.

Khurana, S., Verma, S., Verma, N., Crevar, C.J., and Carter, D.M. (2010). Properly folded bacterially expressed H1N1 hemagglutinin globular head and ectodomain vaccines protect ferrets against H1N1 pandemic influenza virus. PLoS ONE *5*, e11548.

Kilbourne, E.D., Laver, W.G., Schulman, J.L., and Webster, R.G. (1968). Antiviral activity of antiserum specific for an influenza virus neuraminidase. Journal of Virology *2*, 281–288.

Kilbourne, E.D. (2006). Influenza Pandemics of the 20th Century. Emerging Infectious Diseases *12*, 9.

Klein, F., Mouquet, H., Dosenovic, P., Scheid, J.F., Scharf, L., and Nussenzweig, M.C. (2013). Antibodies in HIV-1 Vaccine Development and Therapy. Science *341*, 1199–1204.

Knossow, M., and Skehel, J.J. (2006). Variation and infectivity neutralization in influenza. Immunology *119*, 1–7.

Koopmans, M., Wilbrink, B., Conyn, M., Natrop, G., van der Nat, H., Vennema, H., Meijer, A., van Steenbergen, J., Fouchier, R., Osterhaus, A., et al. (2004). Transmission of H7N7 avian influenza A virus to human beings during a large outbreak in commercial poultry farms in the Netherlands. Lancet *363*, 587–593.

Krammer, F., and Palese, P. (2015). Advances in the development of influenza virus vaccines. Nat Rev Drug Discov *14*, 167–182.

Kreijtz, J.H.C.M., de Mutsert, G., van Baalen, C.A., Fouchier, R.A.M., Osterhaus, A.D.M.E., and Rimmelzwaan, G.F. (2008). Cross-recognition of avian H5N1 influenza virus by human cytotoxic T-lymphocyte populations directed to human influenza A virus. Journal of Virology *82*, 5161–5166.

Lamb, J.R., Woody, J.N., Hartzman, R.J., and Eckels, D.D. (1982). In vitro influenza virus-specific antibody production in man: antigen-specific and HLA-restricted induction of helper activity mediated by cloned human T lymphocytes. Journal of Immunology (Baltimore, Md. : 1950) *129*, 1465–1470.

Lambert, L.C., and Fauci, A.S. (2010). Influenza Vaccines for the Future. N Engl J Med *363*, 2036–2044.

Laursen, N.S., and Wilson, I.A. (2013). Broadly neutralizing antibodies against influenza viruses. Antiviral Research *98*, 476–483.

Lee, L.Y.-H., Ha, D.L.A., Simmons, C., de Jong, M.D., Chau, N.V.V., Schumacher, R., Peng, Y.C., McMichael, A.J., Farrar, J.J., Smith, G.L., et al. (2008). Memory T cells established by seasonal human influenza A infection cross-react with avian influenza A (H5N1) in healthy individuals. J. Clin. Invest. *118*, 3478–3490.

Lee, P.S., and Wilson, I.A. (2015). Structural characterization of viral epitopes recognized by broadly cross-reactive antibodies. Curr. Top. Microbiol. Immunol. *386*, 323–341.

Lee, P.S., Ohshima, N., Stanfield, R.L., Yu, W., Iba, Y., Okuno, Y., Kurosawa, Y., and Wilson, I.A. (2014). Receptor mimicry by antibody F045–092facilitates universal binding to the H3 subtypeof influenza virus. Nature Communications *5*, 1–9.

Lee, P.S., Yoshida, R., Ekiert, D.C., Sakai, N., Suzuki, Y., Takada, A., and Wilson, I.A. (2012). Heterosubtypic antibody recognition of the influenza virus hemagglutinin receptor binding site enhanced by avidity. Proc. Natl. Acad. Sci. U.S.a. *109*, 17040–17045.

Lefranc, M.P., and Lefranc, G. (2001). The Immunoglobulin FactsBook 2001 (Academic Press).

Lefranc, M.P., Giudicelli, V., Ginestoux, C., Bodmer, J., Muller, W., Bontrop, R., Lemaitre, M., Malik, A., Barbie, V., and Chaume, D. (1999). IMGT, the international ImMunoGeneTics database. Nucleic Acids Res. *27*, 209–212.

Lefranc, M.-P. (1998). IMGT Locus on Focus: A new sections of Experimental and Clinical Immunogenetics. Experimental and Clinical Immunogenetics *15*, 1–7.

Leser, G.P., and Lamb, R.A. (2005). Influenza virus assembly and budding in raft-derived microdomains: a quantitative analysis of the surface distribution of HA, NA and M2 proteins. Virology *342*, 215–227.

Li, Y., Myers, J.L., Bostick, D.L., Sullivan, C.B., Madara, J., Linderman, S.L., Liu, Q., Carter, D.M., Wrammert, J., Esposito, S., et al. (2013). Immune history shapes specificity of pandemic H1N1 influenza antibody responses. J. Exp. Med. *210*, 1493–1500.

Lieber, M.R., Ma, Y., Pannicke, U., and Schwarz, K. (2003). Mechanism and regulation of human non-homologous DNA end-joining. Nat. Rev. Mol. Cell Biol. *4*, 712–720.

Lu, Y., Welsh, J.P., and Swartz, J.R. (2014). Production and stabilization of the trimeric influenza hemagglutinin stem domain for potentially broadly protective influenza vaccines. Proc Natl Acad Sci USA *111*, 125–130.

Ma, W., Kahn, R.E., and Richt, J.A. (2008). The pig as a mixing vessel for influenza viruses: Human and veterinary implications. J Mol Genet Med *3*, 158–166.

Matrosovich, M., Tuzikov, A., Bovin, N., Gambaryan, A., Klimov, A., Castrucci, M.R., Donatelli, I., and Kawaoka, Y. (2000). Early Alterations of the Receptor-Binding Properties of H1, H2, and H3 Avian Influenza Virus Hemagglutinins after Their Introduction into Mammals. Journal of Virology *74*, 8502–8512.

Matrosovich, M.N., Matrosovich, T.Y., Gray, T., Roberts, N.A., and Klenk, H.-D. (2004). Human and avian influenza viruses target different cell types in cultures of human airway epithelium. Proc. Natl. Acad. Sci. U.S.a. *101*, 4620–4624.

Mänz, B., Schwemmle, M., and Brunotte, L. (2013). Adaptation of avian influenza A virus polymerase in mammals to overcome the host species barrier. Journal of Virology *87*, 7200–7209.

McCoy, A.J., Grosse-Kunstleve, R.W., Storoni, L.C., and Read, R.J. (2005). Likelihood-enhanced fast translation functions. Acta Crystallogr. D Biol. Crystallogr. *61*, 458–464.

McGuire, A.T., Hoot, S., Dreyer, A.M., Lippy, A., Stuart, A., Cohen, K.W., Jardine, J., Menis, S., Scheid, J.F., West, A.P., et al. (2013). Engineering HIV envelope protein to activate germline B cell receptors of broadly neutralizing anti-CD4 binding site antibodies. J. Exp. Med. *210*, 655–663.

McLean, G.R., Olsen, O.A., Watt, I.N., Rathanaswami, P., Leslie, K.B., Babcook, J.S., and Schrader, J.W. (2005). Recognition of human cytomegalovirus by human primary immunoglobulins identifies an innate foundation to an adaptive immune response. Journal of Immunology (Baltimore, Md. : 1950) *174*, 4768–4778.

Mosmann, T.R., Cherwinski, H., Bond, M.W., Giedlin, M.A., and Coffman, R.L. (1986). Two types of murine helper T cell clone. I. Definition according to profiles of lymphokine activities and secreted proteins. Journal of Immunology (Baltimore, Md. : 1950) *136*, 2348–2357.

Mulligan, M.J., Bernstein, D.I., Winokur, P., Rupp, R., Anderson, E., Rouphael, N., Dickey, M., Stapleton, J.T., Edupuganti, S., Spearman, P., et al. (2014). Serological responses to an avian influenza A/H7N9 vaccine mixed at the point-of-use with MF59 adjuvant: a randomized clinical trial. Jama *312*, 1409–1419.

Muramatsu, M., Kinoshita, K., Fagarasan, S., and Yamada, S. (2000). Class switch recombination and hypermutation require activation-induced cytidine deaminase (AID), a potential RNA editing enzyme. Cell *102*, 553–563.

Murphy, K.M., Travers, P., and Walport, M. (2007). Janeway's Immunobiology (Garland Science).

Nakanishi, Y., Lu, B., Gerard, C., and Iwasaki, A. (2009). CD8(+) T lymphocyte mobilization to virus-infected tissue requires CD4(+) T-cell help. Nature *462*, 510–513.

Nicholson, K.G., Colegate, A.E., Podda, A., Stephenson, I., Wood, J., Ypma, E., and Zambon, M.C. (2001). Safety and antigenicity of non-adjuvanted and MF59-adjuvanted influenza A/Duck/Singapore/97 (H5N3) vaccine: a randomised trial of two potential vaccines against H5N1 influenza. Lancet *357*, 1937–1943.

Nobusawa, E., Aoyama, T., Kato, H., Suzuki, Y., and Tateno, Y. (1991). Comparison of complete amino acid sequences and receptor-binding properties among 13 serotypes of hemagglutinins of influenza A viruses. Virology *182*, 475–485.

O'Brien, K.B., Morrison, T.E., Dundore, D.Y., Heise, M.T., and Schultz-Cherry, S. (2011). A protective role for complement C3 protein during pandemic 2009 H1N1 and H5N1 influenza A virus infection. PLoS ONE *6*, e17377.

Oettinger, M.A., Schatz, D.G., Gorka, C., and Baltimore, D. (1990). RAG-1 and RAG-2, adjacent genes that synergistically activate V(D)J recombination. Science *248*, 1517–1523.

Okomo-Adhiambo, M., Fry, A.M., Su, S., Nguyen, H.T., Elal, A.A., Negron, E., Hand, J., Garten, R.J., Barnes, J., Xiyan, X., et al. (2015). Oseltamivir-resistant influenza A(H1N1)pdm09 viruses, United States, 2013-14. Emerging Infectious Diseases *21*, 136–141.

Okoye, I.S., and Wilson, M.S. (2011). CD4+ T helper 2 cells - microbial triggers, differentiation requirements and effector functions. Immunology *134*, 368–377.

Okuno, Y., Isegawa, Y., Sasao, F., and Ueda, S. (1993). A common neutralizing epitope conserved between the hemagglutinins of influenza A virus H1 and H2 strains. Journal of Virology *67*, 2552–2558.

Oprea, M., and Perelson, A.S. (1997). Somatic mutation leads to efficient affinity maturation when centrocytes recycle back to centroblasts. Journal of Immunology *158*, 5155–5162.

Osterhaus, A.D., Rimmelzwaan, G.F., Martina, B.E., Bestebroer, T.M., and Fouchier, R.A. (2000). Influenza B virus in seals. Science *288*, 1051–1053.

Ostrowsky, B., Huang, A., Terry, W., Anton, D., Brunagel, B., Traynor, L., Abid, S., Johnson, G., Kacica, M., Katz, J., et al. (2012). Low pathogenic avian influenza A (H7N2) virus infection in immunocompromised adult, New York, USA, 2003. Emerging Infectious Diseases *18*, 1128–1131.

Otwinowski, Z., and Minor, W. (1997). Processing of X-ray diffraction data collected in oscillation mode. Methods in Enzymology *276*, 307–326.

Painter, J., and Merritt, E.A. (2006). Optimal description of a protein structure in terms of multiple groups undergoing TLS motion. Acta Crystallogr. D Biol. Crystallogr. *62*, 439–450.

Palese, P.S., and Shaw, M.L. (2007). Orthomyxoviridae: The viruses and their replication (Philadelphia, PA, USA: Fields Virology).

Palese, P., and Wang, T.T. (2011). Why do influenza virus subtypes die out? A hypothesis. MBio *2*, e00150–11.

Pallikkuth, S., Parmigiani, A., Silva, S.Y., George, V.K., Fischl, M., Pahwa, R., and Pahwa, S. (2012). Impaired peripheral blood T-follicular helper cell function in HIV-infected nonresponders to the 2009 H1N1/09 vaccine. Blood *120*, 985–993.

Pang, I.K., and Iwasaki, A. (2011). Inflammasomes as mediators of immunity against influenza virus. Trends Immunol. *32*, 34–41.

Pecorari, F.E.A. (1999). Folding, Heterodimeric Association and Specific Peptide Recognition of a Murine ab T-cell Receptor Expressed in Escherichia coli. Journal of Molecular Biology *285*, 1831–1843.

Peled, J.U., Kuang, F.L., Iglesias-Ussel, M.D., Roa, S., Kalis, S.L., Goodman, M.F., and Scharff, M.D. (2008). The Biochemistry of Somatic Hypermutation. Annu. Rev. Immunol. *26*, 481–511.

Poland, G.A., Jacobson, R.M., and Targonski, P.V. (2007). Avian and pandemic influenza: an overview. Vaccine *25*, 3057–3061.

Pooran Chand, Pravin L Kotian, Ali Dehghani, Yahya El-Kattan, Tsu-Hsing Lin, Tracy L Hutchison, Y Sudhakar Babu, Shanta Bantia, Arthur J Elliott, A., and Montgomery, J.A. (2001). Systematic Structure-Based Design and Stereoselective Synthesis of Novel Multisubstituted Cyclopentane Derivatives with Potent Antiinfluenza Activity. Journal of Medical Chemistry *44*, 4379–4392.

Potter, C.W., and Oxford, J.S. (1979). Determinants of immunity to influenza infection in man. Br. Med. Bull. *35*, 69–75.

Powers, D.C., Kilbourne, E.D., and Johansson, B.E. (1996). Neuraminidase-specific antibody responses to inactivated influenza virus vaccine in young and elderly adults. Clin. Diagn. Lab. Immunol. *3*, 511–516.

Prabakaran, P., Du, L., Shi, W., Feng, Y., Wang, Y., Wang, L., Li, W., Jiang, S., Dimitrov, D.S., Ying, T., et al. (2015). Junctional and allele-specific residues are criticalfor MERS-CoV neutralization by an exceptionallypotent germline-like antibody. Nature Communications *6*, 1–10.

Rambaut, A., Pybus, O.G., Nelson, M.I., Viboud, C., Taubenberger, J.K., and Holmes, E.C. (2008). The genomic and epidemiological dynamics of human influenza A virus. Nature *453*, 615–619.

Riberdy, J.M., Christensen, J.P., Branum, K., and Doherty, P.C. (2000). Diminished primary and secondary influenza virus-specific CD8(+) T-cell responses in CD4-depleted Ig(-/-) mice. Journal of Virology *74*, 9762–9765.

Rini, J.M., Schulze-Gahmen, U., and Wilson, I.A. (1992). Structural evidence for induced fit as a mechanism for antibody-antigen recognition. Science *255*, 959–965.

Rogers, G.N., Paulson, J.C., Daniels, R.S., Skehel, J.J., Wilson, I.A., and Wiley, D.C. (1983). Single amino acid substitutions in influenza haemagglutinin change receptor binding specificity. Nature *304*, 76–78.

Roth, D.B., and Roth, S.Y. (2000). Unequal access: regulating V(D)J recombination through chromatin remodeling. Cell *103*, 699–702.

Ruigrok, V.J.B., Levisson, M., Eppink, M.H.M., Smidt, H., and van der Oost, J. (2011). Alternative affinity tools: more attractive than antibodies? Biochem. J. *436*, 1–13.

Russell, C.A., Jones, T.C., Barr, I.G., Cox, N.J., Garten, R.J., Gregory, V., Gust, I.D., Hampson, A.W., Hay, A.J., Hurt, A.C., et al. (2008). Influenza vaccine strain selection and recent studies on the global migration of seasonal influenza viruses. Vaccine *26*, D31–D34.

Sanders, C.J., Doherty, P.C., and Thomas, P.G. (2011). Respiratory epithelial cells in innate immunity to influenza virus infection. Cell Tissue Res. *343*, 13–21.

Sauter, N.K., Grosse-Kunstleve, R.W., and Adams, P.D. (2004). Robust indexing for automatic data collection. J Appl Crystallogr *37*, 399–409.

Schatz, D.G., Oettinger, M.A., and Baltimore, D. (1989). The V(D)J recombination activating gene, RAG-1. Cell *59*, 1035–1048.

Schäfer, J.R., Kawaoka, Y., Bean, W.J., Süss, J., Senne, D., and Webster, R.G. (1993). Origin of the pandemic 1957 H2 influenza A virus and the persistence of its possible progenitors in the avian reservoir. Virology *194*, 781–788.

Schmidt, A.G., Do, K.T., McCarthy, K.R., Kepler, T.B., Liao, H.-X., Moody, M.A., Haynes, B.F., and Harrison, S.C. (2015). Immunogenic Stimulus for Germline Precursors of Antibodies that Engage the Influenza Hemagglutinin Receptor-Binding Site. Cell Rep *13*, 2842–2850.

Schmidt, A.G., Xu, H., Khan, A.R., O'Donnell, T., Khurana, S., King, L.R., Manischewitz, J., Golding, H., Suphaphiphat, P., Carfi, A., et al. (2013). Preconfiguration of the antigen-binding site during affinity maturation of a broadly neutralizing influenza virus antibody. Proc. Natl. Acad. Sci. U.S.a. *110*, 264–269.

Scholtissek, C., Hoyningen, Von, V., and Rott, R. (1978a). Genetic relatedness between the new 1977 epidemic strains (H1N1) of influenza and human influenza strains isolated between 1947 and 1957 (H1N1). Virology *89*, 613–617.

Scholtissek, C., Rohde, W., Hoyningen, Von, V., and Rott, R. (1978b). On the origin of the human influenza virus subtypes H2N2 and H3N2. Virology *87*, 13–20.

Shapiro, G.S., Ellison, M.C., and Wysocki, L.J. (2003). Sequence-specific targeting of two bases on both DNA strands by the somatic hypermutation mechanism. Mol. Immunol. *40*, 287–295.

Sheu, T.G., Deyde, V.M., Okomo-Adhiambo, M., Garten, R.J., Xu, X., Bright, R.A., Butler, E.N., Wallis, T.R., Klimov, A.I., and Gubareva, L.V. (2008). Surveillance for neuraminidase inhibitor resistance among human influenza A and B viruses circulating worldwide from 2004 to 2008. Antimicrobial Agents and Chemotherapy *52*, 3284–3292.

Shinya, K., Ebina, M., Yamada, S., Ono, M., Kasai, N., and Kawaoka, Y. (2006). Avian flu: Influenza virus receptors in the human airway. Nature *440*, 435–436.

Skehel, J.J., Bayley, P.M., Brown, E.B., Martin, S.R., Waterfield, M.D., White, J.M., Wilson, I.A., and Wiley, D.C. (1982). Changes in the conformation of influenza virus hemagglutinin at the pH optimum of virus-mediated membrane fusion. Proc. Natl. Acad. Sci. U.S.a. *79*, 968–972.

Skehel, J.J., and Wiley, D.C. (2000). Receptor Binding and Membrane Fusion in Virus Entry: The Influenza Hemagglutinin. Annu. Rev. Biochem. *69*, 531–569.

Smith, D.J., Lapedes, A.S., De Jong, J.C., Bestebroer, T.M., Rimmelzwaan, G.F., Osterhaus, A.D.M.E., and Fouchier, R.A.M. (2004). Mapping the antigenic and genetic evolution of influenza virus. Science *305*, 371–376.

Smith, G.J.D., Vijaykrishna, D., Bahl, J., Lycett, S.J., Worobey, M., Pybus, O.G., Ma, S.K., Cheung, C.L., Raghwani, J., Bhatt, S., et al. (2009). Origins and evolutionary genomics of the 2009 swine-origin H1N1 influenza A epidemic. Nature *459*, 1122–1125.

Song, L., Nakaar, V., Kavita, U., Price, A., Huleatt, J., and Tang, J. (2008a). Efficacious recombinant influenza vaccines produced by high yield bacterial expression: a solution to global pandemic and seasonal needs. PLoS ONE *3*, e2257.

Song, L., Nakaar, V., Kavita, U., Price, A., Huleatt, J., Tang, J., Jacobs, A., Liu, G., Huang, Y., Desai, P., et al. (2008b). Efficacious Recombinant Influenza Vaccines Produced by High Yield Bacterial Expression: A Solution to Global Pandemic and Seasonal Needs. Biochim. Biophys. Acta *1844*, 1891–1906.

Stanfield, R.L., Takimoto-Kamimura, M., Rini, J.M., Profy, A.T., and Wilson, I.A. (1993). Major antigen-induced domain rearrangements in an antibody. Structure *1*, 83–93.

Stanfield, R.L., Zemla, A., Wilson, I.A., and Rupp, B. (2006). Antibody elbow angles are influenced by their light chain class. Journal of Molecular Biology *357*, 1566–1574.

Stevens, J., Blixt, O., Tumpey, T.M., and Taubenberger, J.K. (2006a). Structure and Receptor Specificity of the Hemagglutinin from an H5N1 Influenza Virus. Science *312*, 404–410.

Stevens, J., Blixt, O., Paulson, J.C., and Wilson, I.A. (2006b). Glycan microarray technologies: tools to survey host specificity of influenza viruses. Nat. Rev. Microbiol. *4*, 857–864.

Subbarao, K., Klimov, A., Katz, J., Regnery, H., Lim, W., Hall, H., Perdue, M., Swayne, D., Bender, C., Huang, J., et al. (1998). Characterization of an avian influenza A (H5N1) virus isolated from a child with a fatal respiratory illness. Science *279*, 393–396.

Suguitan, A.L., Cheng, X., Wang, W., Wang, S., Jin, H., and Lu, S. (2011). Influenza H5 hemagglutinin DNA primes the antibody response elicited by the live attenuated influenza A/Vietnam/1203/2004 vaccine in ferrets. PLoS ONE *6*, e21942.

Sui, J., Hwang, W.C., Perez, S., Wei, G., Aird, D., Chen, L.-M., Santelli, E., Stec, B., Cadwell, G., Ali, M., et al. (2009). Structural and functional bases for broad-spectrum neutralization of avian and human influenza A viruses. Nat Struct Mol Biol *16*, 265–273.

Sun, S.B., Sen, S., Kim, N.-J., Magliery, T.J., Schultz, P.G., and Wang, F. (2013). Mutational Analysis of 48G7 Reveals that Somatic Hypermutation Affects Both Antibody Stability and Binding Affinity. Journal of the American Chemical Society *135*, 9980–9983.

Takashita, E., Meijer, A., Lackenby, A., Gubareva, L., Rebelo-de-Andrade, H., Besselaar, T., Fry, A., Gregory, V., Leang, S.-K., Huang, W., et al. (2015). Global update on the susceptibility of human influenza viruses to neuraminidase inhibitors, 2013-2014. Antiviral Research *117*, 27–38.

Tamerius, J., Nelson, M.I., and Zhou, S.Z. (2011). Global influenza seasonality: reconciling patterns across temperate and tropical regions. Environmental Health Perspectives *119*, 439–445.

Tan, K.-X., Jacob, S.A., Chan, K.-G., and Lee, L.-H. (2015). An overview of the characteristics of the novel avian influenza A H7N9 virus in humans. Front Microbiol *6*, 140.

Taubenberger, J.K., Reid, A.H., Janczewski, T.A., and Fanning, T.G. (2001). Integrating historical, clinical and molecular genetic data in order to explain the origin and virulence of the 1918 Spanish influenza virus. Philos. Trans. R. Soc. Lond., B, Biol. Sci. *356*, 1829–1839.

Teng, G., and Papavasiliou, F.N. (2007). Immunoglobulin Somatic Hypermutation. Annu. Rev. Genet. *41*, 107–120.

Tharakaraman, K., Raman, R., Viswanathan, K., Stebbins, N.W., Jayaraman, A., Krishnan, A., Sasisekharan, V., and Sasisekharan, R. (2013). Structural determinants for naturally evolving H5N1 hemagglutinin to switch its receptor specificity. Cell *153*, 1475–1485.

Thornburg, N.J., Nannemann, D.P., Blum, D.L., Belser, J.A., Tumpey, T.M., Deshpande, S., Fritz, G.A., Sapparapu, G., Krause, J.C., Lee, J.H., et al. (2013). Human antibodies that neutralize respiratory droplet transmissible H5N1 influenza viruses. J. Clin. Invest. *123*, 4405–4409.

Thornburg, N.J., Zhang, H., Bangaru, S., Sapparapu, G., Kose, N., Lampley, R.M., Bombardi, R.G., Yu, Y., Graham, S., Branchizio, A., et al. (2016). H7N9 influenza virus neutralizing antibodies that possess few somatic mutations. J. Clin. Invest. *126*, 1482–1494.

Thorpe, I.F., and Brooks, C.L. (2007). Molecular evolution of affinity and flexibility in the immune system. Proc. Natl. Acad. Sci. U.S.a. *104*, 8821–8826.

Tong, S., Li, Y., Rivailler, P., Conrardy, C., Castillo, D.A.A., Chen, L.-M., Recuenco, S., Ellison, J.A., Davis, C.T., York, I.A., et al. (2012). A distinct lineage of influenza A virus from bats. Proc Natl Acad Sci USA *109*, 4269–4274.

Tong, S., Zhu, X., Li, Y., Shi, M., Zhang, J., Bourgeois, M., Yang, H., Chen, X., Recuenco, S., Gomez, J., et al. (2013). New World Bats Harbor Diverse Influenza A Viruses. PLoS Pathog *9*, e1003657.

Treanor, J.J., Wilkinson, B.E., Masseoud, F., and Hu-Primmer, J. (2001). Safety and immunogenicity of a recombinant hemagglutinin vaccine for H5 influenza in humans. Vaccine *19*, 1732–1737.

Treanor, J.J. (2014). Expanding the options for confronting pandemic influenza. Jama *312*, 1401–1402.

Treanor, J.J., Campbell, J.D., Zangwill, K.M., Rowe, T., and Wolff, M. (2006). Safety and immunogenicity of an inactivated subvirion influenza A (H5N1) vaccine. N Engl J Med *354*, 1343–1351.

Tweed, S.A., Skowronski, D.M., David, S.T., Larder, A., Petric, M., Lees, W., Li, Y., Katz, J., Krajden, M., Tellier, R., et al. (2004). Human illness from avian influenza H7N3, British Columbia. Emerging Infectious Diseases *10*, 2196–2199.

Ungchusak, K., Auewarakul, P., Dowell, S.F., Kitphati, R., Auwanit, W., Puthavathana, P., Uiprasertkul, M., Boonnak, K., Pittayawonganon, C., Cox, N.J., et al. (2005). Probable person-to-person transmission of avian influenza A (H5N1). N Engl J Med *352*, 333–340.

Vagin, A., and Teplyakov, A. (1997). MOLREP: an Automated Program for Molecular Replacement. J Appl Crystallogr *30*, 1022–1025.

van de Sandt, C.E., Kreijtz, J.H.C.M., and Rimmelzwaan, G.F. (2012). Evasion of Influenza A Viruses from Innate and Adaptive Immune Responses. Viruses *4*, 1438–1476.

Victora, G.D., and Nussenzweig, M.C. (2012). Germinal Centers. Annu. Rev. Immunol. *30*, 429–457.

Wang, F., Sen, S., Zhang, Y., Ahmad, I., Zhu, X., Wilson, I.A., Smider, V.V., Magliery, T.J., and Schultz, P.G. (2013). Somatic hypermutation maintains antibody thermodynamic stability during affinity maturation. Proc Natl Acad Sci USA *110*, 4261–4266.

Wang, H., Feng, Z., Shu, Y., Yu, H., Zhou, L., Zu, R., Huai, Y., Dong, J., Bao, C., Wen, L., et al. (2008). Probable limited person-to-person transmission of highly pathogenic avian influenza A (H5N1) virus in China. Lancet *371*, 1427–1434.

Webster, R.G., Bean, W.J., Gorman, O.T., Chambers, T.M., and Kawaoka, Y. (1992). Evolution and ecology of influenza A viruses. Microbiol. Rev. *56*, 152–179.

Wedemayer, G.J., Patten, P.A., Wang, L.H., Schultz, P.G., and Stevens, R.C. (1997). Structural insights into the evolution of an antibody combining site. Science *276*, 1665–1669.

Weis, W., Brown, J.H., Cusack, S., Paulson, J.C., Skehel, J.J., and Wiley, D.C. (1988). Structure of the influenza virus haemagglutinin complexed with its receptor, sialic acid. Nature *333*, 426–431.

Wharton, S.A., Belshe, R.B., Skehel, J.J., and Hay, A.J. (1994). Role of virion M2 protein in influenza virus uncoating: specific reduction in the rate of membrane fusion between virus and liposomes by amantadine. J. Gen. Virol. *75*, 945–948.

Whittle, J.R.R., Zhang, R., Khurana, S., King, L.R., Manischewitz, J., Golding, H., Dormitzer, P.R., Haynes, B.F., Walter, E.B., Moody, M.A., et al. (2011). Broadly neutralizing human antibody that recognizes the receptor-binding pocket of influenza virus hemagglutinin. Proc. Natl. Acad. Sci. U.S.a. *108*, 14216–14221.

WHO (1980). A revision of the system of nomenclature for influenza viruses: a WHO memorandum. Bull. World Health Organ. *58*, 585–591.

WHO (2014a). Influenza (seasonal). Fact Sheet no. 211 (World Health Organization).

WHO (2014b). Avian influenza. Fact sheet.

WHO (2014c). Influenza at the Human-Animal Interface. World Health Organization.

WHO (2016). Cumulative number of confirmed human cases for avian influenza A(H5N1) reported to WHO, 2003-2016.

Wiley, D.C., Wilson, I.A., and Skehel, J.J. (1981). Structural identification of the antibody-binding sites of Hong Kong influenza haemagglutinin and their involvement in antigenic variation. Nature *289*, 373–378.

Willis, J.R., Briney, B.S., DeLuca, S.L., Crowe, J.E., and Meiler, J. (2013). Human germline antibody gene segments encode polyspecific antibodies. PLoS Comput. Biol. *9*, e1003045.

Wilson, I.A., and Stanfield, R.L. (1994). Antibody-antigen interactions: new structures and new conformational changes. Curr. Opin. Struct. Biol. *4*, 857–867.

Wilson, I.A., Skehel, J.J., and Wiley, D.C. (1981). Structure of the haemagglutinin membrane glycoprotein of influenza virus at 3 Å resolution. Nature *289*, 366–373.

Winarski, K.L., Thornburg, N.J., Yu, Y., Sapparapu, G., Crowe, J.E., and Spiller, B.W. (2015). Vaccine-elicited antibody that neutralizes H5N1 influenza and variants binds the receptor site and polymorphic sites. Proc. Natl. Acad. Sci. U.S.a. *112*, 9346–9351.

Winter, G. (2010). xia2: an expert system for macromolecular crystallography data reduction. J Appl Crystallogr *69*, 1260–1273.

Wrammert, J., Koutsonanos, D., Li, G.-M., Edupuganti, S., Sui, J., Morrissey, M., McCausland, M., Skountzou, I., Hornig, M., Lipkin, W.I., et al. (2011). Broadly cross-reactive antibodies dominate the human B cell response against 2009 pandemic H1N1 influenza virus infection. J. Exp. Med. *208*, 181–193.

Wu, Y., Cho, M., Shore, D., Song, M., Choi, J., Jiang, T., Deng, Y.-Q., Bourgeois, M., Almli, L., Yang, H., et al. (2015). A potent broad-spectrum protective human monoclonal antibody crosslinking two haemagglutinin monomers of influenza A virus. Nature Communications *6*, 7708.

Xiong, X., Coombs, P.J., Martin, S.R., Liu, J., Xiao, H., McCauley, J.W., Locher, K., Walker, P.A., Collins, P.J., Kawaoka, Y., et al. (2013). Receptor binding by a ferret-transmissible H5 avian influenza virus. Nature *497*, 392–396.

Xiong, X., Corti, D., Liu, J., Pinna, D., Foglierini, M., Calder, L.J., Martin, S.R., Lin, Y.P., Walker, P.A., Collins, P.J., et al. (2015). Structures of complexes formed by H5 influenza hemagglutinin with a potent broadly neutralizing human monoclonal antibody. Proc Natl Acad Sci USA *112*, 9430–9435.

Xiong, X., Xiao, H., Martin, S.R., Coombs, P.J., Liu, J., Collins, P.J., Vachieri, S.G., Walker, P.A., Lin, Y.P., McCauley, J.W., et al. (2014). Enhanced human receptor binding by H5 haemagglutinins. Virology *456-457*, 179–187.

Xu, R., Ekiert, D.C., Krause, J.C., Hai, R., Crowe, J.E., and Wilson, I.A. (2010). Structural Basis of Preexisting Immunity to the 2009 H1N1 Pandemic Influenza Virus. Science *328*, 357–360.

Xu, R., Krause, J.C., McBride, R., Paulson, J.C., Crowe, J.E., and Wilson, I.A. (2013). A recurring motif for antibody recognition of the receptor- binding site of influenza hemagglutinin. Nat Struct Mol Biol *20*, 363–370.

Xu, Z., Zan, H., Pone, E.J., Mai, T., and Casali, P. (2012). Immunoglobulin class-switch DNA recombination: induction, targeting and beyond. Nature Reviews Immunology *12*, 517–531.

Yaari, G., Vander Heiden, J.A., Uduman, M., Gadala-Maria, D., Gupta, N., Stern, J.N.H., O'Connor, K.C., Hafler, D.A., Laserson, U., Vigneault, F., et al. (2013). Models of somatic hypermutation targeting and substitution based on synonymous mutations from high-throughput immunoglobulin sequencing data. Front Immunol *4*, 358.

Yamada, S., Suzuki, Y., Suzuki, T., Le, M.Q., Nidom, C.A., Sakai-Tagawa, Y., Muramoto, Y., Ito, M., Kiso, M., Horimoto, T., et al. (2006). Haemagglutinin mutations responsible for the binding of H5N1 influenza A viruses to human-type receptors. Nature *444*, 378–382.

Yamashita, M., Krystal, M., Fitch, W.M., and Palese, P. (1988). Influenza B virus evolution: co-circulating lineages and comparison of evolutionary pattern with those of influenza A and C viruses. Virology *163*, 112–122.

Yuan, J., Zhang, L., Kan, X., Jiang, L., Yang, J., Guo, Z., and Ren, Q. (2013). Origin and molecular characteristics of a novel 2013 avian influenza A(H6N1) virus causing human infection in Taiwan. Clin. Infect. Dis. *57*, 1367–1368.

Zhang, W., Shi, Y., Lu, X., Shu, Y., Qi, J., and Gao, G.F. (2013). An Airborne Transmissible Avian Influenza H5 Hemagglutinin Seen at the Atomic Level. Science *340*, 1463–1467.

Zhirnov, O.P. (1990). Solubilization of matrix protein M1/M from virions occurs at different pH for orthomyxo- and paramyxoviruses. Virology *176*, 274–279.

Zhou, T., Zhu, J., Wu, X., Moquin, S., Zhang, B., Acharya, P., Georgiev, I.S., Altae-Tran, H.R., Chuang, G.-Y., Joyce, M.G., et al. (2013). Multidonor analysis reveals structural elements, genetic determinants, and maturation pathway for HIV-1 neutralization by VRC01-class antibodies. Immunity *39*, 245–258.

Zhu, J., and Paul, W.E. (2010). Heterogeneity and plasticity of T helper cells. Cell Res. *20*, 4–12.

Zhu, X., Guo, Y.H., Jiang, T., Wang, Y.D., Chan, K.H., Li, X.F., Yu, W., McBride, R., Paulson, J.C., Yuen, K.Y., et al. (2013). A Unique and Conserved Neutralization Epitope in H5N1 Influenza Viruses Identified by an Antibody against the A/Goose/Guangdong/1/96 Hemagglutinin. Journal of Virology *87*, 12619–12635.

Zhu, X., Viswanathan, K., Raman, R., Yu, W., Sasisekharan, R., and Wilson, I.A. (2015). Structural Basis for a Switch in Receptor Binding Specificity of Two H5N1 Hemagglutinin Mutants. Cell Rep *13*, 1683–1691.

Zuo, T., Sun, J., Wang, G., Jiang, L., Zuo, Y., Li, D., Shi, X., Liu, X., Fan, S., Ren, H., et al. (2015). Comprehensive analysis of antibody recognition in convalescent humans from highly pathogenic avian influenza H5N1 infection. Nature Communications *6*, 1–12.